NAVAL FACILITIES ENGINEERING SERVICE CENTER
Port Hueneme, California 93043-4370

Technical Report
TR-2093-SHR

EFFECTIVE STRESS DRYDOCK ANALYSIS

by

J.M. Ferritto

September 1998

19990618 038

Sponsored by
Naval Facilities Engineering Command, Code 15
1510 Gilbert Street
Norfolk, VA 23511-2699

Approved for public release; distribution is unlimited.

DTIC QUALITY INSPECTED 4

Printed on recycled paper

REPORT DOCUMENTATION PAGE

Form Approved
OMB No. 0704-018

Public reporting burden for this collection of information is estimated to average 1 hour per response, including the time for reviewing instructions, searching existing data sources, gathering and maintaining the data needed, and completing and reviewing the collection of information. Send comments regarding this burden estimate or any other aspect of this collection information, including suggestions for reducing this burden, to Washington Headquarters Services, Directorate for Information and Reports, 1215 Jefferson Davis Highway, Suite 1204, Arlington, VA 22202-4302, and to the Office of Management and Budget, Paperwork Reduction Project (0704-0188), Washington, DC 20503.

1. AGENCY USE ONLY *(Leave blank)*	2. REPORT DATE	3. REPORT TYPE AND DATES COVERED
	September 1998	Final: July 1998 - Sep 1998

4. TITLE AND SUBTITLE

EFFECTIVE STRESS DRYDOCK ANALYSIS

5. FUNDING NUMBERS

6. AUTHOR(S)

J.M. Ferritto

7. PERFORMING ORGANIZATION NAME(S) AND ADDRESSE(S)

Naval Facilities Engineering Service Center
1100 23rd Ave.
Port Hueneme, CA 93043-4370

8. PERFORMING ORGANIZATION REPORT NUMBER

TR-2093-SHR

9. SPONSORING/MONITORING AGENCY NAME(S) AND ADDRESSES

Naval Facilities Engineering Command, Code 15
1510 Gilbert Street
Norfolk, VA 23511-2699

10. SPONSORING/MONITORING AGENCY REPORT NUMBER

11. SUPPLEMENTARY NOTES

12a. DISTRIBUTION/AVAILABILITY STATEMENT

Approved for public release; distribution is unlimited.

12b. DISTRIBUTION CODE

13. ABSTRACT *(Maximum 200 words)*

Recent earthquakes have emphasized the high damage threat the soil liquefaction phenomenon poses to waterfront structures. These experiences have shown that both the nature of waterfront facilities, such as earth-retaining structures, and the depositional environment of the coastal marine soil contribute to major liquefaction damage. Drydocks are critical structures containing high value ships and as such represent a class of structure which can not fail during an earthquake. Consequently, drydock certification studies have been conducted to evaluate the safety of drydocks under all possible load conditions. The recent development of effective stress finite difference technology now permits a more accurate assessment of these structures. The newly developed FLAC computer program was evaluated as part of this study and a demonstration case performed on the drydock located at Naval Station, San Diego. The results of this study show that the drydock has adequate factors of safety for the static load considered. This is in agreement with the drydock certification study. This analysis shows the drydock to be at yield levels during dynamic earthquake loading. The levels of liquefaction are limited and controlled. The FLAC analysis is better able to represent the actual loading conditions on the drydock than the traditional hand calculations performed in the drydock certification studies. As a result the more accurate FLAC analysis shows a lower level of loading both under static and dynamic conditions and higher factors of safety. The conclusion of this study is that for the conditions established in the drydock certification report, the drydock is safer than indicated in the report under dynamic loading.

14. SUBJECT TERMS	15. NUMBER OF PAGES
Earthquakes, drydocks, soil, analysis	98
	16. PRICE CODE

17. SECURITY CLASSIFICATION OF REPORT	18. SECURITY CLASSIFICATION OF THIS PAGE	19. SECURITY CLASSIFICATION OF ABSTRACT	
Unclassified	Unclassified	Unclassified	UL

Executive Summary

Recent earthquakes, particularly those in Kobe, Japan, Guam, and California as well as previous earthquakes in Alaska, Japan, and Chile, have emphasized the high damage threat the soil liquefaction phenomenon poses to waterfront structures. These experiences have shown that both the nature of waterfront facilities, such as earth-retaining structures, and the depositional environment of the coastal marine soil contribute to major liquefaction damage. Drydocks are critical structures containing high value ships and as such represent a class of structure which can not fail during an earthquake. Consequently, drydock certification studies have been conducted to evaluate the safety of drydocks under all possible load conditions. The recent development of effective stress finite difference technology now permits a more accurate assessment of these structures.

The newly developed FLAC computer program was evaluated as part of this study and a demonstration case performed on the drydock located at Naval Station, San Diego. The results of this study show that the drydock has adequate factors of safety for the static loads considered. This is in agreement with the drydock certification study. This analysis shows the drydock to be at yield levels during dynamic earthquake loading. The levels of liquefaction are limited and controlled. The response of the drydock is controlled. The FLAC analysis is better able to represent the actual loading conditions on the drydock than the traditional hand calculations performed in the drydock certification studies. As a result the more accurate FLAC analysis shows a lower level of loading both under static and dynamic conditions and higher factors of safety. It is important to note the limitation in this study which involved lack of specific site soil properties and a need for estimating of soil material properties. To minimize these limitations the soil properties were varied over a wide range and the results did not change appreciably. Additionally several earthquake records were used to treat possible variability in ground motion.

The conclusion of this study is that for the conditions established in the drydock certification report, the drydock is safer than indicated in the report under dynamic loading. The threat of liquefaction induced damage is less than indicated by the quasi-static approach used in certification report. For a bedrock motion of 0.2g, the drydock would be at yield levels at the intersection of the wall and floor and would undergo several cycles of controlled inelastic yielding. This level of motion would have about a 50 percent probability of exceedance in 50 years. The drydock would sustain moderate damage at a bedrock ground motion level of 0.4g and be near collapse at a bedrock ground motion of 0.6g. The study relates the FLAC analysis results to damage levels and combines the damage with the probability distribution of seismic exposure. The expected damage level over a 50-year exposure would be about 13 percent.

This report presents a recommended approach for conducting future drydock certification studies and defines a limited additional follow-up study.

Contents Page

Introduction

Recent earthquakes, particularly those in Kobe, Japan, Guam, and California as well as previous earthquakes in Alaska, Japan, and Chile, have emphasized the high damage threat the soil liquefaction phenomenon poses to waterfront structures. These experiences have shown that both the nature of waterfront facilities, such as earth-retaining structures, and the depositional environment of the coastal marine soil contribute to major liquefaction damage. Over twenty years ago it was noted in a study of the Naval Air Station (NAS) North Island, California, liquefaction under design earthquake levels could result in damage in the vicinity of such critical structures as aircraft carrier berths, aviation fuel tank farms, and underground utility service lines. Unfortunately, almost all previous studies of the liquefaction problem have been concerned with either conventional building foundations or with analyses of dams, and procedures for analysis are not available on the effect of liquefaction on Navy types of specialized structures. Recent advances in computer codes and constitutive soil models is of major significance to the Navy since the Navy must locate in areas where the water table is high. Even if liquefaction (a loss of shear stress from a loss of effective confining stress) does not occur, a buildup of pore pressure is probable both in sands and clays. This pore pressure buildup can be of major significance to structural behavior. This work deals only with that type of stationary drydock often referred to as a graving dock. It does not consider structures as floating drydocks, lift docks, marine railroads, or similar strictures.

A graving dock is a permanent structure constructed at the water's edge capable of being closed off and dewatered to allow docking of a vessel in the dry. This basin like structure is constructed such that the ship may be floated in and the water removed from the basin allowing the ship to settle down on blocking propositioned on the drydock floor. Graving docks or dock sections may be classified according to the types of foundation design:

Fully hydrostatic

Partially relieved

Fully relieved

Often an actual drydock may be composed of sections of all three types of foundations. The recommended type of construction design depends upon the soil and underlying foundation conditions at the site. A fully hydrostatic drydock structure is generally constructed in sandy or pervious soils. This dock structure must be capable of resisting the total maximum hydrostatic water pressure, both vertically and horizontally. The partially relieved drydock structure is designed to reduce the hydrostatic pressure on the floor of the dock. The water pressure is relieved by providing a filter course under the floor, which permits a flow of water into a pipe collection system or allows seepage through holes in the floor slab. Sufficient pumping capacity must be provided to remove

the water seepage. The fully relieved structure is used where the soil conditions permit total relief of the hydrostatic pressure from the floors and sidewalls. The pressure is relieved by continuously draining and pumping the groundwater from the structure.

The basic structural elements of a graving dock are the floor and sidewalls. Common materials of construction are concrete, sheet piling, and composite steel and concrete sections. The load on the floor is transmitted directly to the underlying soil foundation. If the underlying soil has insufficient bearing capacity, piling is generally incorporated into the drydock foundation design. Entrance structures, crane rails, and pumping systems are other important elements in a drydock.

Often an actual drydock may be composed of sections of all three types of foundations. The recommended type of design depends upon the soil and underlying foundation conditions at the site. A fully hydrostatic drydock structure is generally constructed in sandy or pervious soils. This dock structure must be capable of resisting the total maximum hydrostatic water pressure, both vertically and horizontally. The partially relieved drydock structure is designed to reduce the hydrostatic pressure on the floor of the dock. The water pressure is relieved by providing a filter course under the floor, which permits a flow of water into a pipe collection system or allows seepage through holes in the floor slab. Sufficient pumping capacity must be provided to remove the water seepage. The fully relieved structure is used where the soil conditions permit total relief of the hydrostatic pressure from the floors and sidewalls. The pressure is relieved by continuously draining and pumping the groundwater from the structure.

The basic structural elements of a graving dock are the floor and sidewalls. Common materials of construction are concrete, sheet piling, and composite steel and concrete sections. The load on the floor is transmitted directly to the underlying soil foundation. If the underlying soil has insufficient bearing capacity, piling is generally incorporated into the drydock foundation design. Entrance structures, crane rails, and pumping systems are other important elements in a drydock. Before analytical procedures can be discussed it is important to discuss design concepts of drydocks and various types of loadings possible. The underlying soil is a major factor in the selection of the type of drydock design. The soil type and permeability determine the degree to which water pressure can be relieved and whether dewatering is feasible. Each of the three types of drydock section (the fully hydrostatic, the fully relieved and the partially relieved) may be built with or without piles. For the full hydrostatic type, piles may be used to engage soil beneath the drydock to contribute to the holddown weight. For the fully and partially relieved types, piles may be used to improve the elastic modulus of the foundation or to reinforce the soil at locations of excessive soil pressure, e.g., beneath the toes of walls or under ship blocking.

Fully Hydrostatic A drydock is classified as fully hydrostatic unless there is a relief drainage system that lowers the natural hydraulic head on the walls and floor. No material, including rock, can be considered impervious in the sense that it will eliminate the hydraulic pressure on the structure. The full buoyancy of the drydock must be resisted by

one or more of the following: (1) weight of concrete; (2) weight of soil below the dock engaged by holddown devices; or (3) weight of earth resting on a ledge formed by the projection of the floor slab beyond the sidewalls and for friction of the earth on the sidewalls. Theoretically, a fully hydrostatic drydock can be built for almost any site or foundation condition. However, for a large, deep drydock, economic considerations may force the choice of another type. Indicated below are the two basic construction techniques for fully hydrostatic drydock:

Fully Relieved A fully relieved drydock section requires a drainage system to eliminate the pressure on the floor and walls so that these elements may be of minimum size. The pressure relief type may be built for most foundation conditions if the flow of water is naturally cut off by a not-too-pervious soil, or by natural or artificial means. The exception is drydocks constructed in the wet. For drydocks in rock it may be necessary to line the rock excavation with concrete, or pressure-grout to seal any fissures and provide weep holes through the floor and sidewall concrete lining. Where the soil is impervious, or nearly so, and the volume of seepage water to be handled is small, this water can be drawn off through drainage courses placed under the floor and against the walls. This drainage course may or may not be supplemented by a pipe system to carry the seepage water into the drydock chamber for disposal by pumping. The volume of seepage water which must be pumped during the life of a drydock will depend on the degree of permeability of the soil. A very pervious soil condition consisting of a homogenous sand (permeability coefficient equal to 0.01 feet per minute) of indefinite depth cannot be practically dewatered by conventional methods and therefore cannot be constructed to provide a fully relieved type structure. For a fully relieved drydock to be built in pervious soil, a suitable cutoff must be provided outside the drydocks down to an underlying impervious stratum. A drydock may have immediate surrounding soil of granular material underlain by an impervious stratum. A sheet pile cutoff, perhaps originally a part of the construction cofferdam and located at a distance from the drydock, when driven to the impervious layer, can provide the necessary obstruction for cutting off the large volume of seepage flow that would otherwise reach the drydock. Granular materials generally found at these drydock sites must be excluded from the relief system flow. This requires the use of carefully designed filter courses and a system of drainage pipes adjacent to the walls and under the floor. The amount of pumping for this type will depend on the efficiency of the cutoff and permeability of the soil.

Partially Relieved A partially relieved drydock section has relief provided for the floor only. This reduces the uplift and the amount of concrete required. It also minimizes the difficulty in constructing a cofferdam. A partially relieved drydock would generally be arranged with a cutoff wall surrounding the floor area and a filter course under the floor with a system of collector pipes which carry the seepage water into a collecting tunnel. As an alternative to a collector system, holes through the floor would allow the seepage water to flow into the drydock chamber and then through trenches to the collecting tunnel. A filter course would normally be required beneath the floor slab. Two factors determine whether a drydock is to be of the partially relieved type. The first is if the quantity of water to be removed is within acceptable limits. The second factor is an economic one

and involves an analysis to determine if the acquisition cost plus the operating and maintenance charges over a period of years are less than the corresponding costs for a fully hydrostatic dock of much heavier cross section requiring little or no maintenance for continual seepage pumping.

Drydock Construction

The performance of a drydock can depend upon the manner it was constructed. It is important in the review and analysis of a drydock to fully understand the construction process employed and the influence of the method of construction in the design of the structure and its expected performance. The method of construction can establish the static stress state on the walls of the drydock. Soil parameters such as k_0 represent the ratio of horizontal to vertical soil pressure and are established during backfilling operations. This factor is significant in establishing wall factors of safety.

An important design consideration is the location of the entrance to the drydock. An entrance which is to be located in deep water may need an extensive cofferdam or require construction by the tremie method. In this case a fully hydrostatic design would probably be required. Economic tradeoffs exist between the amount of dredging to reach an inshore entrance location and the added cost of deep water construction.

The cross-section dimensions are an important factor in the design of drydocks which must resist full or partial uplift. The depth is particularly significant because hydrostatic uplift varies directly with the depth, and the sidewall moments vary with the cube of depth. This also affects the design of pump wells. The total weight and floor bending moments are functions of the drydock width. During construction the quantity of seepage and the possibility of heaving depend on the drydock width.

Excavation of materials in preparation for the foundation is the first step in the construction process. In some materials excavation may be accomplished by dredging. Normally excavation is accomplished by dewatering and conventional dry-land excavation techniques. Usually dry construction, when possible, is the most economical. Cofferdams may be used when required as cutoffs of water to the site. In impervious sites drainage layers are installed below the floor slab.

The floor slab may be poured in the dry or underwater. The tremie method is necessary for underwater construction. Tremie concrete is brought to about 2 feet below the top of the finished slab, with the remainder poured in the dry. The drydocks constructed underwater are usually of the fully hydrostatic type. Incremental construction load case must be examined since the partially completed structure does not have the benefit of wall weight to overcome buoyancy. Hold down piles may be used if the weight of the floor slab is insufficient to overcome the total buoyancy. Tremie concrete can also be used in the sidewalls. Straight wall, noncellular-type sheet piles have been used particularly in the vertical portion of entrance walls. The usual method of anchoring the

sheet pile walls has been to run steel walers along the piling and support the walers laterally by wire cables or rods

Previous Experience

Drydocks used by the Navy may be reinforced concrete, unreinforced concrete, or cofferdam in cross-section. The large buoyant or hydrostatic uplift forces that tend to act upon a dewatered drydock must be opposed either by huge gravity sections (fully hydrostatic), or else the uplift pressures must be reduced. Thus, it is often more economical to design the drydock to either be fully relieved, wherein the hydraulic head beneath the drydock is held at essentially floor level; or partially relieved, that is, drydock stability is attained by a combination of gravity sections and sections (floor) with reduced hydrostatic pressures. It is noted however, that even drydocks that are defined as being totally relieved may have some portions, such as the pumphouse or the entrance sill, which rely Upon gravity loads to maintain their stability. Thus, in addition to failures due to loss of foundation support, failures in the subsurface drainage system could lead to floor breach/blow up, uncontrolled flooding, failure of the dock walls, and freezing of the entrance caisson (due to jamming). Subsurface erosion around the periphery of the drydock could also lead to failures of the adjacent slabs or crane rails. These difficulties could be a result of such things as breaching of flow-cutoffs, clogged drainage blankets, improperly functioning pressure relief systems, and the presence of erosion cavities or "pipes".

As noted above, numerous problems can occur during operation of these kinds of docks. Foundation problems may manifest themselves in terms of irregular pressure distributions and flow variations due to the development of voids; large settlements, either under ship blocks or under adjacent crane rails; floor breach/blow up; wall or floor slab collapse; entrapment of the caisson gate; uncontrollable water or soil and water inflows. Such problems may be caused by a loss of a drainage blanket, loss of subsurface support from erosion; breached flow- cutoffs such as split sheeting; failure of pumping or dewatering system valves or pumps; blockage of under-drains; drainage lines; filters; and drainage blankets. The intent is to concentrate on the soil-structure problems; i.e., those related to the drydock walls and foundation and the effect of liquefaction on soil loading.

U-frame locks are very similar to drydocks. Two such structures are the Port Allen and Old River locks on the Mississippi River. Both of these structures have been extensively instrumented and analyzed. Duncan and Clough (1969) performed a nonlinear analysis of the locks in which incremental construction was used to simulate construction including excavation, dewatering, concrete placement, backfill placement, increase in ground water level, filling of the lock and temperature changes. The analysis represents an excellent rigorous procedure using finite element techniques to model a problem. However one must remember it is still a mathematical model and actual construction stresses can only be approximated.

Port Allen Lock. This structure is 84 feet wide, 68 feet high and 1,200 feet long. Backfill extends to 50 feet above floor level. The base slab is 11.5 feet thick. The wall is a very stiff cantilever with an EI value of 12 x 106 kip-ft^2 at the base. The lock overlies 65 feet of overconsolidated silt with clay and sand lenses. Below this is 105 feet of medium compact sand with gravel. Backfill behind the walls was a clean fine sand (D_R = 70%). Observations of the lateral deflections during construction were made and compared to computed results. The structure was built in a dewatered open excavation. It is important to note that the deposition (placement) of the wall backfill dominated the deflection pattern of the structure. The wall and slab edge settled more than the center of the slab resulting in the wall tilting 0.5 inch into the backfill at the top. Filling the lock with water resulted in the wall deflecting about 1/8-inch inward. Note the wall response is linked with the floor deflection. Displacement of subsoil upon filling was downward and outward beneath the floor slab causing the backfill to move upward and inward increasing wall pressures. This increase may have been caused in part by high temperatures. The lock was shown to be sensitive to temperature changes. The walls moved 3/4-inch with seasonal changes of 40°F. Thirty percent fluctuations were observed in lateral pressure.

Old River Lock This lock is 75 feet wide, 1,200 feet long and 78 feet deep. Backfill was placed to 65 feet above floor level. The base slab was 12.5 feet thick. The structure rests on 100 feet of medium compact sand overlying clay. The dominant weight of the backfill and lock wall again resulted in the wall tilting outward into the backfill. The mobilized angle of friction was 28 degrees (about the same as Port Allen). Upon filling with water the wall deflected inward and the earth pressure decreased. This is in contrast to the increased pressure observed at Port Allen. Both of these locks show the significance of the wall pressures and deflections on the total floor slab-wall response, and that edge settlements tilt the wall into the backfill. Moments in the base slab are dominated by settlement patterns. Maximum center floor slab moment occurs with the lock empty (tension on top). Maximum wall moments occur with the lock empty. Temperature is significant. For these reasons conventional retaining wall analysis is not well suited to drydock analysis.

Instrumented Drydock Tests Loads on the keel blocks have been measured for several ships. Deflection surveys were run on drydocks before and after docking and strains were measures on one snips nulls. Results showed that keel block load varies with time and takes a number of days to stabilize. The effect of temperature variations of 20 degrees had an effect on keel block load. Test results for the USS FORRESTAL at Graving Dock 8 at the Norfolk Naval Shipyard noted a drop in temperature of 21°F which reduced the maximum load in the skeg area from 122 tons/ft to 92 tons/ft. Results of tests on the VALLEY FORGE docked at the Norfolk Shipyard indicate considerable redistribution of load occurs with time. Data was compared with a previous drydocking of the same ship and showed while the general shape of the keel block load profile is similar there can be as much as 30 percent variation at the same location with different dockings. The USS BENNINGTON was drydocked at the Norfolk Naval Shipyard. This drydock rests on piles driven into a soft foundation of mud. The tests were repeated at the San Francisco Naval Shipyard which rests on rock. Results for the San Francisco drydock test indicated

variation in settlement with time and temperature. An interesting comparison of the test results shows a variation in keel block load determined on similar ships at the same shipyard and for similar ships in different shipyards. There was as much variation in the keel-block loads determined on similar ships in the same shipyard as the variation in the loads for similar ships in different shipyards. Note the Norfolk dock rests on piles driven into a soft mud base whereas the San Francisco dock rests on rock. Forrest (1982) measured wall rotation

Navy Certification Studies Previous certification reports noted the following for West Coast drydocks:

Bremerton Drydock no. 4: Ultimate moment in floor adjacent to wall exceeds allowable in 0.15 earthquake loading

Mare Island Drydock no. 3: Drydock could not resist seismic loads.

Long Beach Drydock no. 1: Liquefaction possible; also flotation and wall instability possible

Long Beach Drydock no. 2: High liquefaction potential and possible floor failure

Long Beach Drydock no. 3: High liquefaction potential subject to floatation and floor failure

Experience has shown, however, that because of unknown or misunderstood soil conditions, faulty construction, inaccurate design assumptions, or other factors, drydocks do not always function as intended. Although such structures can tolerate some deviations, serious failures have occurred. Perhaps of equal importance is the uncertainly and lack of assurance of ship safety over extended periods of time. Foremost among these ships are the nuclear submarines which may be vulnerable during long periods of very complex overhaul in both Navy and commercial docks.

A certification study was performed for Drydock 3, Mare Island Naval Shipyard. The contract study found the factors of safety against static and earthquake loads to be less than 1.0. The drydock was reanalyzed by the Naval Civil Engineering Laboratory; the level of safety depended upon the amount of tension permitted in the mass concrete walls. Levels of up to 180 psi were calculated as the demand; it was assumed that the structure capacity was over 200 psi. Other unknowns was the strength of construction joints.

Facets of Drydock Analysis

The complete analysis of a drydock must include the various conditions which could cause failure - static and dynamic application of loads, variation in water elevation, failure of drainage devices (pumps, drains, etc.), breach of cutoffs, and deterioration of the

structure or soil foundation. It becomes obvious that many failure modes and interactions are possible; no single analytical technique can begin to fully and accurately represent the actual structure. Some assumptions and simplifications must be made to attempt to segment and model the problem.

Static Soil-Structure Analysis Several alternatives can be used to analyze drydock structures to determine foundation interaction. The simplest uses beam column analysis representing the soil as equivalent springs. Nonlinearity of soil behavior may be approximated by parabolic soil stiffness functions. More complex procedures are available such as finite element analysis techniques. The concrete drydocks may be modeled accurately; however, the interface between soil and structure is the key to satisfactory results. Some codes incorporate specific nodal tie elements to allow nonlinear slippage between the soil and concrete interface. Static analysis of total stress is typical within the present state-of-the-art.

Dynamic Soil-Structure Analysis Some of the finite element codes used for static soil-structure analysis are capable of treating total-stress dynamic analysis by using time history incremental analysis using time step integration. Coupled with the total stress analysis are supplemental programs which can generate pore pressure histories in an approximate uncoupled manner. This has application to estimating seismically induced liquefaction, but is not amenable to accurate load estimation on vertical drydock walls. Effective stress material models are under development. One application will be discussed at length below.

Seepage The seepage analytical technique is perhaps the most developed of the several discussed. Full three-dimensional finite element arid finite difference codes are available that can model the most complex geometry and determine water surface location and flow rates under transient and steady state conditions. Drains, pumps, and cutoffs may all be represented. In this manner, the seepage conditions and possible seepage failure modes under a drydock can be evaluated. Although the technology is available, the types of problems studied have been limited to major structures such as dams.

Consolidation Programs are available for one-, two-, and three-dimensional consolidation. This procedure analyzes the generation and dissipation of pore water pressure established by a loading or change in water conditions. Finite element techniques are available which form a suitable solution by application of a generalized variational principle to the static equations of equilibrium solving for displacements and pore pressures.

Finite Element Stress Modeling The earth-structure interaction problem has been of great importance in geotechnical engineering. The interaction of a retaining wall with a frictional soil backfill was studied by Coulomb in 1776 and Rankine in 1857. Their work is in use even today. Both theories assume the earth as a rigid-plastic mass material governed by Mohr-Coulomb failure and the structure as rigid. Terzagihi (1936) and others demonstrated limit conditions and the dependence of earth pressure on the wall

deformation and flexibility. Empirical and semi-empirical techniques are generally used in design of many earth-support systems giving a conservative estimate of loading and deformation.

The finite element approach offers the ability to simulate in a better manner soil behavior and boundary conditions. As a result, this approach is a major tool in sizable geotechnical projects. However, idealizations of the problem must be made. These idealizations often entail less than a full three-dimensional analysis and some compromise at boundaries. The retaining wall soil interface is a complex nonlinear junction which must behave differently in tension than in compression; slippage and friction may be paramount to realistic solutions. Numerous material models will simulate some aspects of soil behavior such as nonlinearitiy, time dependence, dilation and shear-volume change effects; however, often a material model may represent one phenomenon or type of test data and completely miss another. The choice of material model is critical to a valid solution. If shear induced deformations are of major significance, then a curve-fit model using volumetric stress-strain data will not produce satisfactory results; or, if the problem involves mainly volume change, use of empirically fit shear modulus parameters might not be suitable. Each model presents certain capabilities and certain complexities. The more test data types capable of being simulated, generally the greater the capability, hut also the higher the complexity, cost of rise, and increased data input required.

Key Analysis Elements

As suggested previously, any satisfactory procedure for drydock certification will have to encompass directly measurable or recorded design information, as well as indirect information, such as observations made during original construction or during subsequent operations. For example, during construction at Pascagoula, it was noted that the contractor experienced unusually soft driving conditions in the sheet pile cells. Toward the end of construction, some leakage was also observed from floor vents just inboard of the gate. This knowledge, combined with design information and analysis, provided a preview of some of the subsequent problems experienced. From the geotechnical aspect, several critical items for certification can be singled out. These items might best be treated under the following categories:

1. Applied Loads - Investigate supports for static loads of dock, ship, cranes, and equipment

2. Foundation-Structure Interactions - Assure that sidewalls and adjacent entrance walls are not overstressed by hydrostatic and local soil pressures

3. Hydrostatic Relief and Drainage Systems - Assure that all drainage and pressure relief systems are in sound condition

4. Subsurface Erosion - Detect any subsurface voids or erosion channels adjacent to the dock

5. Deformation-Related Problems - Assure that deformations do not interfere with any drydock operations

6. Earthquake Effects - Assure stability during seismic loading

These categories will be discussed with regard to basic descriptions and engineering design data, field examinations and measurements, and applicable analysis.

Applied Loads Basic data should include a description of wall and floor foundation type, floor thickness, spacing, size and type of piling, design floor loading, and design pile loading. A description of the soil layers beneath and adjacent to the dock would be required, including stratum thickness, groundwater levels, and soil characteristics. Elevations of soil and foundation bearing levels and pile tips relative to the soil layers depended upon to carry the loads should be detailed. Loading conditions on the dock and all associated crane tracks and equipment should be defined. Field inspections should be conducted in conjunction with detailed knowledge of past drydock performance. In addition to inspection of obvious cracking, settling, or yielding of the dock or adjacent pavements arid crane rails, all deformations should be precisely measured. This should include, for example, comparisons between measurements at dock- empty and dock-flooded stages. Supplementary field measurements might include current soil explorations and testing programs, which might entail test pits along crane tracks to determine the condition of supporting piling, geophysical testing, arid other types of nondestructive soil testing. Sonic, geophysical, or other techniques can also be used to check the soundness or, if necessary, the extent of foundation materials and sheet piling. Estimates must be made of the condition of all these structural items as well as the expected rates of deterioration.

Foundation-Structure Interactions This item is concerned with insuring that the sidewalls, entrance, and other structures are riot overstressed by either soil or hydrostatic pressures. Basic engineering requirements include properties of the backfill materials behind the sidewalls and walls or bulkheads adjacent to the dock entrance and within cells of cofferdams. It is necessary to denote the location, dimensions, and properties of wall drainage systems, filters, arid piping. The location, dimensions, and characteristics of special hydrostatic control wells or drains must be stated. This information permits analysis of the soil and hydrostatic loading on walls and bulkheads, of the stability of cells, and of other characteristics. Care must be taken during inspection to observe such items as wall tilting, free flowing leakage, openings in or bulging of cell walls. Entrance bulkheads must be given special attention to detect problems such as excessive erosion or loss of backfill material. Infiltration rates should be estimated and the proper functioning of cell drainage systems assured. Additional testing can include penetrometer probing of filled areas arid measurements of piezometric and soil pressure gradients behind walls and cells.

Again, precise measurement and analysis of wall displacements between flooded and empty dock stages can provide valuable insight toward drydock condition.

Hydrostatic Relief and Drainage Systems The locations, dimensions, and engineering properties of all sub- drainage features must be defined, including subfloor blankets, filters and pipe drains, wall backfill drainage, and any special hydrostatic control or relief wells. Tip elevations of cut-off walls, cofferdam, or bulkhead sheet piles must be identified in relation to the soil profiles. All manholes, pipes, and drainage passages must be clean and properly aligned. Evidence of any gradual reduction in seepage from wall or floor drains must be noted, since this could result from clogging or some other form of malfunction. Hydrostatic heads and pressure gradients beneath the floor and behind walls should be determined, using piezometers, for both dock-flooded and dock-empty conditions. Measurements made during pumping from particular drainage wells can be compared with analytical results of the flow regime beneath the dock. In this way, any anomalies in pressure gradients under the sidewalls, the entrance sill, or other areas can be recognized. All records must be maintained for comparison to permit estimates of rate of drainage system deterioration.

Subsurface Erosion The danger posed to a drydock by underground erosion or piping warrants special consideration. It is critical that no incipient flow channels or voids develop beneath or around a drydock. This could lead to uncontrolled flooding or complete loss of support for the dock and for adjacent work areas. Construction records must be studied in detail with regard to compaction control, design and gradation of filters, filter thickness, size of pipe perforations, and other information. All this information must be considered in relation to the grain size and gradation of the local soils and backfill materials. It must be determined whether or not all construction dewatering systems have been removed or sealed up. Attention must be directed toward any evidence of sediment accumulating in drainage and filling tunnels or seepage collector pipes or of sediment moving through cracks. Analysis of in-flowing water for suspended or dissolved solids can be a valuable indicator of drydock condition. Any progressive increase in the quantity of seepage must be noted. Localized settlements of paved areas around the dock can be an indicator of soil loss or voids. Examination of the harbor bottom near the drydock entrance for evidence of holes, craters, heaves, or other anomalies is valuable. Voids beneath the floor may be detected through the vent holes, but generally nondestructive detection of voids beneath the substantial concrete thickness of a drydock floor is an unresolved problem. Field measurements may include borehole permeability tests and pumping tests in selected areas with measurements of flow rates. Use of dyes, isotopes, or measurement of chloride content can be used to detect sources of seepage flows. Bathymetric surveys of the entrance bottom and adjacent areas can suggest any deteriorating conditions. Pressure head measurements and pumping tests can be used together with an analysis of the flow regime around and beneath a dock to detect any anomalies in flow paths or hydraulic gradients.

Deformation-Related Problems It is important to insure that settlements and earth movements adjacent to the drydock do not adversely affect the safety of equipment

operation. Basic information here includes surface and subsurface soil profiles, data on possible negative skin friction acting on piles and walls, and estimates of possible subsidence or distortion levels. The cause and nature of any soil movements must be determined and their significance evaluated. This aspect of drydock certification entails placement and monitoring of bench marks for both vertical and lateral movements. Use of inclinometers and deformation gages are valuable in this regard. Piezometers and soil stress measurement combined with theoretical analysis can be valuable in evaluating structure response.

Earthquake Effects Because many drydocks are located in seismic regions, such as the West Coast, the central Atlantic coast, or even the northeastern Great Lakes area, it is necessary to assure that the dock and associated crane rail foundations and other structures can withstand anticipated earthquake effects. Basic information required here is knowledge of adjacent native soils and fills and the geometry, stiffness, and mass of involved structures. A major factor for consideration is earthquake-induced Soil liquefaction which could destroy not only pressure relief and drainage systems bit also the dock itself. This is the main topic of this report and will be addressed below. The stress conditions around a drydock during seismic loading can be complex, making it difficult to predict liquefaction potential in all but the more extreme cases. Where limited liquefaction can be expected to occur at depth, the results on the dock and upon the adjacent facilities are also difficult to predict. Even in cases where liquefaction may not be a problem, such as beneath the drydocks at Mare Island which are reported to be founded on a stiff clay problems regarding dynamic lateral pressures arise. Previous analysis procedures for handling dynamic soil pressures were for the most part empirical quasi-static approaches. Thus, the ability to analyze the resistance of the dock walls, entrance walls, floor support piling, and other structures to ground acceleration forces can improved by more accurate new tools such as effective stress modeling.

Ship Rigidity A problem of concern is the treatment of the ship and its load distribution on the slab and soil. Often for lack of a better analysis the ship is treated as rigid or totally flexible. To examine this problem a beam on elastic foundation concept was studied, Ferritto, (1979). An idealized model and ship weight distribution was made. A comparison was made between the soil pressure distribution for a rigid model ship and for 2 levels of ship flexibility. The flexible solution allows greater soil stress; however, the amount of flexibility appears to be of minor effect for this case. The conclusion was that the ship flexibility should be considered but that an exact description of the ship flexibility is not critical.

Load Combinations and Failure Modes

It is important in an analysis of a drydock to have a firm understanding of the design concept used and the construction procedure. The following loading conditions must be considered:

1. Ship in basin flooded
2. Ship in basin empty
3. Superflooded condition
4. Rapid basin drawdown
5. Basin empty
6. Seismic loading
7. Seepage pressure (acting with above)

From an analysis viewpoint the following elements must be considered:

1. The soil stress distribution and amplitude around the structure
2. The nonlinear soil-structure interaction effects
3. The pore pressure and seepage pressure effects, on soil strength and structure pressures

Current engineering practice is limited in its ability to treat all these problems simultaneously in a single analysis. It is desired to utilize the best-suited techniques to analyze the highly complex nonlinear soil-structure interaction problem and to evaluate the capabilities of current available material models. It is essential to understand the sensitivity of the solution to variation in the input parameters and choice of model. Since the analytical solution can be used in conjunction with measured field data on drydock performance, the possible variation in computed solution must be understood.

The general types of loadings considered are shown in Figure 1. In general the following has been noted to occur. Case A imposes maximum wall moment. Case B imposes maximum uplift. Case C imposes maximum base bearing. Cases E and F impose maximum local floor shear and moment. Thus each case must be evaluated.

In general the following failure modes are possible:

1 Wall yielding
2. Floor failures under ship loading
3. Hydrostatic failure, resulting in either heaving or uncontrolled flooding

General Structural Analysis Procedures

The most common methods for analysis of a structure's seismic response are pseudostatic analysis procedures, response spectrum and time history dynamic analysis procedures. These methods are briefly outlined below.

Pseudostatic Methods Pseudo-static methods utilize dynamic characteristics of the structure and ductility features to estimate base seismic shear forces. These base shear forces are then applied to the structure in a static analysis to simulate dynamic behavior. This practical design approach has been utilized for many years and was the highly predominant choice before availability of modern computers. This design approach can

provide reliable results, provided good judgment is used in the selection of dynamic characteristics and ductility factors. Pseudo-static methods typically analyze the behavior of the structure independent of the soil-support system. Designer must exercise judgment in evaluating the impact of the soil-structure interaction. This is accomplished with a de-coupled design approach where soil deformations are taken into account using separate analysis.

Response Spectrum Method The response spectrum method is based on the normal mode method of analysis. The approach involves determining the design spectrum for the site, and entering the spectrum at the natural period of each significant mode of vibration in order to obtain the amplitude of response for that mode. For each given mode, this amplitude is used together with the mode shape and a modal participation factor (computed from the structure component weights and the mode shape) in order to obtain the structure's maximum response at any location for that mode. However, because these maximum responses from each mode will occur at different times, detailed approaches to evaluating and combining these responses are used. This approach is limited to elastic analysis.

Time History Method of Analysis The dynamic time history procedure is applicable to either linear or nonlinear structure models. Time history procedures compute the structure model's time-dependent response to input motion time histories, through numerical integration of the model's equations of motion. When applied with linear elastic models, the material properties represented in the model are unchanged throughout the duration of the ground shaking. However, if a nonlinear model is used, the material properties are updated to reflect effects of changing inelastic deformation during the ground motion. Under such conditions, a nonlinear time history analysis is more exact. A variation is the case where a soil-structure system is being modeled that contains significant soil-structure interaction, and the non-linear behavior of the soil is particularly important, a class of "equivalent linear" models that approximate the non-linear behavior of the soil is sometimes used.

Drydock Soil-Structure Interaction

The seismic response of a drydock is affected by the interaction of the structure with the surrounding and underlying soil, both soil and structure responding to the seismic ground motion. This is a complex phenomenon and represents a number of different elements or components. One basic component resulting from the size of the drydock is the change in the seismic waves when they interact with an inclusion in a propagating medium. This is initiated when incident seismic waves propagating away from the causative fault and through the geologic media encounter a drydock whose inertial and stiffness characteristics differ from those of the surrounding soils. As these incident ground waves strike the structure/foundation, they are reflected and refracted. The resulting motions of the foundation generate inertia forces and motions throughout the overlying structure, which further alter the motions of the foundation and the surrounding

soil. Soil structure interaction also represents the coupling effect of the structure to the surrounding soil through a mass and stiffness effect. This is prevalent in soil retaining structures such as quaywalls and drydocks. The lateral stiffness of structural elements embedded in the soil such as piles is another example of a case where the fundamental response of the structure is influenced by the lateral stiffness of the supporting soil.

This dynamic process can have several effects on the response of the structure. First, it alters the motions, stresses, and deformations in the soil relative to free field conditions away from the structure. Second, a structure founded on soil will respond as a softer dynamic system with a longer natural period than that of the same structure founded on rock. Finally, the dissipation of part of the structure's vibrational energy by hysteric action of the soil and by the radiation of waves away from the structure will increase the structure's effective damping. The potential significance of each effect, and whether the combined effects actually increase or decrease the seismic response of the structure, will depend on many factors related to: (a) the amplitudes, wavelengths, directions of approach, and relative phasing of the incident seismic waves; (b) the stratigraphy and material properties of the site soil materials; and (c) the configuration, stiffness, mass, and damping characteristics of the structure and its foundation.

Coupled vs. Uncoupled Model Structural analysis models are available that can provide an integrated analysis of both soil and structure systems simultaneously. These are termed "coupled" or "integrated" analyses tools. The alternative approach to soil structure coupled analysis is an iterative approach using different tools to model the soil and structure separately, and then make adjustments and rerun each model based on the results of the opposite model. This "uncoupled" approach is commonly used. When the analysis includes non-linear systems, the coupled approach becomes more complicated, and less used.

General Methods of Analysis for Drydocks

Several different methods can be used for seismic dynamic analysis of a drydock. These methods range from spring-dashpot models to continuum (boundary element) or finite element models of the foundation and underlying soil medium (e.g., see summary by Werner, 1991 The following is intended to be a brief summary of the approaches. Many examples of the current technology for substructure and direct methods of dynamic analysis are available as computer programs. These programs encompass a range of methodologies, are established and well documented in the technical literature, and have typically been used to provide analytical correlations in major soil structure interaction test programs emanating from the study of nuclear power plants. The following is based on the ASCE Seismic Guidelines for Ports of which this writer was a member of the committee which produced that document.

Spring-Dashpot Methods In these methods, the stiffness of the foundation-soil system is represented as equivalent springs and the damping of the system as equivalent dashpots, in which separate sets of springs and dashpots can be associated with horizontal translation,

vertical translation, rocking rotation, and torsional rotation of the foundation. The traditional beam-on-elastic foundation approach can model a drydock wall or floor.

Equivalent Linear Finite Element Use of the program SHAKE is the most common approach for computing 1-dimensional soil amplification of a level ground representation of a soil profile. Two-dimensional codes based on this concept are used to include the presence of a structure. FLUSH and SASSI are two such computer analysis tools. The equivalent linear procedure uses a nonlinear material model which is a function of the strain level. The actual material properties selected for use are based on the average level of strain in the response. Once the strain level is established, a set of elastic material properties is computed from the nonlinear material model at the established strain level. The soil-structure is then analyzed by elastic analysis.

The FLUSH Code (Lysmer et al., 1975) uses a direct method of analysis of a two-dimensional finite element soil-structure system representation with an equivalent linear model of horizontally layered soils on a rigid base, and seismic input motions from vertically propagating shear waves. It approximates out-of-plane radiation damping effects through the use of in-plane dashpots attached to each soil node point. For many years, FLUSH has been among the most widely used SSI analyses procedures in engineering practice. An advanced version of FLUSH (named SUPERFLUSH) has been developed that has several new features, including accommodation of simultaneous horizontal and vertical excitations, traveling wave effects, and non-horizontal soil layers and topography (Udaka, et al., 1981).

The CLASSI Program (Luco and Wong, 1982 and 1987; Luco et al., 1988a) employs a substructure approach in conjunction with a general three-dimensional structural model and a boundary element approach to compute foundation-soil impedances for a linear viscoelastic and horizontally layered soil medium. The superstructure properties used as input to CLASSI are its fixed base modes of vibration, which are computed externally by any arbitrary structural analysis program. Originally developed to accommodate rigid surface foundations of arbitrary shape, CLASSI can now also accommodate deformable surface foundations, embedded rigid foundations of arbitrary shape, and embedded deformable foundations of cylindrical shape, as well as spatially random input motions from arbitrarily incident seismic waves.

The SASSI Program (Lysmer et al., 1981; Ostadan, 1983; Tabatabaie et al., 1982; Bechtel, 1991) is a three-dimensional finite element program for SSI analysis of a structure located on or within horizontal soil layers with equivalent linear material properties, and subjected to input motions from arbitrarily incident seismic waves. It uses a substructuring method termed the flexible volume method, in which the excavated soil that is replaced by the foundation is modeled and subtracted from the structure, and the SSI is assumed to occur over a volume rather than at the boundaries of the foundation. This simplifies the computation of the foundation-soil impedance matrix, and eliminates the need for a separate analysis to obtain foundation input motions that include scattering effects. The equivalent linear model in SASSI cannot be automatically iterated after each

dynamic analysis run; rather, this iteration must be accomplished manually. Also, SASSI uses octahedral strain as the strain ordinate in its equivalent linear model.

The HASSI-8 Program (Katayama et al., 1991) is the latest in the HASSI family of programs which uses a hybrid model consisting of a three-dimensional finite element model of the structure and a near field segment of soil, and an analytical solution to represent the far field soil region. This latest version accommodates free-field motions from arbitrarily incident body waves, considers the site to be comprised of horizontally layered soils with an equivalent linear material model, and incorporates scattering effects into the computation of the foundation input motion The equivalent linear soil model in HASSI-8 is defined in terms of octahedral strain.

Linear Finite Element Linear finite element programs have been in use since the 1960's. SAP was one of the early programs used. Much of the development work was in support of nuclear power plant design.

Nonlinear Finite Element General purpose nonlinear finite element computer codes have existed for over thirty years starting with such early codes as NONSAP. Other more recent codes include ADINA and ABBACUS, LINOS and TRANL. These codes have a family of material models included which range from bilinear models to curved stress strain models. More complex soil models include models which represent two and three dimensional failures surfaces such as the cap model, the bounding surface plasticity model and numerous others. In each of these cases a set of constitutive relationships is used to define the strain/deformation to the stress state. The analytical solution process utilizes a time step integration procedure which divides the loading into a number of time step increments.

The TRANL Program (Baylor et al., 1974; Isenberg et al., 1978) is a fully nonlinear three-dimensional finite element program that incorporates nonlinear material models for the continuum and structural elements, debonding and rebonding along the soil-structure interface, and large deformations. It uses a 'soil island" approach in which free field ground motions corresponding to any desired combination of incident seismic waves are computed along a fictitious boundary enclosing a volume of soil (termed the soil island) that surrounds the location of the structure. Then, the structure is inserted into this soil island, the above free field motions are applied along the boundaries of the island, and the seismic response of the soil-structure system is computed. TRANL does not have wave-transmitting boundaries; therefore, the size of the soil island must be sufficiently large to minimize the interference of back reflections from the boundaries.

In addition to the above programs other significant efforts have been directed toward the development of nonlinear SSI analysis procedures. Examples of such efforts are (a) the use of nonlinear constitutive models based on mathematical functions, mechanical models, or plasticity theory (e.g. Pyke, 1979; Vaughn and Isenberg, 1983); (b) discrete element methods using finite difference equations applied to a network of material zones to approximate the differential equations of motion for a continuum (Cundall,

1976); (c) the use of nonlinear soil models coupled with pore water pressure models within an effective stress framework, in order to incorporate pore pressure effects during the seismic analysis of the soil medium (Finn, 1990; Prevost, 1981; NRC, 1985); and (d) the use of boundary elements for an elastic layered far field region together with a nonlinear model of the soil and structure near-field region (Wolf and Darbe, 1984 and 1986). It is noted that the above referenced work of Prevost, Cundall, and Finn has been used primarily to assess pore pressure effects and the stability of soil deposits, earth structures, and retaining-structure/soil systems (e.g., Roth et al., 1991), and have not yet been widely applied to SSI analyses for critical buildings, tanks, etc.

Nonlinear Effective Stress Finite Element/Finite Difference The generation of porewater fluid pressure is a controlling factor in the occurrence of liquefaction. The inclusion of porewater pressure in a total stress calculation to determine the actual stress state in the soil itself is termed an "effective stress analysis" Over the last decade progress has been made in effective stress analysis by inclusion of specific element degrees of freedom to track the porewater pressure. These computer analysis programs have complex nonlinear material models which are capable of representing the nonlinear shear and volumetric behavior of soil such as to not only predict the deformation state but also the porepressure changes. Both finite element and finite difference procedures are used for problem solution. Computer programs include DYNAFLO, DESRA, and FLAC among others.

The Effective Stress Finite Difference Code FLAC

FLAC is a two-dimensional explicit finite-difference program which can simulate the behavior of structures built of soil, rock or other materials that undergo plastic flow when their yield limits are reached. Materials are represented by polyhedral elements within a two-dimensional grid that is adjusted by the user to fit the shape of the object to be modeled. Each element behaves according to a prescribed linear or non-linear stress/strain law in response to applied forces or boundary restraints. The material can yield and flow, and the grid can deform (in large-strain mode) and move with the material that is represented. The explicit, Lagrangian, calculation scheme and the mixed-discretization zoning technique used in FLAC ensure that plastic collapse and flow are modeled accurately. Because no matrices are formed, large calculations can he in made without excessive memory requirements. The drawbacks of the explicit formulation (i.e., small time step limitation and the question of required damping) are overcome by automatic inertia scaling and automatic damping that does not influence the mode of failure.

Both finite difference and finite element methods translate a set of differential equations into matrix equations for each element, relating forces at nodes to displacements at nodes. Although FLAC equations are derived by the finite difference method, the resulting element matrices, for an elastic material, are identical to those of the finite element method (for constant strain tetrahedra). FLAC differs in the following respects.

1. The "mixed discretization" scheme is used for accurate modeling of plastic Collapse loads and plastic flow. This scheme is believed to be physically more justifiable than the "reduced integration" scheme commonly used with finite elements.

2. The full dynamic equations of motion are used, even with modeling systems that are essentially static. This enables FLAC to follow physically unstable processes without numerical distress.

3. An "explicit" solution scheme is used (in contrast to the more usual implicit methods). Explicit schemes can follow arbitrary nonlinearly in stress/strain laws in almost the same computer time as linear laws, whereas implicit solutions can take significantly longer to solve nonlinear problems Furthermore, it is not necessary to store any matrices, which means that (a) a large number of elements may be modeled with a modest memory requirement, and (b) a large-strain simulation is hardly more time-consuming than a small-strain run, because there is no stiffness matrix to be updated.

There are two disadvantages. Linear simulations run longer with FLAC than with equivalent finite element programs. FLAC is most effective when applied to non-linear or large-strain problems, or to situations in which physical instability may occur. The solution time with FLAC is determined by the ratio of the longest natural period to the shortest natural period in the system being modeled. Certain problems are very inefficient to model (e.g., beams, represented by solid elements rather than structural elements, or problems that contain large disparities in elastic moduli or element sizes).

Basic Features FLAC offers a wide range of capabilities to solve complex problems in geomechanics. FLAC has special numerical representations for the mechanical response of geologic materials. The program has ten built-in material models: the "null" model, three elasticity models (isotropic, transversely isotropic and orthotropic elasticity), and six plasticity models (Drucker-Prager, Mohr-Coulomb. strain-hardening/softening, ubiquitous-joint, bilinear strain-hardening/softening ubiquitous-joint. and modified Cam-clay). Each zone in a FLAC grid may have a different material model or property, and a continuous gradient or statistical distribution of any property may be specified. Additionally, an interface, or slip-plane, model is available to represent distinct interfaces between two or more portions of the grid. The interfaces are planes upon which slip and/or separation are allowed, thereby simulating the presence of faults, joints or frictional boundaries. The code has for types of structural elements: beam, cable, pile and shell.

Boundary conditions and initial conditions can be specified. Either velocity (and displacement) boundary conditions or stress (and force) boundary conditions may be specified at any boundary orientation. Initial stress conditions, including gravitational loading, may also be given, and a water table may be defined for effective stress calculations. All conditions may be specified with gradients.

FLAC incorporates the facility to model confined groundwater flow and pore-pressure dissipation, and the full coupling between a deformable porous solid and a viscous fluid flowing within the pore space. The fluid is assumed to obey the isotropic form of Darcy's law. Both the fluid and the grains within the porous solid are deformable. Non-steady flow is modeled, with steady flow treated as an asymptotic case. Fixed pore pressure and constant-flow boundary conditions may be used, and sources and sinks (wells) may be modeled. The flow model can also be run independently from the mechanical calculation. All zones are assumed to be fully saturated, so problems involving phreatic surfaces cannot be modeled.

Dynamic analysis can be performed with FLAC using the dynamic-calculation module. User-specified acceleration, velocity or stress waves can be input directly to the model either as an exterior boundary condition or an interior excitation to the model. FLAC contains absorbing and free-field boundary conditions to simulate the effect of an infinite elastic medium surrounding the model. The dynamic calculation can be coupled to the groundwater flow model.

FLAC Soil Model Properties

Mohr-Coulomb Relation The basic criterion for material failure in FLAC is the Mohr-Coulomb relation, which is a linear failure surface corresponding to shear failure:

$$f_s = \sigma_1 - \sigma_3 N_\phi + 2c(N_\phi)^{1/2}$$

where

N_ϕ $= (1 + \sin\phi) / (1 - \sin\phi)$
σ_1 = major principal stress (compressive stress is negative),
σ_3 = minor principal stress,
ϕ = friction angle, and
c = cohesion.

Shear yield is detected if $f_s < 0$. The two strength constants, ϕ and c, are conventionally derived from laboratory triaxial tests. The Mohr-Coulomb criterion loses its physical validity when the normal stress becomes tensile but, for simplicity, the surface is extended into the tensile region to the point at which σ_3 equals the uniaxial tensile strength, σ_t . The minor principal stress can never exceed the tensile strength, f_t. tensile yield is detected if f_t is greater than zero.

Drucker-Prager Relation Drucker-Prager strength parameters can be estimated from cohesion and friction angle properties. For example, assuming that the Drucker-Prager

failure envelope circumscribes the Mohr-Coulomb envelope, the Drucker-Prager parameters q_ϕ and k_ϕ are related to ϕ and c by

$$q_\phi = \frac{6}{\sqrt{3}(3(-\sin\ \phi)}(\sin\ \phi)$$

$$k_\phi = \frac{6}{\sqrt{3}(3(-\sin\ \phi)}(c\cos\ \phi)$$

Post-failure Properties In many instances, particularly in mining engineering, the response of a material after failure has initiated is an important factor in the engineering design. Consequently, the post-failure behavior must be simulated in the material model. In FLAC, this is accomplished with properties that define four types of post failure response:

(1) shear dilatancy;
(2) shear hardening / softening;
(3) volumetric hardening / softening; and
(3) tensile softening.

These properties are only activated after failure is initiated, as defined by the Mohr-Coulomb relation or the tensile-failure criterion. Shear dilatancy is simulated with the Mohr-Coulomb, ubiquitous-joint and strain-softening Mohr-Coulomb and ubiquitous-joint models. Shear hardening / softening is simulated with the strain-softening Mohr-Coulomb and ubiquitous-joint models, and volumetric hardening / softening is simulated with the modified Cam-clay model. Tensile softening is simulated with the strain-softening Mohr-Coulomb and ubiquitous-joint models.

Shear Dilatancy Shear dilatancy, or dilatancy, is the change in volume that occurs with shear distortion of a material. Dilatancy is characterized by a dilation angle, ψ, which is related to the ratio of plastic volume change to plastic shear strain. This angle can be specified in the Mohr-Coulomb ubiquitous joint and strain-hardening / softening models in FLA3D. Dilation angle is typically determined from triaxial tests or shear-box tests. The dilation angle is found from the plot of volumetric strain versus axial strain. The initial slope for this plot corresponds to the elastic regime, while the slope used to measure the dilation angle corresponds to the plastic regime. For soils, rocks and concrete, the dilation angle is generally significantly smaller than the friction angle of the material. Vermeer and de Borst observe that values for the dilation angle are approximately between 0 and 20 degrees whether the material is soil, rock, or concrete. The default value for dilation angle is zero for all the constitutive models in FLAC.

Shear Hardening / Softening The initiation of material hardening or softening is a gradual process once plastic yield begins. At failure, deformation becomes more and more

inelastic as a result of micro-cracking in concrete and rock and particle sliding in soil. This also leads to degradation of strength in these materials and the initiation of shear bands. In FLAC, shear hardening and softening are simulated by making Mohr-Coulomb properties (cohesion and friction, along with dilation) functions of plastic strain. These functions are accessed from the strain-softening model.

Volumetric Hardening / Softening Volumetric hardening corresponds to irreversible compaction; increasing the isotropic pressure can cause permanent volume decrease. This behavior is common in materials such as lightly cemented sands and gravels and overconsolidated clays.

Tensile Softening At the initiation of tensile failure, the tensile strength of a material will generally drop to zero. The rate at which the tensile strength drops, or tensile softening occurs, is controlled by the plastic tensile strain.

Liquefaction FLAC contains a built-in constitutive model (named the "Finn model") that incorporates a relationship between irrecoverable volume strain and shear strain into the standard Mohr-Coulomb plasticity model. The model captures the basic mechanisms that can lead to liquefaction in sand. In addition to the usual parameters (friction, moduli, etc.), the model needs the four constants. Martin et al. (1975) describe how these may be determined from a drained cyclic test. Alternatively, one may use some trial values to model an undrained test and compare the results with a corresponding laboratory test; the constants could then be adjusted to obtain a better match. In the Finn model there is logic to detect a strain reversal in the general case. In Martin et al. (1975), the notion of a strain reversal is clear, because they consider one-dimensional measures of strain. In a three-dimensional analysis, however, there are at least six components of the strain-rate tensor. Rules are used to locate extreme points in strain space. Once shear strain is computed the change in volume strain is computed. In particular, the number of "cycles" detected depends strongly on the relative magnitude of horizontal and vertical motion; hence, the rate of buildup of pore pressure will also be sensitive to this ratio.

Structural Modeling Considerations

An extremely important element of the seismic dynamic analysis of a structure is the development of a model that provides a reasonable representation of the structure's inertial, stiffness, and damping characteristics. For a pseudostatic analysis, only the stiffness characteristics of the structure (and the surrounding soil) is represented. Some fundamental considerations in the model development process are outlined below.

Inertia The inertia of a structure is typically represented by lumping the mass of the structure at discrete node points within the model, which also corresponds to locations of the model's dynamic degrees of freedom. If the structure's actual weight is concentrated at a few discrete locations, the masses are lumped at these locations, or where weight is

more nearly uniformly distributed within the structure, the lumped masses (and corresponding dynamic degree-of-freedom locations) are also more uniformly spaced.

Stiffness The stiffness of a structure is a quantity that is used to compute the internal forces in the structure if the displacements of the structure are known. For simple structures that can be represented as a single-degree-of-freedom system, the stiffness is represented as a spring constant that is multiplied by the displacement to obtain the internal force. For multi-degree-of-freedom systems, the structure's stiffness is represented as a stiffness matrix. If the non-linear behavior of the structure is to be represented in the dynamic analysis, the stiffness quantities will vary as a function of the level of deformation imposed within the structure at a given instant in time due to the seismic excitations.

The estimation of the stiffness characteristics for linear elastic structural elements can be readily obtained from elastic structural analysis theory in terms the elastic modulus and Poisson's ratio. For nonlinear structural elements, the stiffness characteristics are usually based on a bilinear model composed of an initial linear stiffness and a yield level. More complex nonlinear material models are available for concrete and soils. Generally, the seismic response of most structures will be nonlinear, because load levels are high, the nonlinear characteristics of the structural materials, and the surrounding soil materials exhibit nonlinear material behavior.

For many structures at ports where soft soils typically predominate, soil-structure interaction effects will be important and the presence of the soil will also be an important factor in estimating the overall stiffness of the structure for seismic analysis purposes. Because of the complexity of all of these characteristics in many structures, the estimation of the structure's stiffness characteristics is often not straightforward. Experience and sound judgment are important ingredients of the estimation of these characteristics.

Damping When a structure is subjected to any type of applied dynamic excitation (e.g., from wind, earthquake, vibrating machinery, etc.) and the excitation stops, the structure's motion during its free vibration will gradually reduce and eventually come to rest. The properties of the structure that cause this to occur are termed its energy dissipation characteristics. These same properties also play a major role in the structure's response to earthquake ground motions, and are related to the characteristics of the structural and non-structural elements and of the foundation-soil system.

Energy dissipation in the structure during strong earthquake shaking occurs from repeated cycles of elastic and inelastic loading and unloading. Example sources of energy dissipation within the structure are: (a) cracking of concrete and yielding of steel reinforcement in reinforced concrete members or connections; (b) yielding of steel members and/or connections; (c) friction in structural connections; and (d) movement, cracking, or yielding of non-structural elements. The structure's ability to absorb energy in these ways depends on the design and detailing of its members and connections and on their material properties. Of course, once a member fails in fracture or buckling, it can no

longer dissipate energy. Within the foundation-soil system, energy dissipation occurs during earthquake shaking due to the nonlinear behavior of the soil materials and also due to the radiation of waves away from the from the vibrating structure and foundation and through the underlying soil medium. These sources of energy dissipation depend on the foundation's configuration, embedment, and mass, and on the properties and stratigraphy of the underlying soil and rock materials.

Estimates of damping ratios for various types of structural elements have been developed by Newmark and Hall (1982). The most common design assumption is 5 percent of critical.

Static Drydock Analysis

The drydock located at the Naval Station, San Diego was chosen as a typical Navy drydock for analysis with the FLAC code. The drydock is fully hydrostatic with a base width of about 92 feet and depth of about 42 feet. A certification study was performed by Ferver Engineering Company in 1979 and the results of that study provided the source of information to define the geometry and material properties. Ferver Engineering Company performed a static analysis of the reinforced concrete wall and floor using soil density and a $k_0 = 0.5$. Figure 2 shows a cross-section of the drydock. For this study, the drydock was modeled by a series of structural beam elements with properties based on the cross-section. Initially the soil field was modeled as soil elements using the Mohr-Coulomb material model, Figure 3. The soil properties were based on the density and k_0 used in the Ferver report. Figure 4 shows the beam elements. Figure 5 shows the equilibrium horizontal soil stress and Figure 6 shows the vertical stress. Figure 7 shows the equilibrium pore water pressure.

The drydock was analyzed for the empty, flooded and docked-ship cases. Ship loads for an AD37 ship appeared to be a severe case based on the Ferver report. The results of the static case are shown in Figure 8 for the drydock wall and Figure 9 for the floor. The wall and floor ultimate capacities are taken from the Ferver report. These were not verified as part of this study. It is interesting to note that the flooded case produces the least stress condition by counter-balancing the soil forces. The floor moments are influenced by the wall loading. Worst case factors of safety under static loads are about 1.6.

A soil profile representative of the properties of the site was defined based on the best available but very limited information contained in the Ferver report. Figure 10 is the closest soil boring log representative of the site. The soil profile shown in Figure 10 was used to establish the material properties and zones for use in the analysis. The water table was at a depth of about 7 feet. The top two layers were medium dense cohesionless material which could liquefy; the Finn material model was used to model these layers. The next layer below was a clay layer modeled using the Mohr-Coulomb material model. The next 2 layers were very dense to medium dense sands which could show some pore water

pressure increase and were modeled using the Finn material model. The remaining layers were dense clays and sands and were modeled using the Mohr Coulomb material model. The analysis loading cases were repeated and the results are shown in Figures 11 and 12. As can be seen the more accurate representation of the material properties characterized in the FLAC analysis results in a lower assessment of the loadings on the wall and floor. The more detailed analysis is better able to capture the soil stiffness and load distribution. This subsequently results in factors of safety are in the range of over 1.7.

Dynamic Analysis – Soil Column

A grid was established for modeling a depth of 100 feet based on the soil profile and material models discussed above . The grid layers, Figure 13, were set to correspond to the soil layers in the boring log. The vertical sides of the grid were bounded by free-field elements to simulate an infinite boundary. Horizontal acceleration consisting of 12 seconds of the El Centro earthquake scaled to 0.2g was applied along the base, Figure 14. The results indicate that the motion was initially amplified until liquefaction of the upper layers occurred and the surface motion subsided, Figure 15. The top layer reached a level of zero confinement, Figure 16, and the next layer experienced a significant reduction in confinement, Figure 17. The clay layer saw an increase in pore water pressure, Figure 18.

Dynamic Analysis – Drydock wall

The drydock wall was modeled using beam elements and typical loose cohesionless soil material properties. This case was meant to directly analyze the assumed conditions used in the Ferver drydock certification study. Figure 19a shows the idealized grid and Figure 19b shows the El Centro acceleration record. Figure 20 shows the maximum moment at the base of the drydock wall. The upper figure is from an analysis in which the wall was modeled as elastic and it can be seen that the response exceeds yield at several points. The lower figure is from an analysis in which the wall was modeled elasto-plastic. Figures 21 a and b show the effective vertical stress in the soil at various depths. Figures 22a and b show the average effective confining stress and Figures 23a and b show the pore pressure. As can be seen there is a significant drop in confining stress. If liquefaction is defined as zero average effective stress then full liquefaction occurred in the top 20 feet and near liquefaction in the remainder. This analysis compares favorably to the computations in drydock certification study. Both show that if liquefaction occurs the moment in the wall will exceed yield levels. This analysis further shows that the occurrences of yielding are controlled. The analysis however uses a generic soil property which can be improved by a more accurate assessment of the soil profile as shown above in the soil column studies and not possible in the closed form certification study.

Dynamic Analysis – Drydock Structure

The drydock model shown in Figure 11 was subjected to 12 seconds of shaking using the El Centro earthquake record. Figure 24 shows the moments at the base of the wall and the center of the floor for the drydock empty case. The wall moment reaches approximate yield levels briefly on two occasions. This response is categorized as at the onset of yielding under controlled conditions which do not lead to excessive deformation. Figure 25 shows the vertical stress contours and Figure 26 shows the horizontal stress contours. Figure 27a shows the average effective stress in the soil for the top two layers. Full liquefaction occurs in the top layer. The actual soil profile has a medium dense second layer and a non-liquefying clay third layer. Layers below these are medium to very dense. The actual soil profile produces less pore pressure development than generic loose soil assumptions which would be expected. Figure 27b shows the average stress in the grid at the corner of the drydock wall and floor intersection. Liquefaction occurs briefly at this location.

The analysis was repeated for the case of the drydock with a ship. Figure 28 Shows the moments in the wall and floor. The wall response approaches yield levels on three occurrences but the response is controlled. Three different earthquake records were used:

1966 Parkfield M 6.1 Cholame, Shandon, California Array No. 2
1940 El Centro M 6.9 Imperial Valley Irrigation District
1984 Morgan Hill M 6.1 Gilroy #4

The results of the three earthquakes scaled to 0.2g bedrock motion were quite similar and only the results of the El Centro earthquake are reported. In addition to the use of the Finn soil model discussed above, an additional soil model attributed to Seed was used. This model used standard penetration blowcounts for estimating soil properties. Results were similar to the Finn model, although data preparation was facilitated.

Limitations In Analysis

The material properties used in this analysis were estimated based on the boring log shown in Figure 10. The only information available was the soil layer description and blow count data for the upper 40 feet. From this information the shear and bulk modulus, friction angle, cohesion, and dilation angle were estimated. The lack of detailed soil properties limits the analysis. No information on soil damping was available. To offset this limitation soil properties were varied over a wide range and results were not appreciably affected.

The load level used in the study was a base (100-ft deep level) acceleration of 0.2g which was amplified by the soil properties to about 0.6g at the surface. Variation of damping levels was not performed. This level of motion corresponds to an earthquake with a 50 percent probability of exceedance in 50 years exposure.

Discussion of Results

The results of this study show that the drydock has adequate factors of safety for the static loads considered. This is in agreement with the drydock certification study. This analysis shows the drydock to be at yield levels during dynamic earthquake loading. The levels of liquefaction are limited and controlled. The response of the drydock is controlled. The FLAC analysis is able to better represent the actual loading conditions on the drydock than the traditional hand calculations performed in the drydock certification studies. As a result the more accurate FLAC analysis shows a lower level of loading both under static and dynamic conditions. It is important to note the limitation in this study which involved gross estimating of soil material properties. To minimize these limitations the soil properties were varied over a wide range and the results did not change appreciably.

It is interesting to note that the weight of the drydock walls and the high static pore pressure acting on the underside of the floor causes concave bending of the floor. Loads resulting from drydock flooding or the presence of a ship tend to offset this concave bending.

The nature of the seismic shaking causes drydock wall and floor deformations which tend to cause volumetric expansion in the soil immediately surrounding the drydock. As the walls deform away from the soil, the soil tends to stretch to fill the void. The tendency toward volumetric expansion results in a tendency toward reduction in pore pressure. This is evidenced by reduction in pore pressure contours as shown in Figure 29. To further examine the validity of this phenomenon, half of the drydock was modeled as a generic structure. Figure 30 shows the pore pressure is reduced in the vicinity of the vertical wall. Figure 31 shows the magnified deformation pattern showing the settlements resulting from the shaking in the soil backfill. This soil movement in the form of volumetric expansion produces a tendency toward reduced pore pressures in the vicinity of the drydock wall. This occurrence would have the effect of stabilizing the soil and limiting liquefaction occurrence. The occurrence of this phenomenon is a function of soil properties and wall flexibility. It probably can not be counted upon to occur in all cases and to be present during repeated earthquake loading and occurrences of liquefaction. Although experience has shown that post liquefaction effects on soils tend to make them more homogeneous and at an average density.

The above analyses were based on the conditions assumed in the Ferver drydock certification study – that the soil was at a k_0 value equal to 0.5. To evaluate the effect of higher k_0 which might be present a k_0 of 1.0 was used. Figure 32 shows the static moment in the drydock wall which is increased compared to the k_0 equal to 0.5 case. Figure 33 shows the static moments in the floor which are increased at the ends joining the walls and reduced at the center. The factor of safety of the drydock floor in the reduced section region joining the wall is about 1.0 under this condition. Figure 34 shows the dynamic moments in the wall and floor which are not substantially different than the k_0 equal to 0.5 case.

Figure 35 gives the probability of not exceeding acceleration levels for a 50-year exposure at the site in San Diego. From Figure 35, Figure 36 can be constructed which shows the distribution of probability for a bin size of 0.1g. The analysis was repeated at bedrock ground motion acceleration levels of 0.4g and 0.6g. The purpose of the addition cases was to be able to categorize damage over the life of the structure. In general the structure experienced some yielding at 0.4g and substantial yielding at 0.6g. Figure 37 has been developed from previous studies and forms a basis for evaluating damage as a function of earthquake return time. Five categories of damage are established ranging from Minimal to Collapse. Additionally limits of elastic behavior, repairability and no-collapse are identified. Figure 37 is intended as a broad generalization to translate engineering analysis results into terms which can be appreciated by managers interested in facility performance. Using the results of the FLAC analysis combined with engineering judgement Figure 38 was constructed. By combining the probability distribution in Figure 36 with the damage in Figure 38, the expected damage to the drydock over its 50-year life is expected to be 13 percent. Most of the exposure emanates from the 0 to 0.25g segment of seismic exposure. Response in this range is elastic with limited damage. Figure 39 plots damage for several return-time earthquakes. Figure 40 shows the range of the navy's new seismic criteria and other codes. In general the performance of the San Diego drydock is consistent with the new Navy criteria.

Suggested approach for Future Certification Studies

It is suggested that future drydock certification studies be planned around the use of the FLAC computer program. This would entail definition of the geometry of the drydock in sufficient detail to be able to generate the model. Soil test should be conducted in the vicinity of the drydock to define the site soil profile and establish the soil mechanical properties. A site seismicity study should be conducted to establish the levels of seismic ground shaking to be used in the analysis. Having adequately defined the drydock section properties, the soil material properties, and the level of loading, an accurate analysis can be conducted to establish factors of safety and reliability of operation.

Need for Additional Study

The following items need to be better defined:

- Procedures for estimating soil mechanical properties from boring logs.
- Effects of soil properties on drydock response
- Determination of which are the critical parameters affecting response
- Quantification of damping and effect of variation of damping on response
- Effect of material parameter variation in Finn soil model on pore pressure development
- Calibration of the Finn soil model against actual soil data
- Strength of drydock walls including tensile capacity
- Seismic criteria development for drydock certification

References

Baylor, J.L et al (1974). TRANL: A 3-D Finite Element Code for Transient Nonlinear Analysis. DNA-3501F, Weidlinger Associates, New York NY, June.

Bechtel (1991). SASSI Theoretical Manual. Bechtel Corporation, San Francisco CA.

C. A. Coulomb. "Esai sur une application des reyles des maximis at minimis a quelques problemes de statique," Memoires Academic Royal des Sciences, vol. 7, 1776.

Cundall, PA. (1976). Explicit Finite Difference Methods in Geomechanics', Second Conf. in Numerical Methods in Geomechanics. Blacksburg VA, June.

Electric Power Research Institute (EPRI) (1989). Proceedings: EPRI/NRC Workshop on Seismic Soil-Structure Interaction Analysis Techniques using Data from Lotung. Taiwan EPRI NP-6154, Vols. 1 and 2, March.

Finn, W.D.L (1990). "Analysis of Deformations, Stability, and Porewater Pressures in Port Structures', Proc. of Workshop on Seismic Safety Planning for Port of Los Angeles Vol., 3, Los Angeles CA, March.

Isenberg, J,, et al (1978). Nonlinear Soil-Structure Interaction. EPRI NP-941, Elec. Power Res. Inst., Palo Alto CA, Dec.

Katayama, I et al (1991). 'Wave Scattering Effect in Soil-Structure Interaction', Trans. of Eleventh Int. Conf. on Struct. Mech. in Reactor Technology (SMIRT-II' Vol. K. Tokyo, Japan, pp.153-158, Aug.

Luco, J.E. and Wong, H.L., (1982). 'Response of Structures to Nonvertically Incident Seismic Waves', Bull. of Seismol. Soc. of Amer.. Vol. 72, No.1, pp.265-302 Feb.

Luco, J.E. and Wong, H.L (1987). 'Seismic Response of Structures Embedded in a layered Half Space', J. of Earth Q. Eng. and Struct. Dyn., Vol.15, pp. 233-245, Feb.

Lysmer, J. (1965). Vertical Motion of Rigid Footings. Ph.D. Dissertation, Univ. of Michigan, Ann Arbor MI, Aug.

Lysmer, J. (1978). Analytical Procedures in Soil Dynamics UCB/EERC-78/29, Univ. of Calif., Berkeley CA, Earthquake Eng. Res. Ctr., Dec.

Lysmer, J., et al (1975). FLUSH. A Computer Program for Approximate 3-D Analysis of Soil-Structure Interaction Problems. EERC 75-30, Univ. of Calif., Berkeley CA, Earthquake Eng. Res. Ctr, Nov.

Lysmer, J. et al (1981). SASSI. A System for Analysis of Soil-Structure Interaction. UCB/GT81-02, Univ. of Calif.

Military Handbook 1025/1 Piers and Wharves 30 Oct. 1987

Military Handbook 1025/2 Dockside Utilities For Ship Service 1 May 1988

Military Handbook 1025/3 Cargo Handling Facilities 12 Sept. 1990

Military Handbook 1025/4 Seawalls, Bulkheads and Quaywalls 30 Sept. 1988

Military Handbook 1025/5 Ferry Terminals and Small Craft Berthing Facilities 12 Sept. 1990

Military Handbook 1025/6 General Criteria For Waterfront Construction 15 May 1988

National Research Council (1985). Liquefaction of Soils during Earthquakes National Academy Press, Washington, D.C.

Naval Civil Engineering Laboratory Report R939 "The Seismic Design Of Waterfront Retaining Structures" January 1993

Ostadan, F. (1983). Dynamic Analysis of Soil-Pile Structure Systems, Ph.D. Dissertation, University of California. Berkeley CA. May

Prevost J.(1981). DYNA-FLOW: A Nonlinear Transient Finite Element Analysis Program. Report 81-SM-1, Princeton University, Dept of Civil Engineering, Princeton NJ.

Pyke, R.M. (1979). 'Nonlinear Soil Models for Irregular Cyclic Loading', J. of Geotech. Eng.. ASCE. Vol. 11, No.6, pp. 715-726, June

W. J. Rankine. "On the stability of loose earth," Transactions Royal Society, London, vol. 147, 1857

Roth, W.H. et al (1991). 'Pleasant Valley Dam: An Approach to Quantifying the Effects of Foundation Interaction', Proc. of Seventeenth Int. Cont. on Large Dams ' Vienna, Austria, pp. 1199-1228,

Tabatabale, M. (1982). The Flexible Volume Method for Dynamic Soil-Structure Interaction Ph.D. Dissertation, University of California, Berkeley CA, Feb.

K. A. Terzaghi. "Fundamental fallacy in earth pressure computations," Journal of the Boston Society of Civil Engineers, vol. 23, 1936, p 71.

Udaka,T. et al(1981) 'Soil-Structure Analysis for Varying Seismic Environments and Boundary Conditions' Trans. of Sixth Int. Conf. on Struct. Mech. in Reactor Tech. Paper K3, Vol. K(a), Paris, France, Aug. 17-21.

Vaughn, D.K. and Isenberg, J. (1983). 'Non-Linear Rocking Response of Model Containment Structures', Earthq. Eng. and Struct. Dyn Vol.11, pp.275-296.

Wolf, J P and Darbe, G.R (1986). 'Nonlinear Soil-Structure Interaction Analysis based on Boundary Element Method in Time Domain with Application to Embedded Foundation', J. of Earthq. Ent. and Struct. Dyn Vol.14, pp 385-400, Jan.-Feb.

Yim, S. and Chopra, A.K. (1955). 'Simplified Earthquake Analysis of Multistory Structures with Foundation Uplift', J. of Struct. Ens. Div., ASCE. Vol.111, No.12, pp. 2708-2731, Dec.

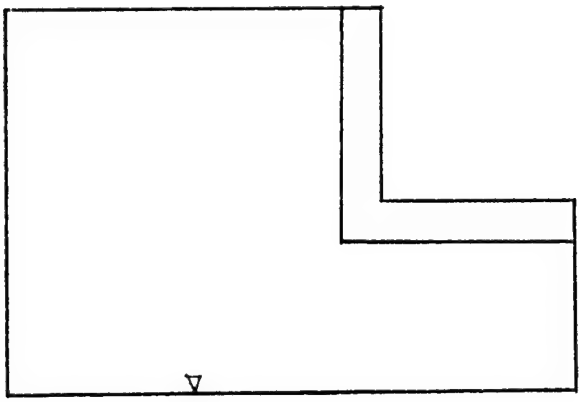

A

Soil density 120 lb/cu ft

Water pressure at base

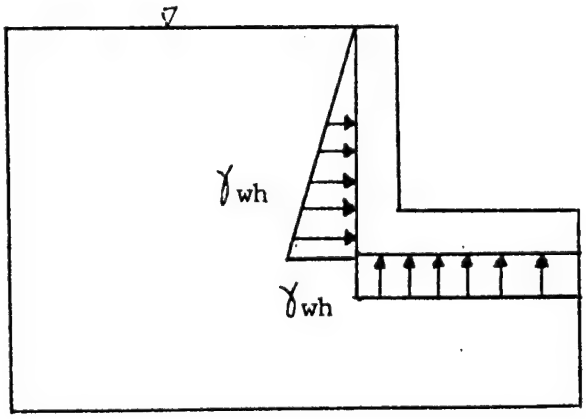

B

Soil density 57.6 lb/cu ft

Water pressure at surface

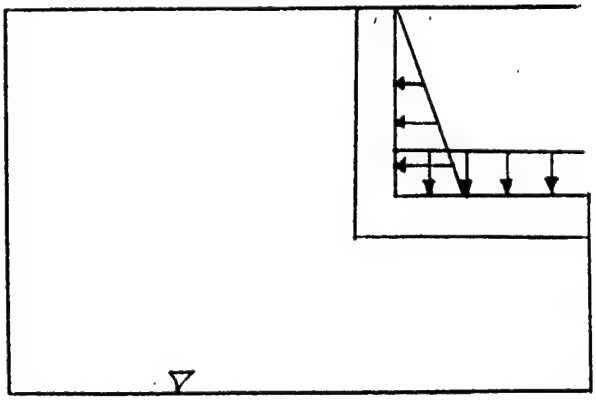

C

Soil density 120 lb/cu ft

Water pressure at base

Internal water pressure

flooded or superflooded

Figure 1. Drydock loading cases.

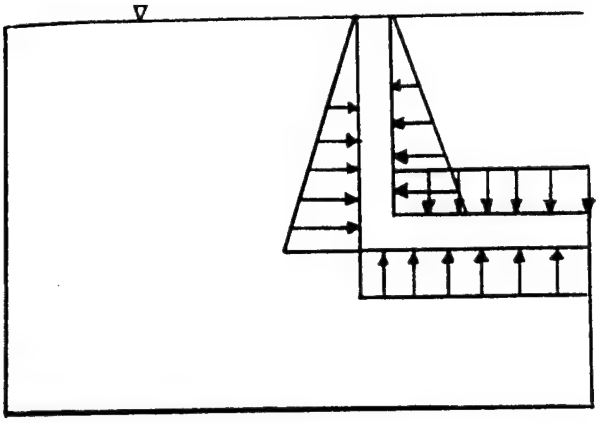

D

Soil density 57.6 lb/cu ft

Water pressure at surface

Internal water pressure

Flooded or superflooded

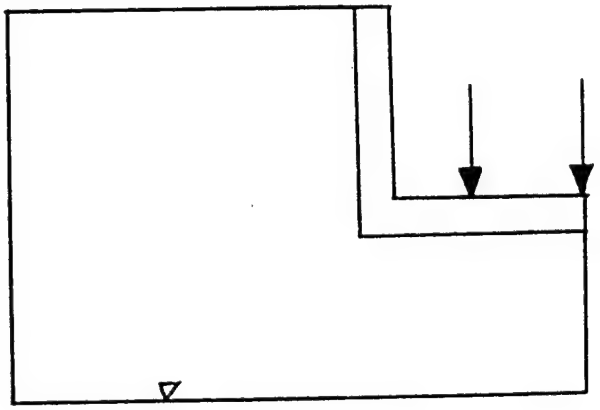

E

Soil density 120 lb/cu ft

Water pressure at base

Ship load through blocking

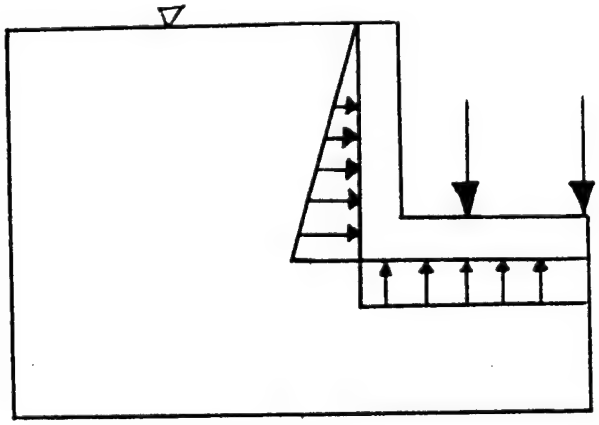

F

Soil density 57.6 lb/cu ft

Water pressure at surface

Slip load through blocking

Figure 1. Continued.

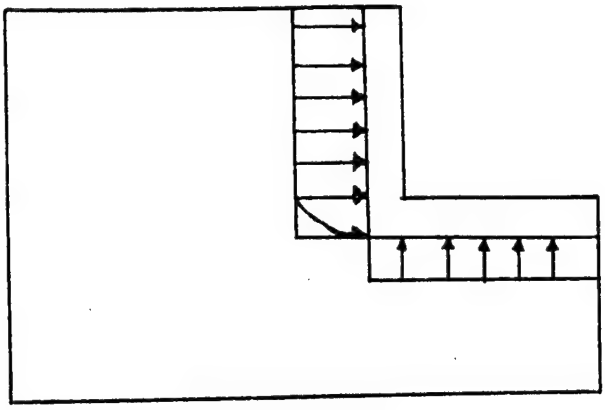

Liquefaction

Approximate Analysis

Soil Density 57.6

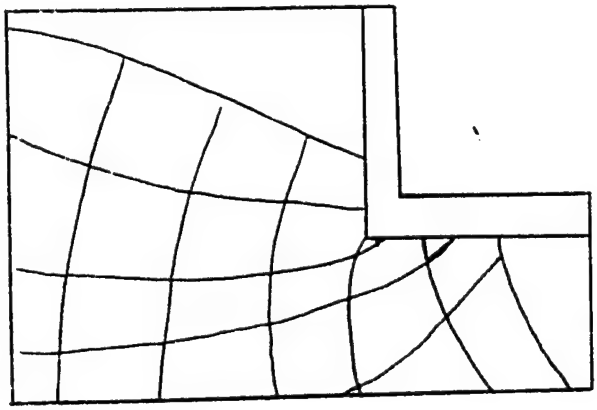

Partial Drawdown

from Seepage Analysis

Figure 1. Continued.

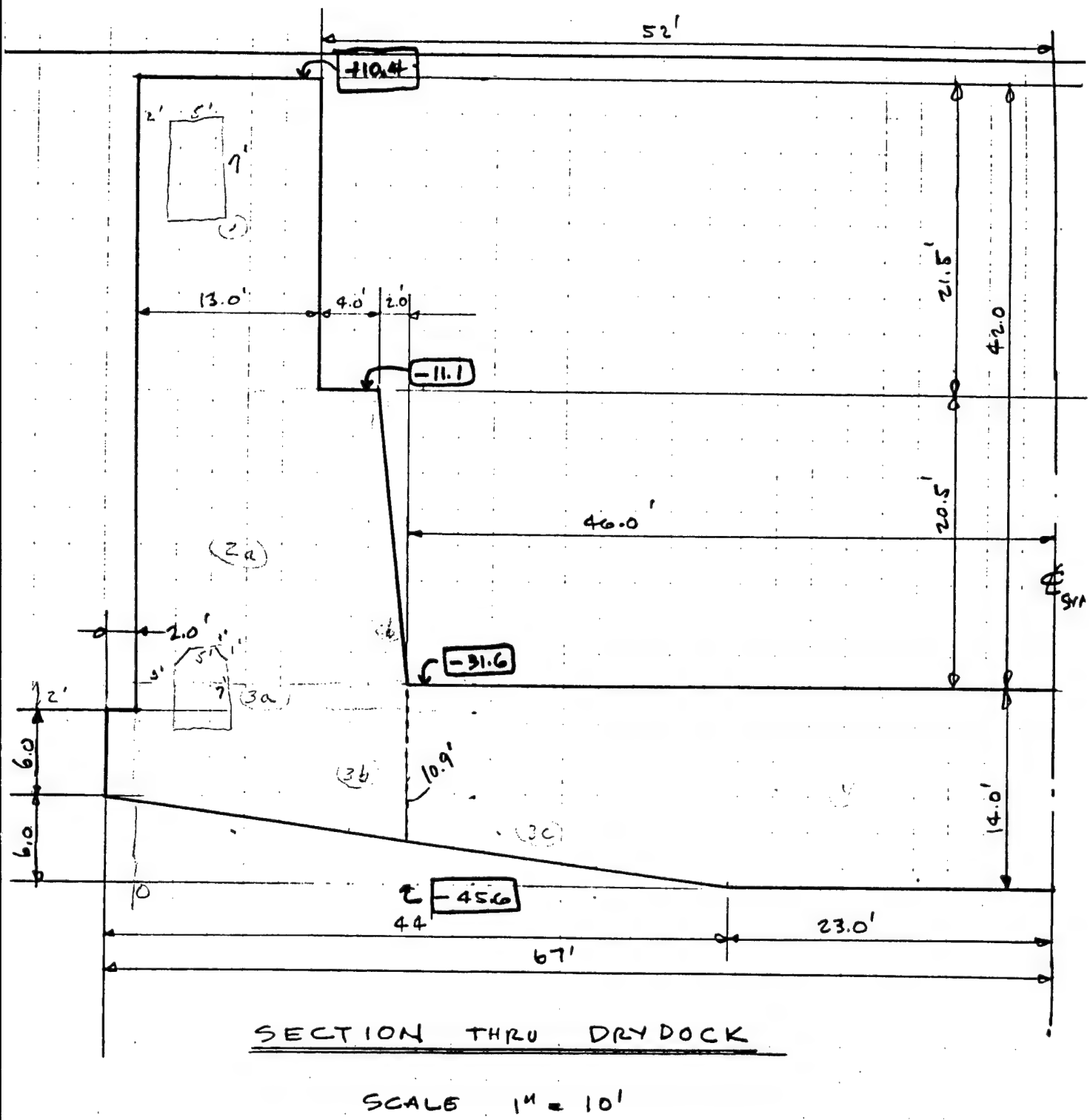

Figure 2. Naval Station, San Diego, drydock cross-section.

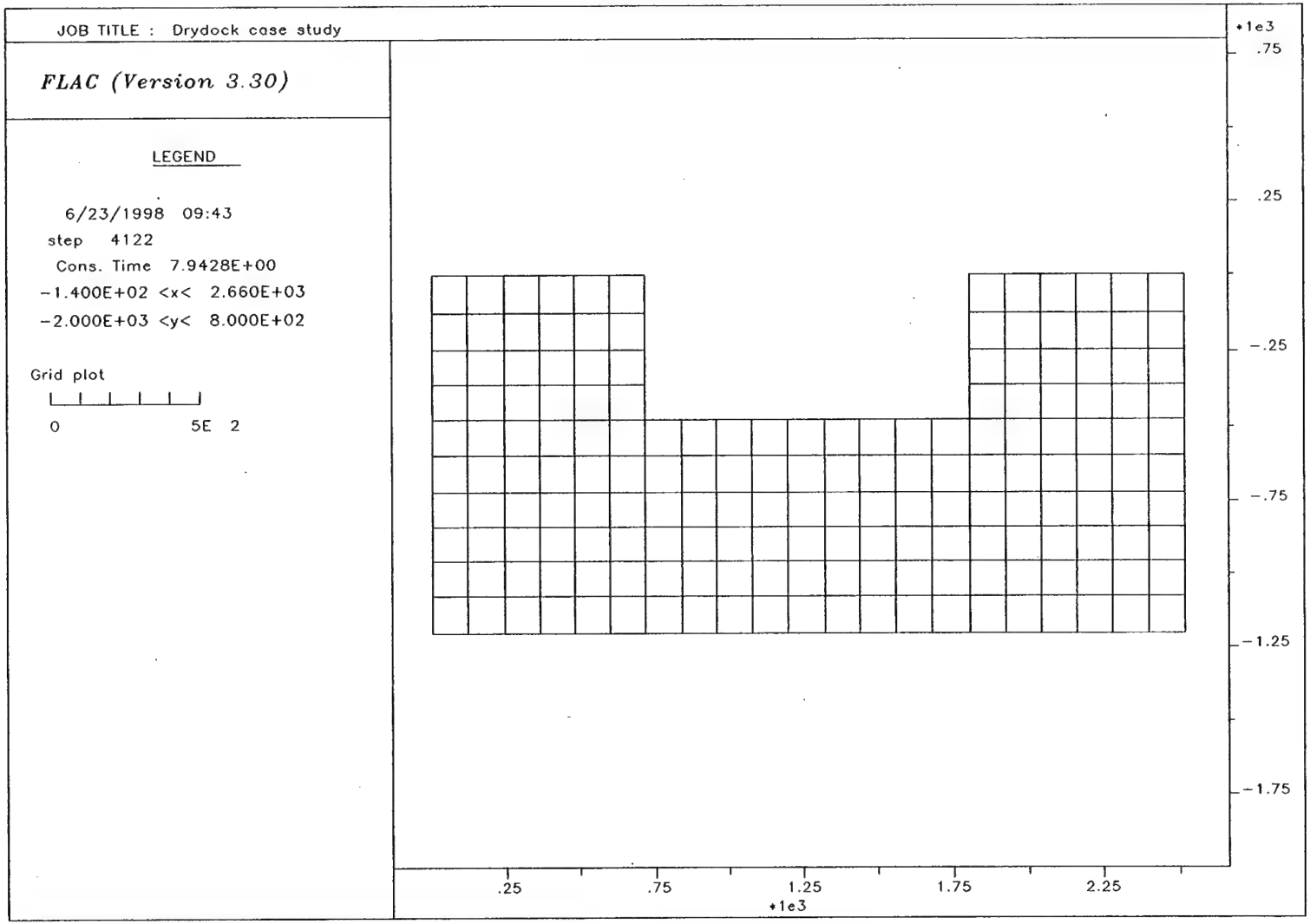

Figure 3. FLAC grid for drydock analysis.

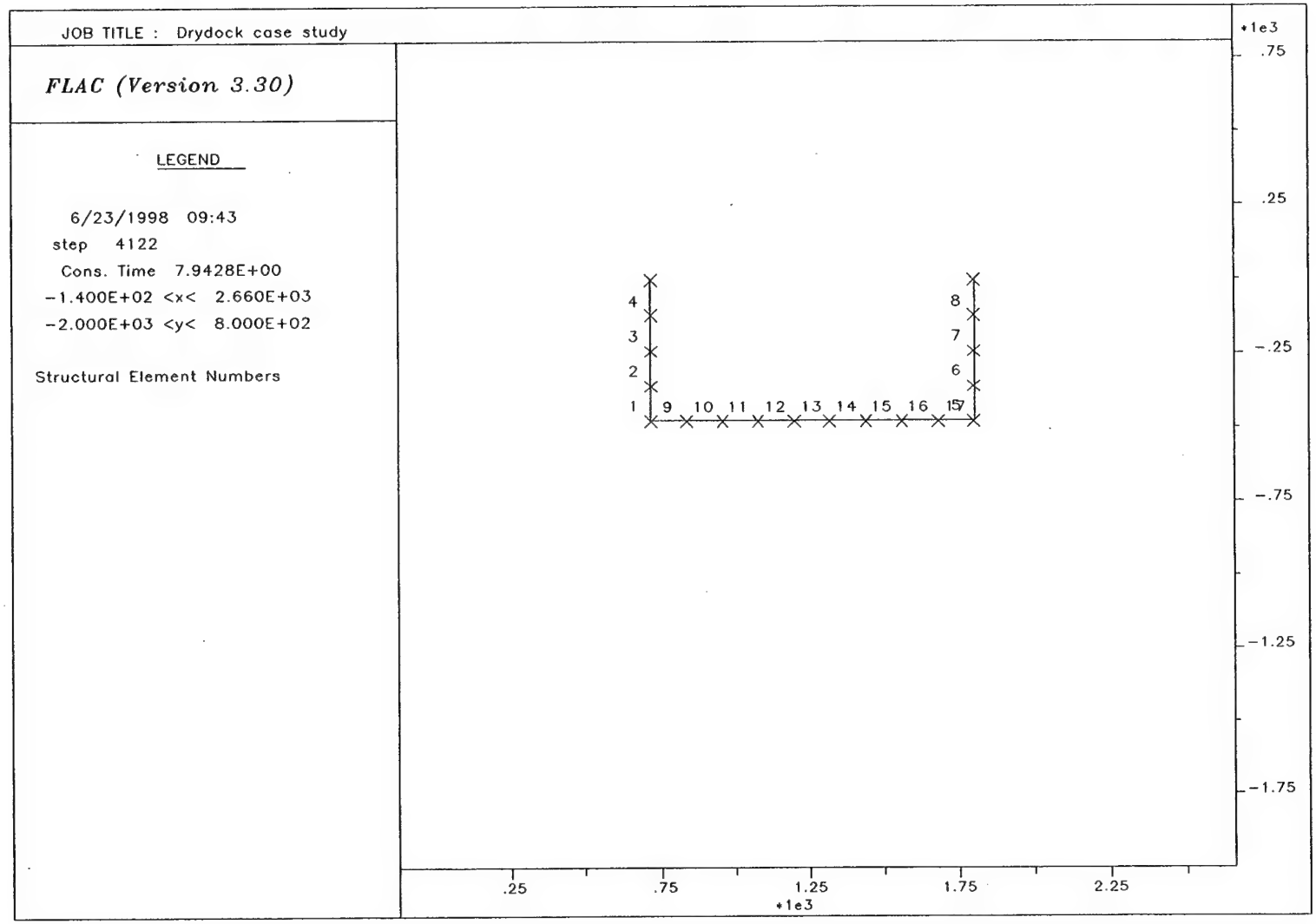

Figure 4. Drydock structure elements.

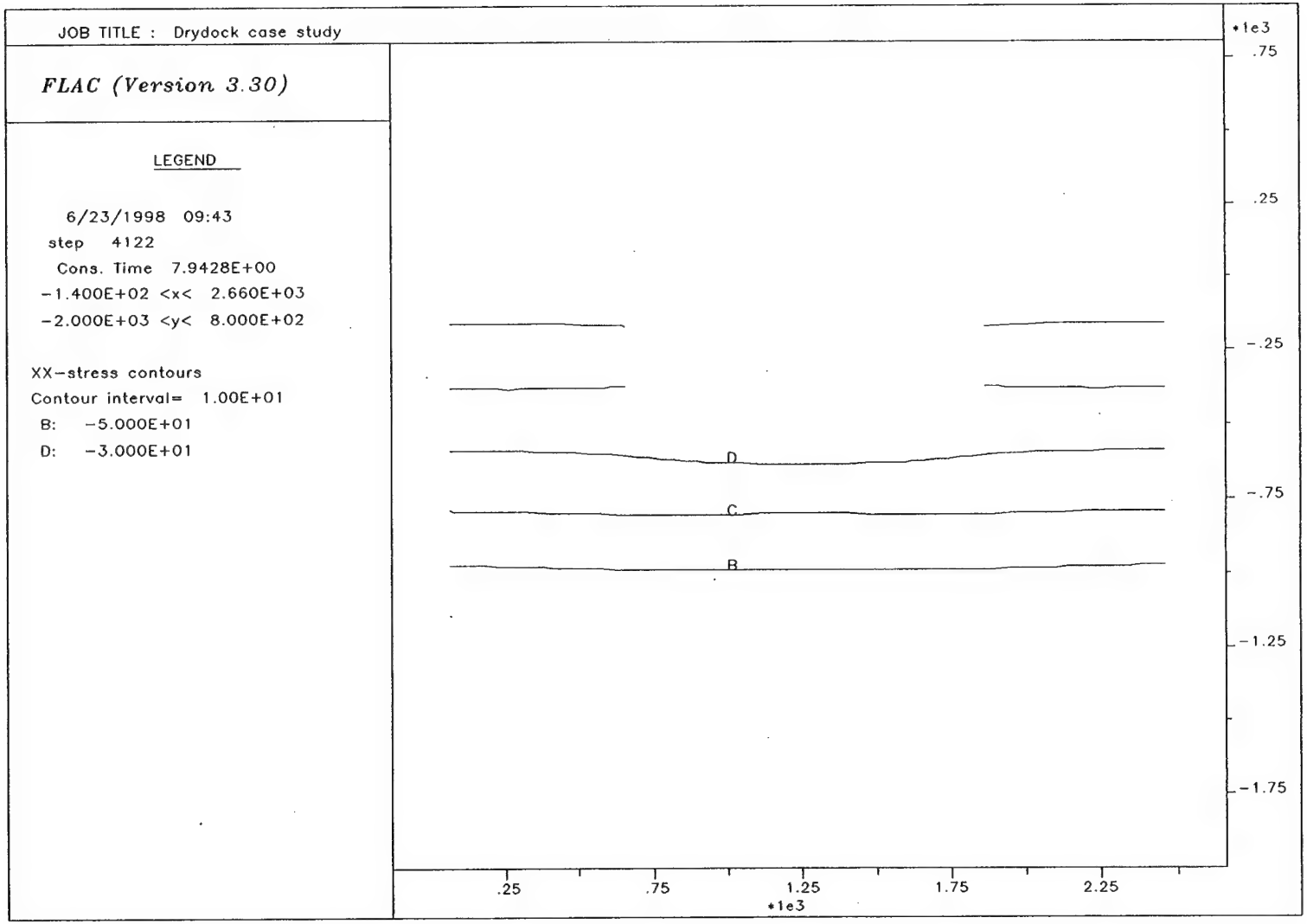

Figure 5. Sxx, horizontal soil stress.

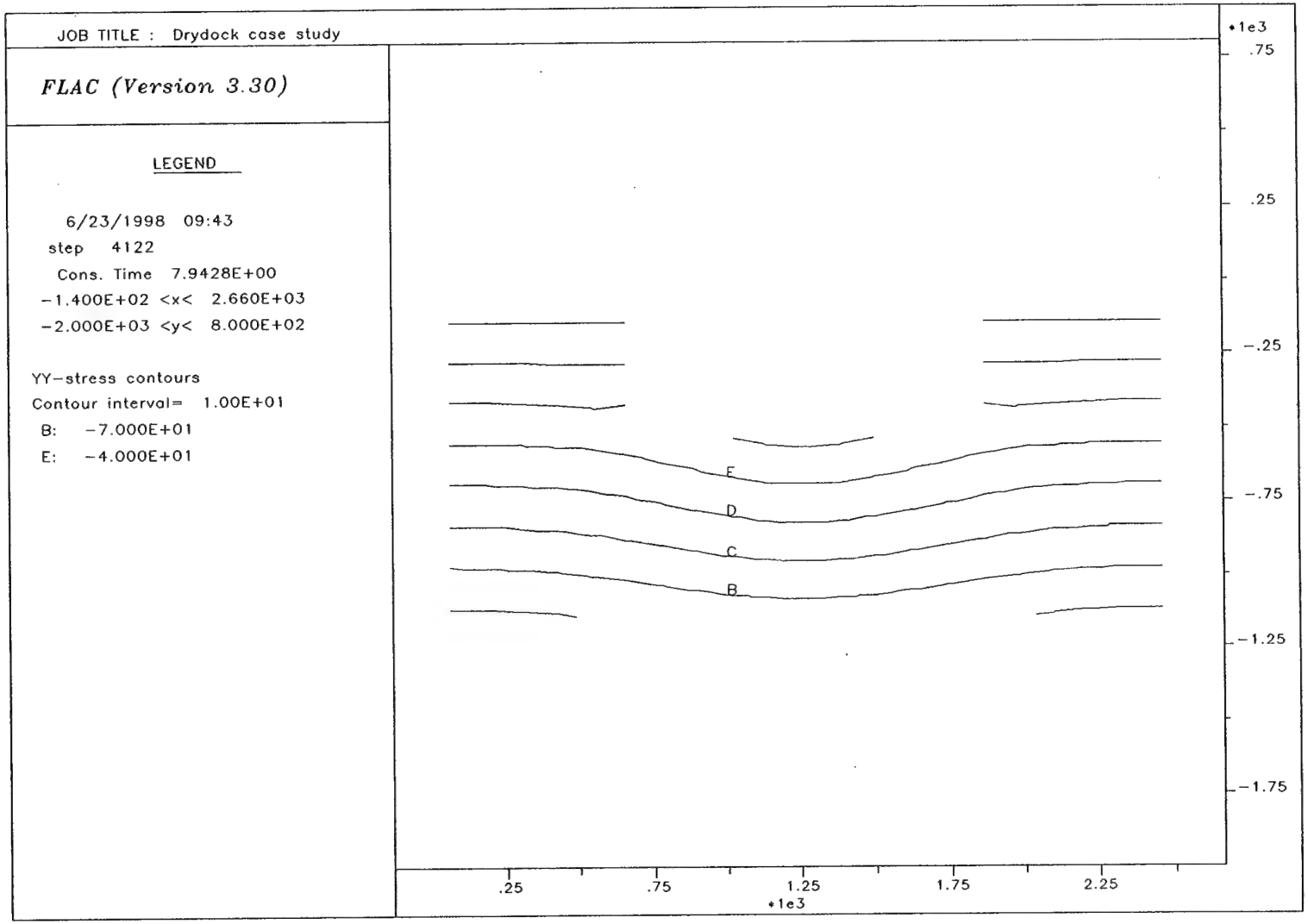

Figure 6. Syy vertical soil stress.

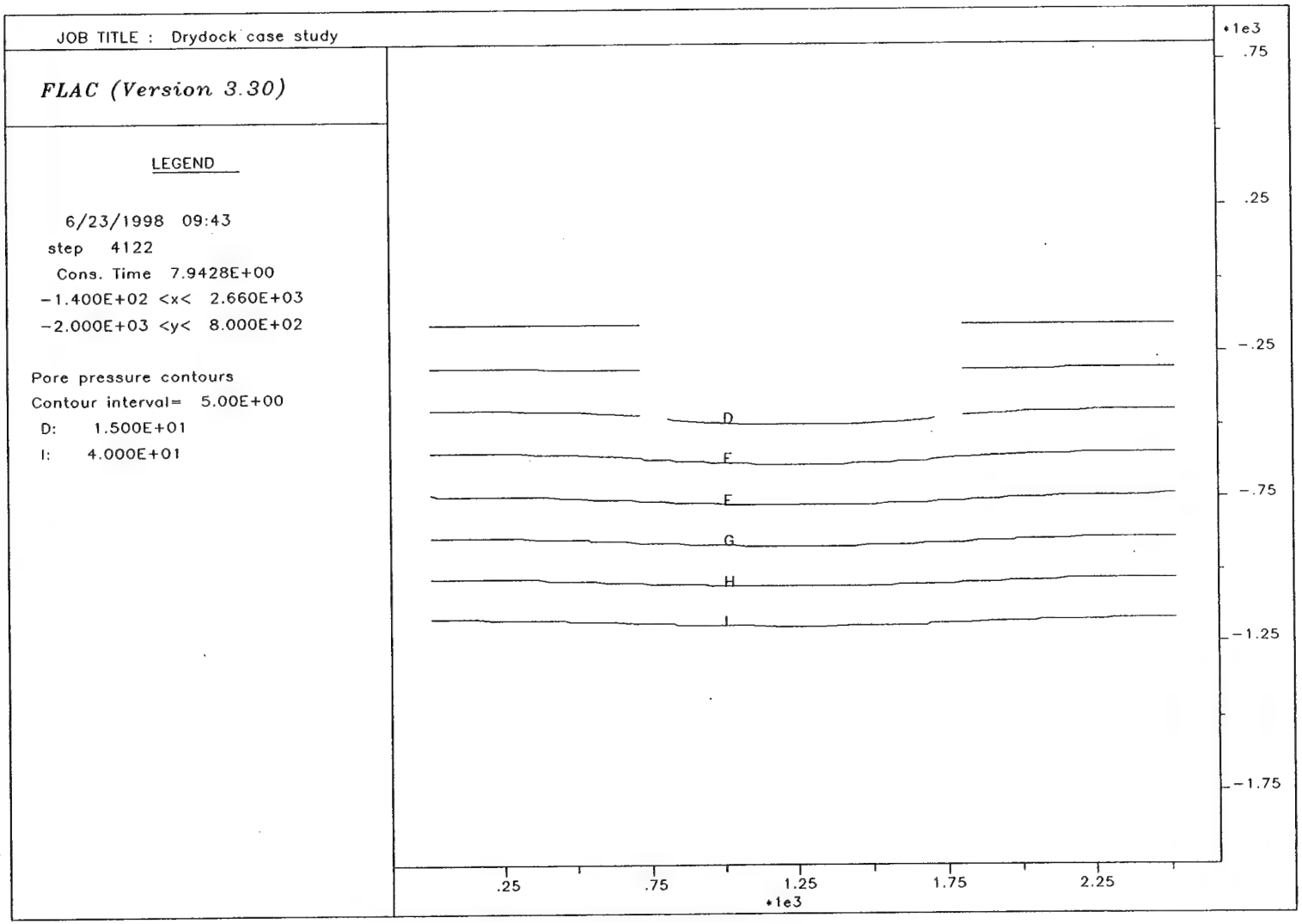

Figure 7. Pore pressure.

Figure 8 . Drydock wall static moment.

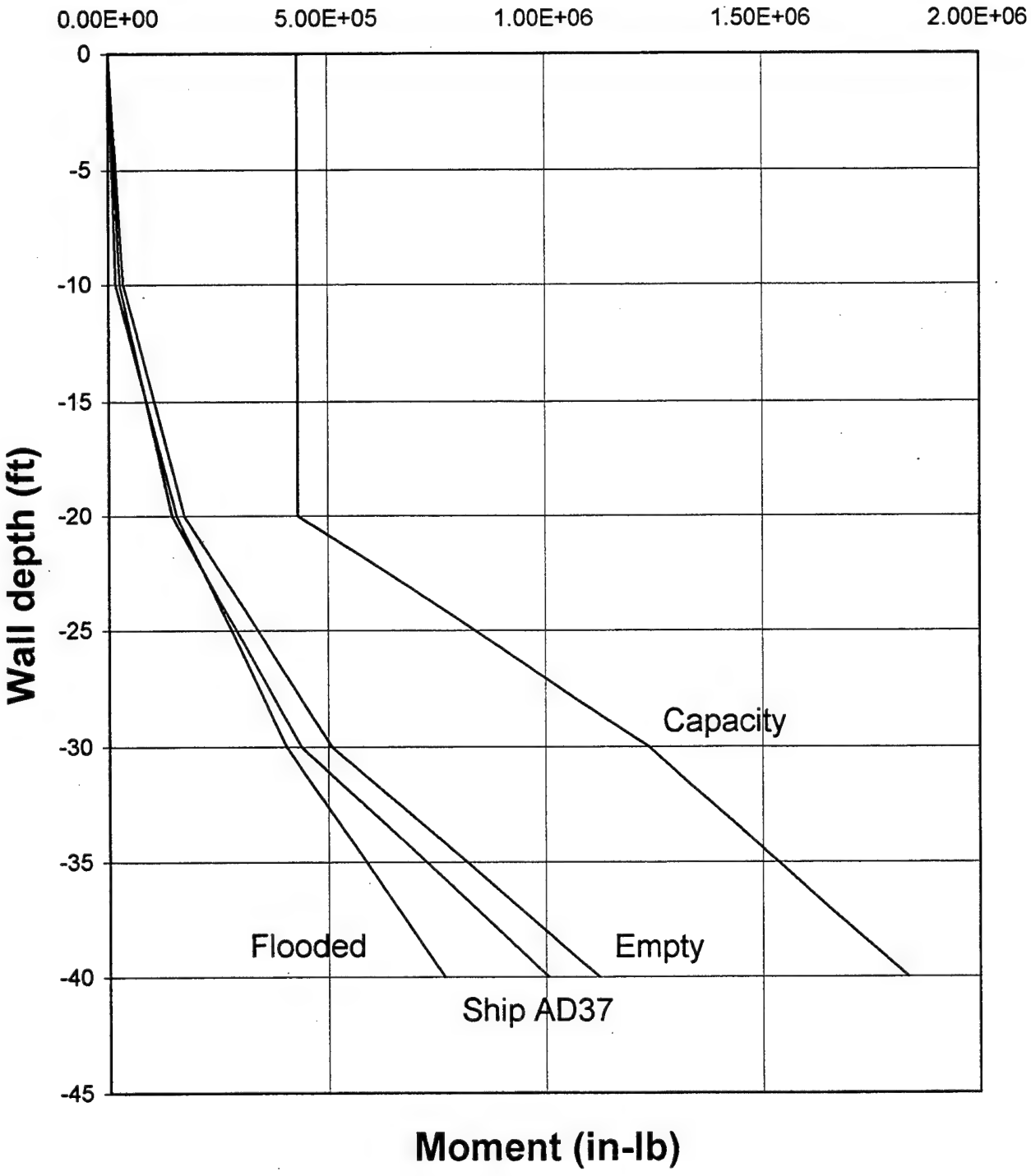

Figure 9 . Floor moments.

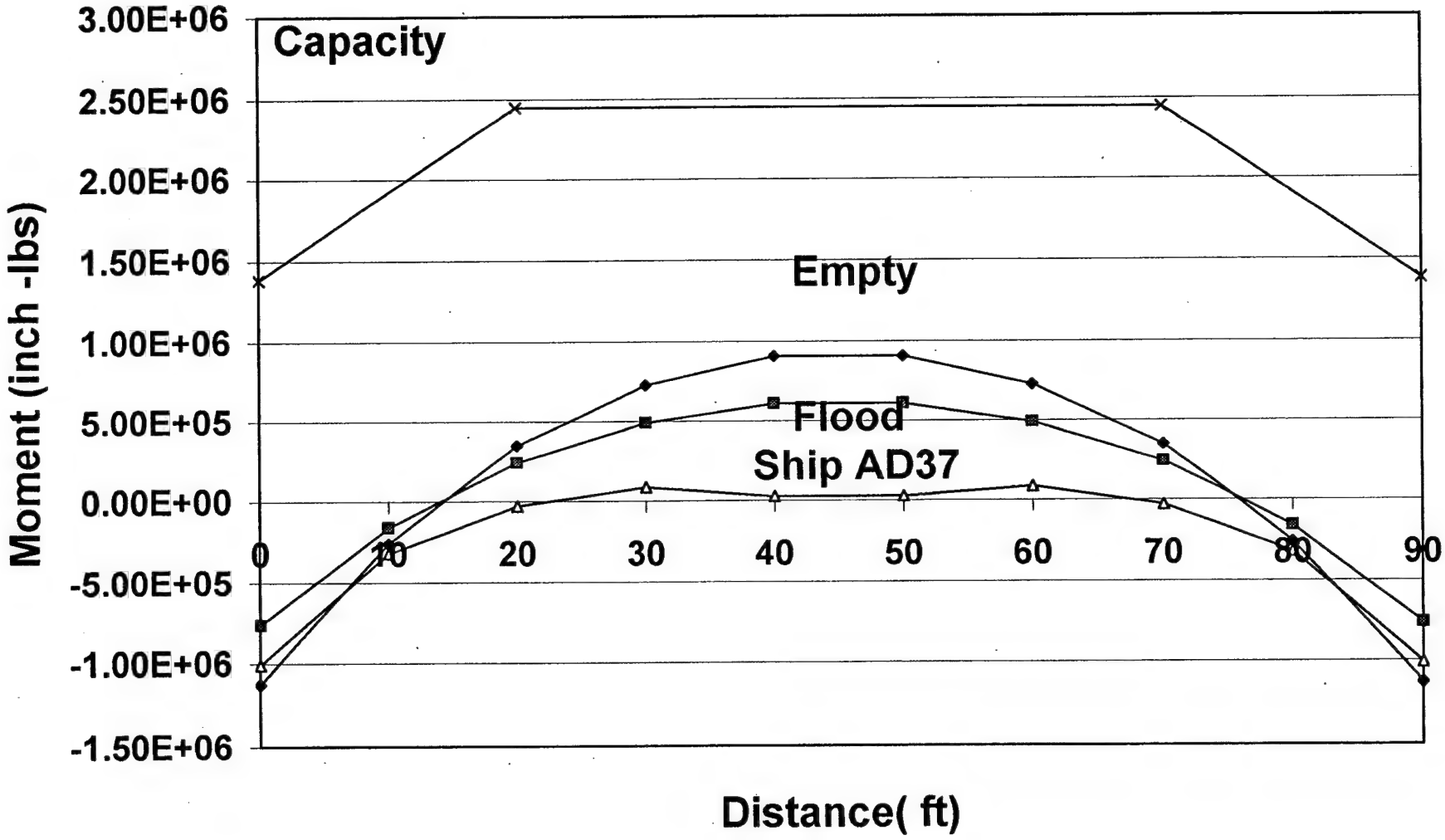

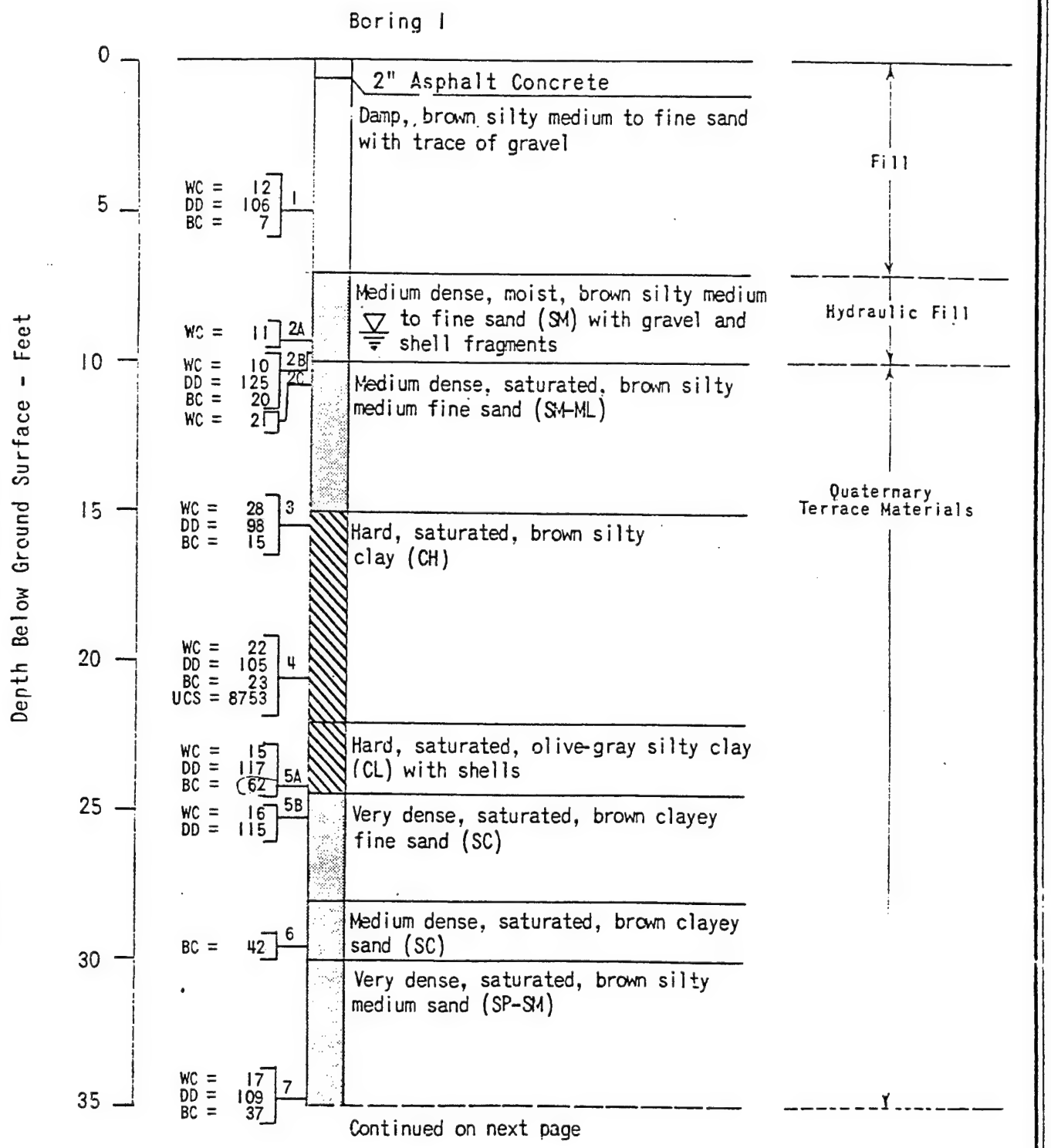

Figure 10. Soil boring log.

LOG OF TEST BORING 1 US NAVAL STATION GAS TURBINE SITE		
WOODWARD – GIZIENSKI & ASSOCIATES CONSULTING SOIL AND FOUNDATION ENGINEERS AND GEOLOGISTS SAN DIEGO, CALIFORNIA		
DR. BY: GS	APPROX. SCALE: 1" = 5'	PROJ. NO: 73-265
CK'D BY:	DATE: 10/31/73	FIGURE NO: 2

APPENDIX C
SHT 4 OF 24

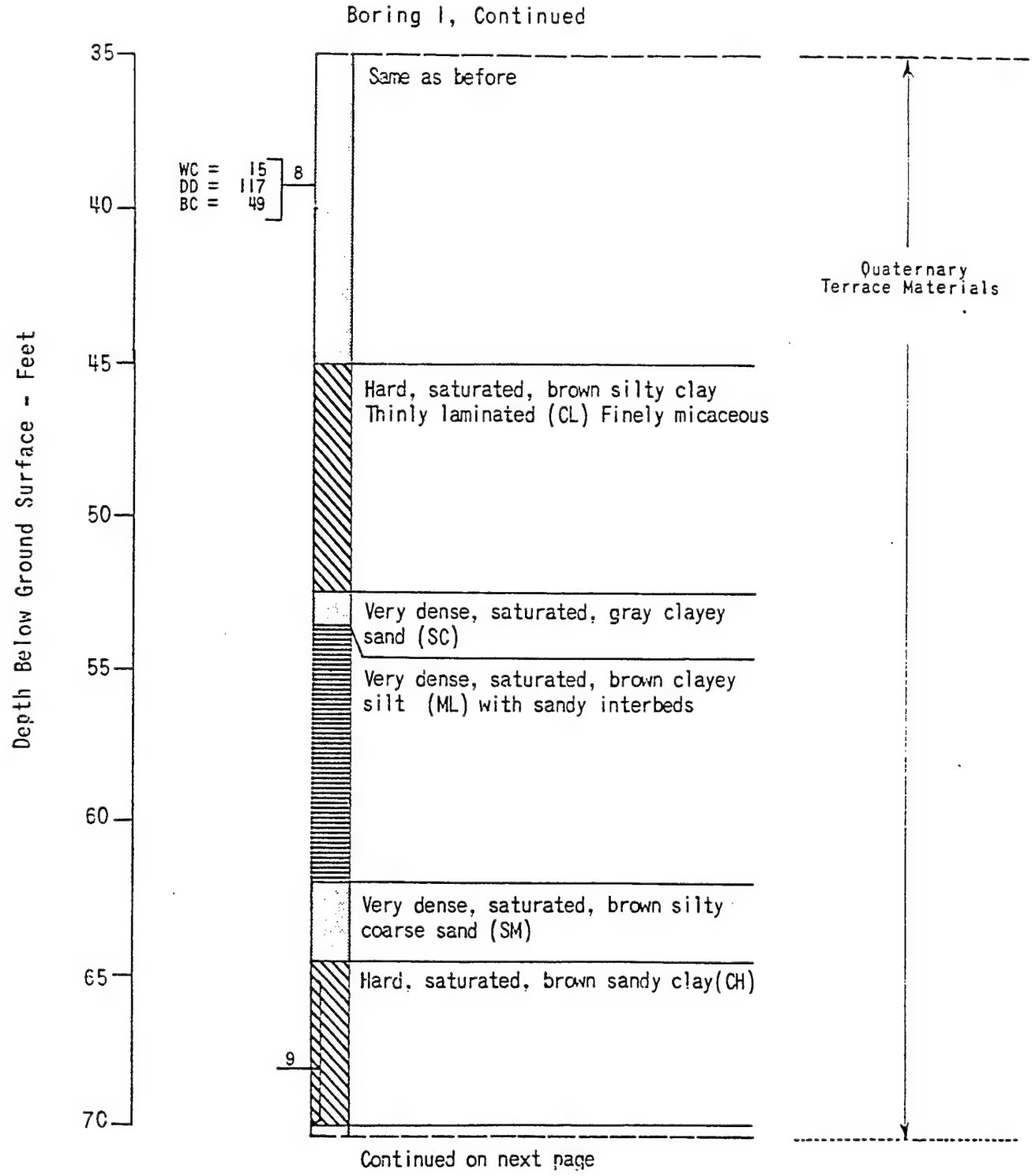

Figure 10. Continued.

LOG OF TEST BORING 1, CONTINUED US NAVAL STATION GAS TURBINE SITE		
WOODWARD – GIZIENSKI & ASSOCIATES CONSULTING SOIL AND FOUNDATION ENGINEERS AND GEOLOGISTS SAN DIEGO, CALIFORNIA		
DR. BY: GS	APPROX. SCALE: 1" = 5'	PROJ. NO: 73-265
CK'D BY: [illegible]	DATE: 10/31/73	FIGURE NO: 3

APPENDIX 1C SHT 5 OF 24

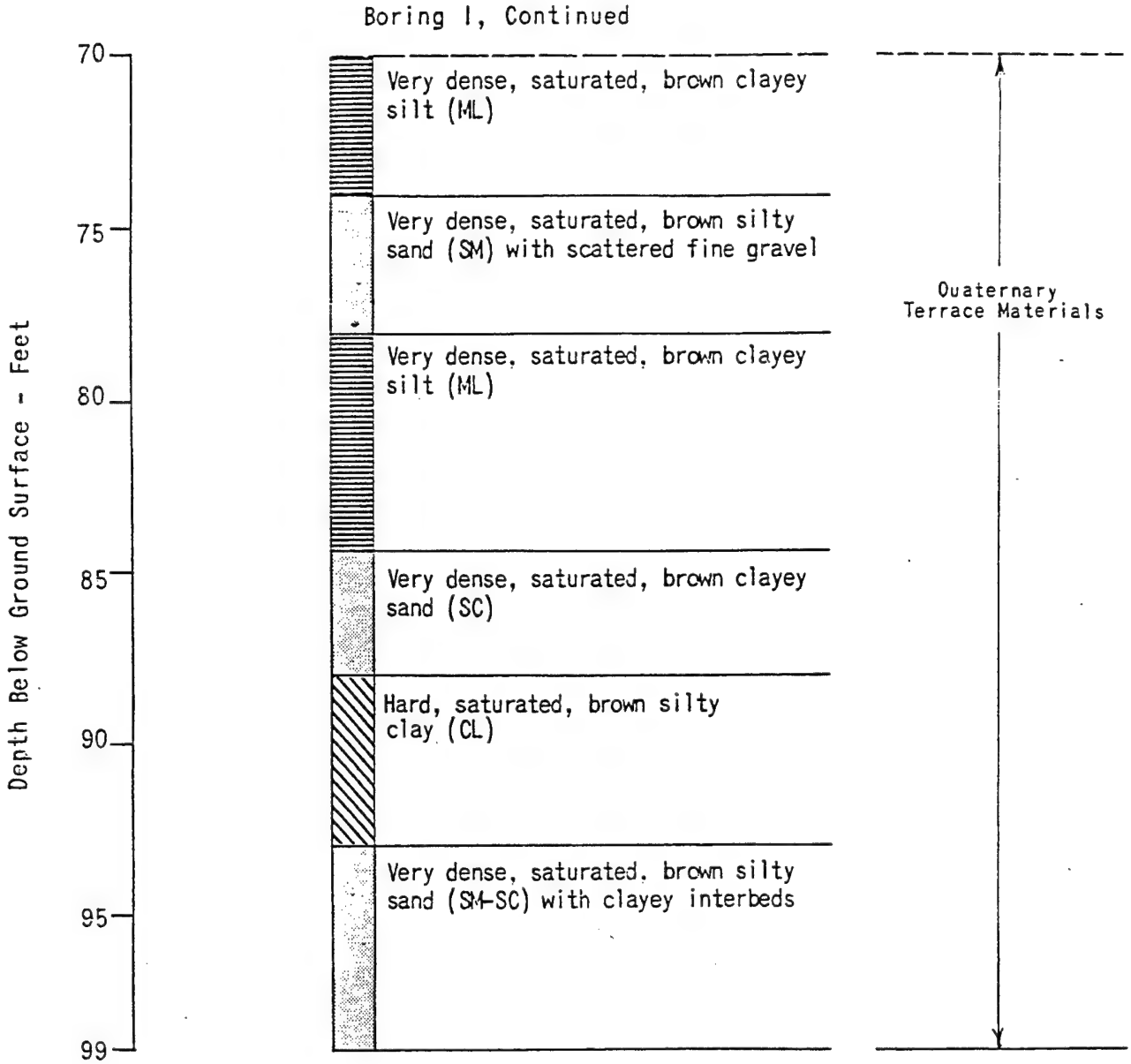

Figure 10. Continued.

LOG OF TEST BORING I, CONTINUED US NAVAL STATION GAS TURBINE SITE		
WOODWARD - GIZIENSKI & ASSOCIATES CONSULTING SOIL AND FOUNDATION ENGINEERS AND GEOLOGISTS SAN DIEGO, CALIFORNIA		
DR. BY: GS	APPROX. SCALE: 1" = 5'	PROJ. NO: 73-265
CK'D BY: [illegible]	DATE: 10/31/73	FIGURE NO: 4

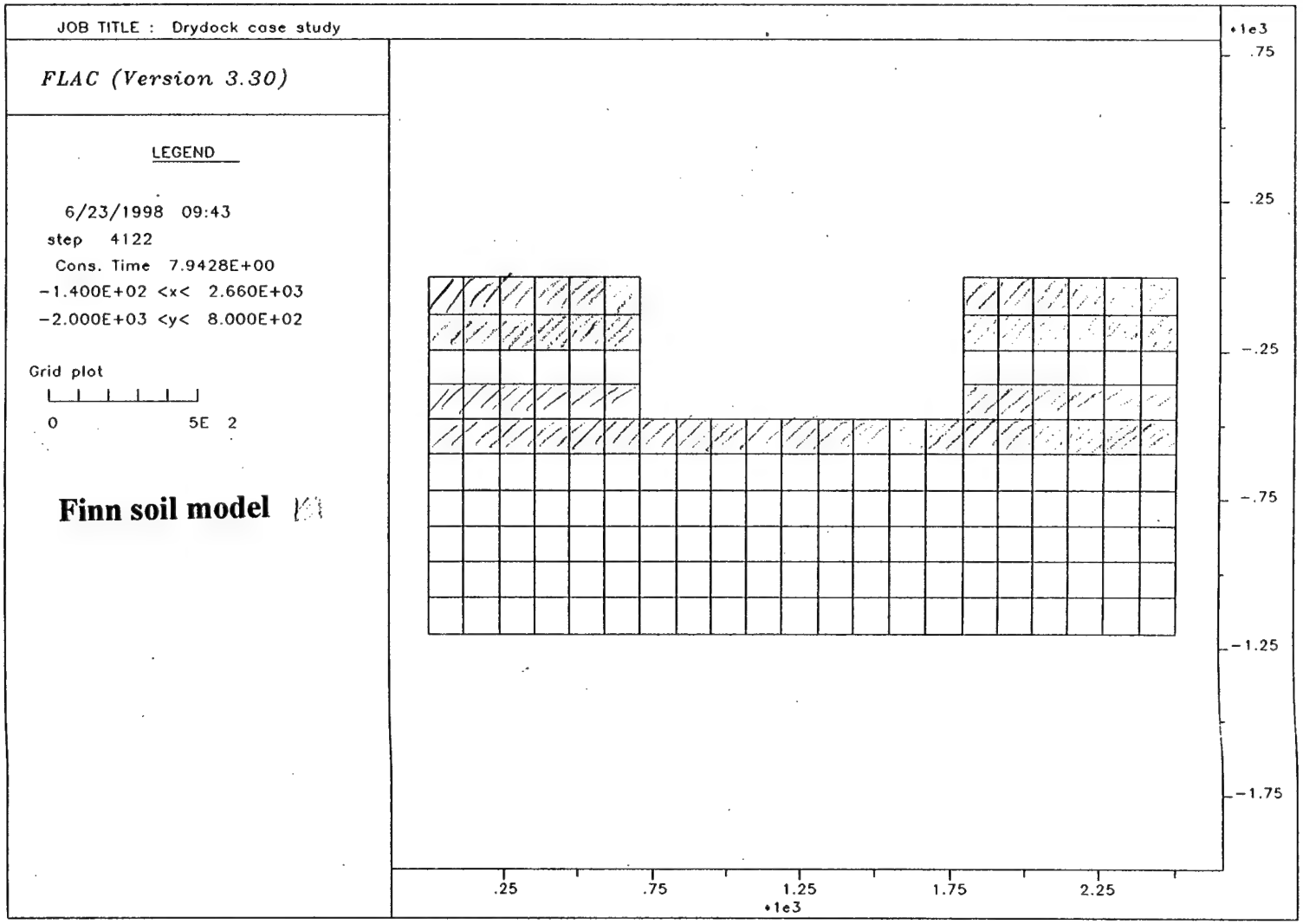

Figure 11. FLAC soil grid showing soil layers

Figure 11 . Drydock wall static moment.

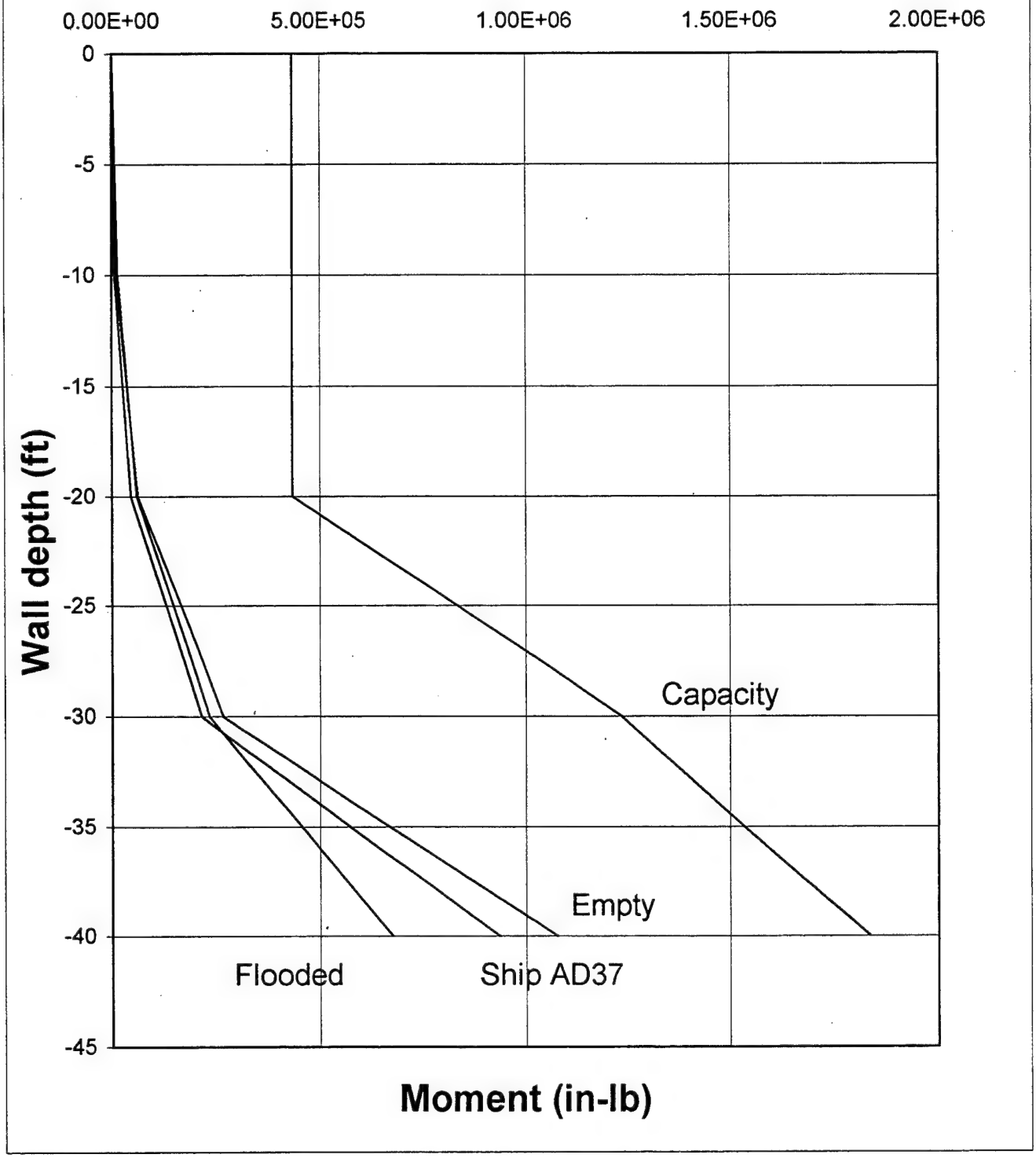

Figure 12 . Floor moments.

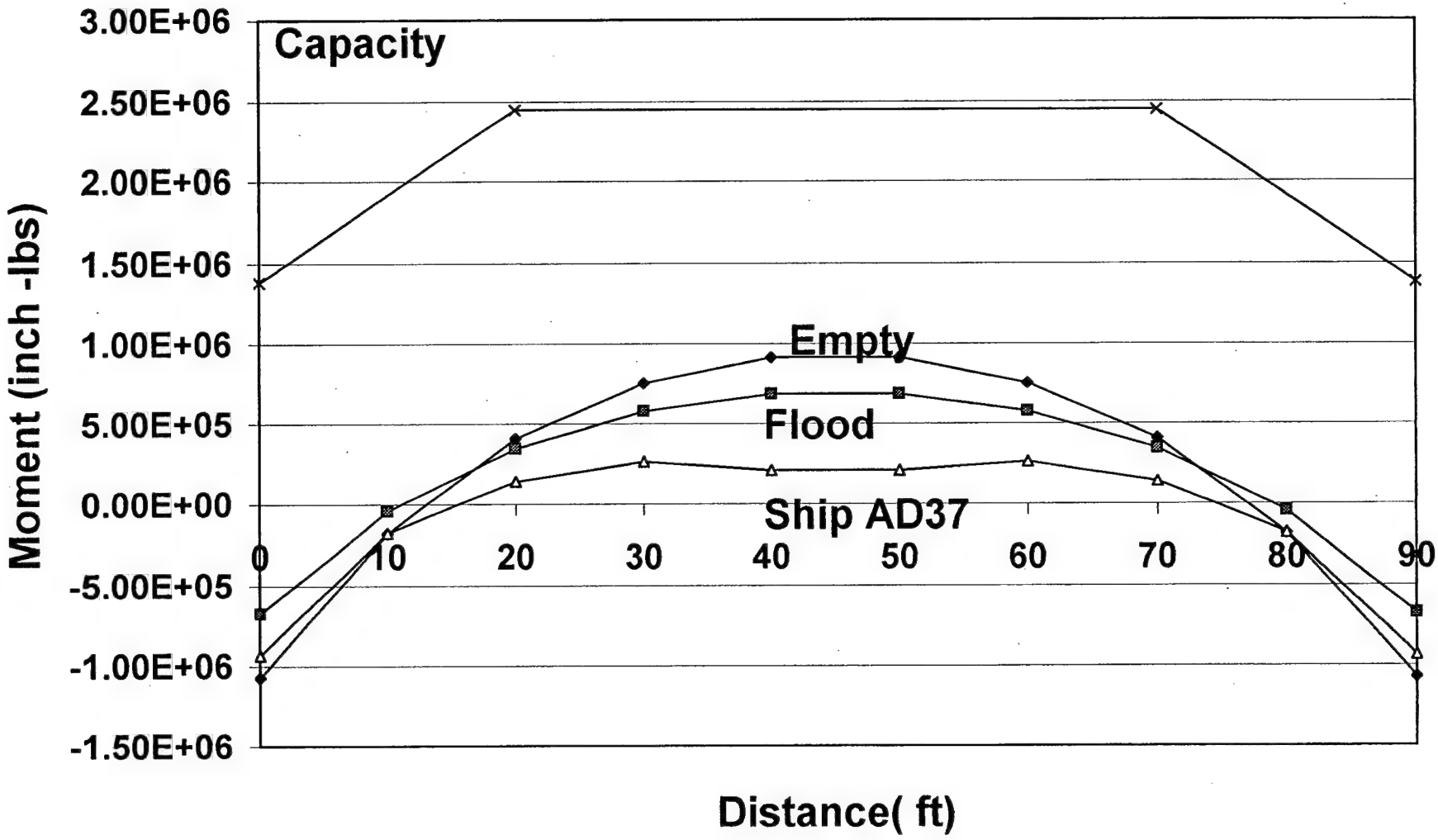

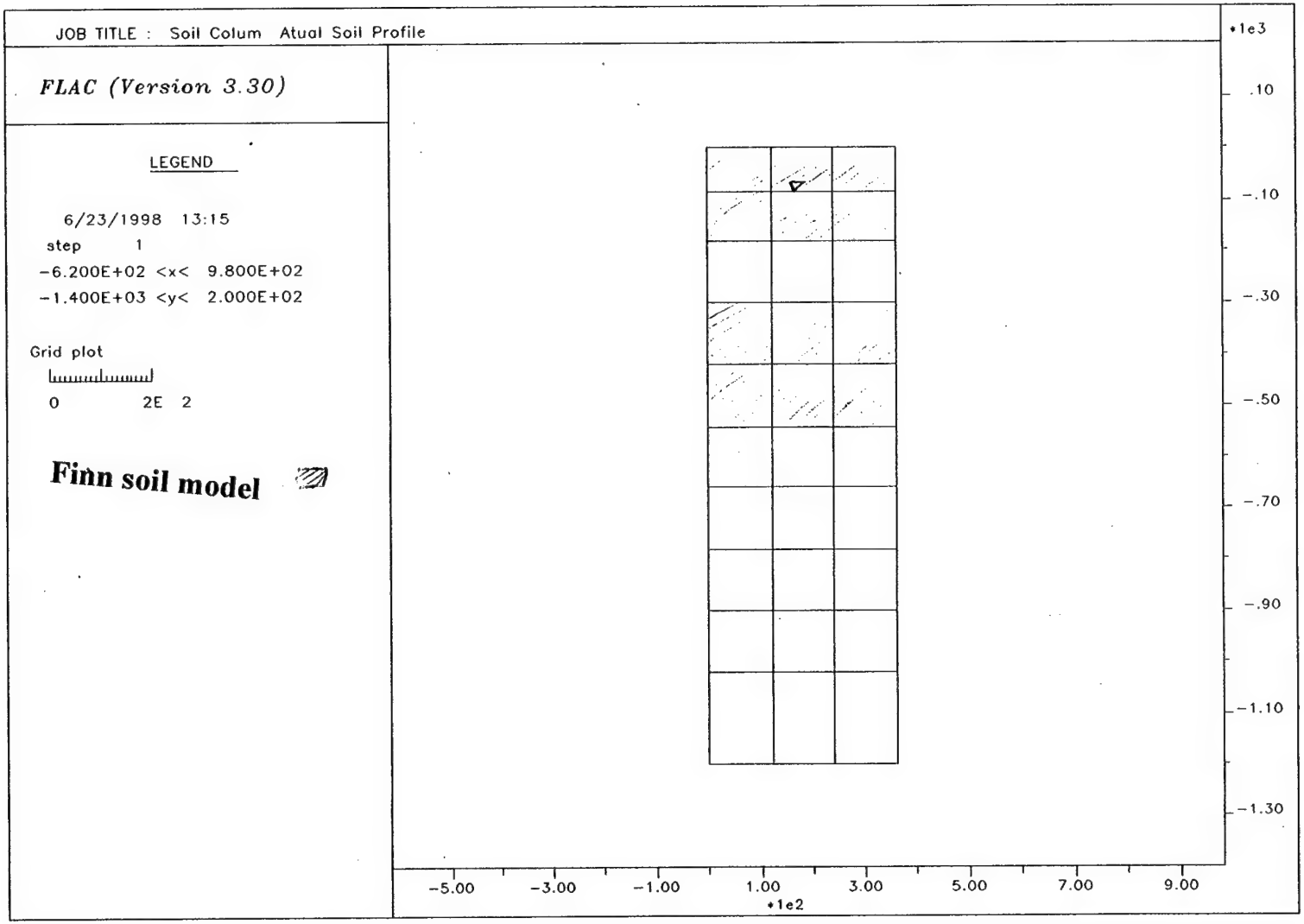

Figure 13. FLAC grid for soil column analysis.

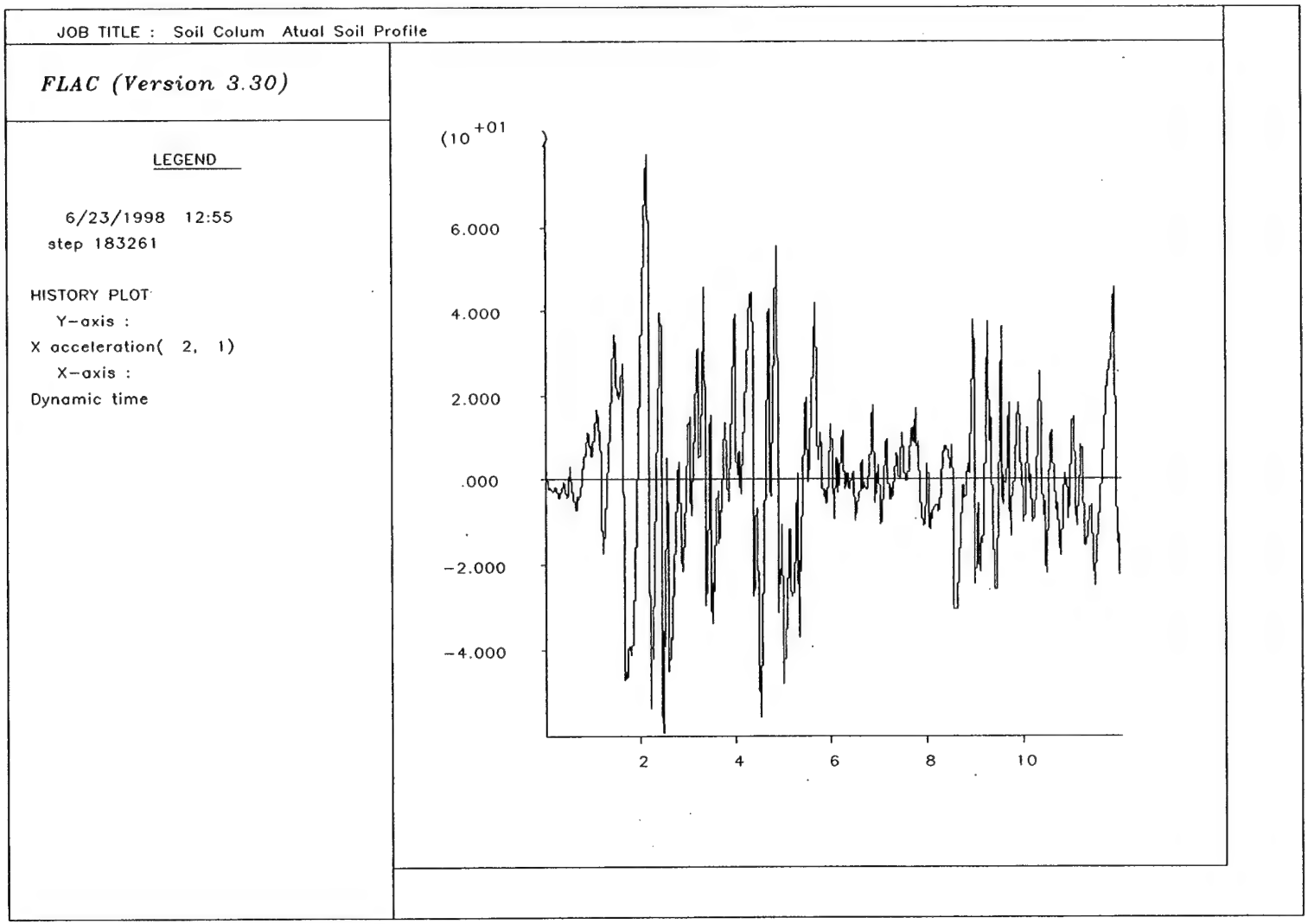

Figure 14. El Centro earthquake applied to base.

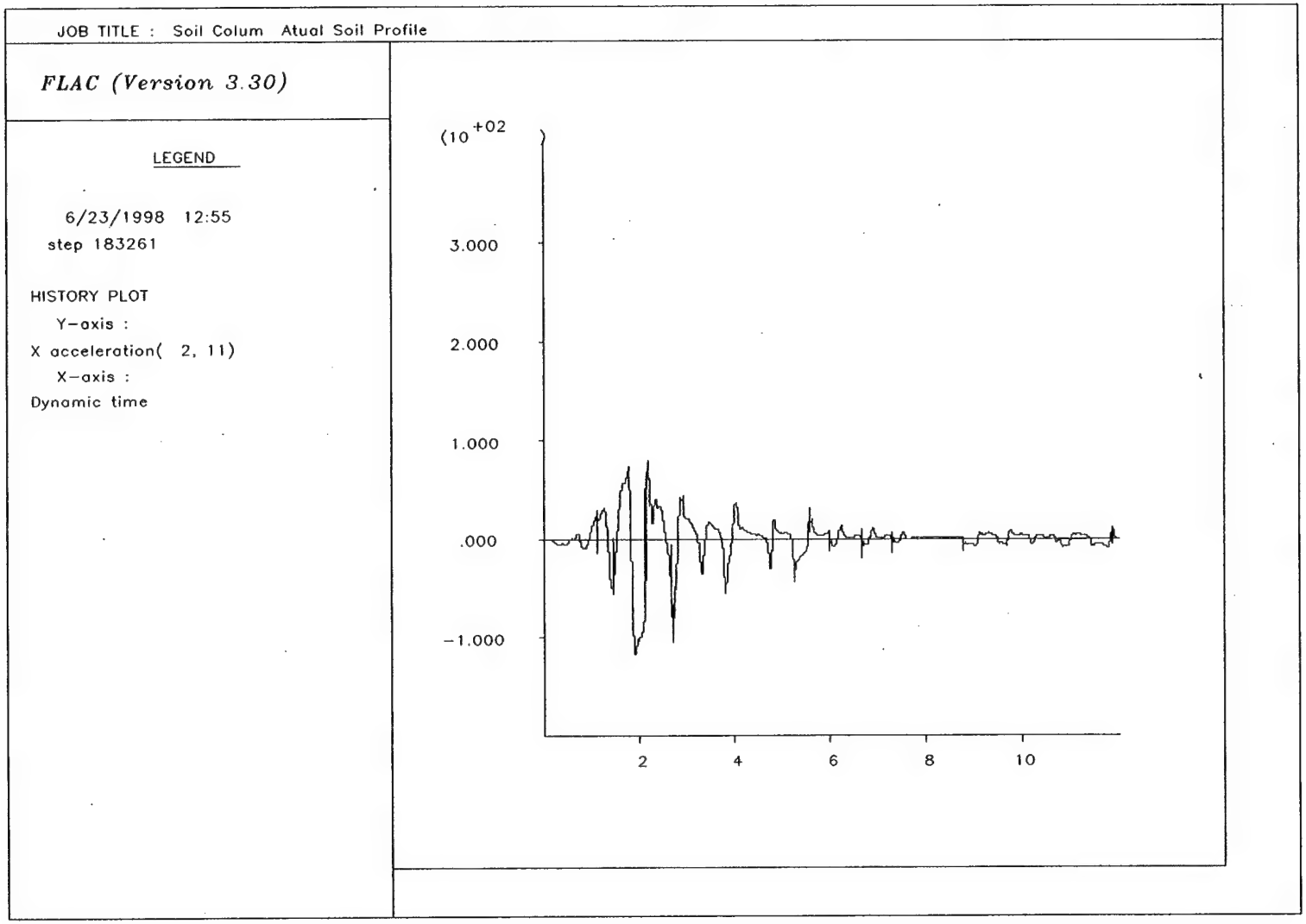

Figure 15. Surface acceleration.

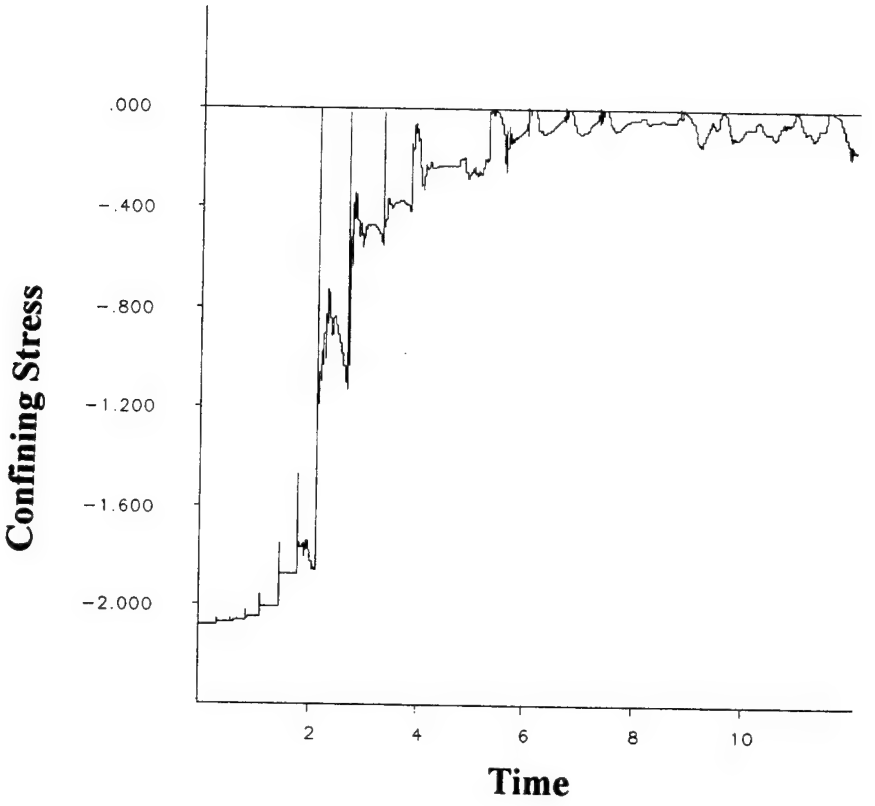

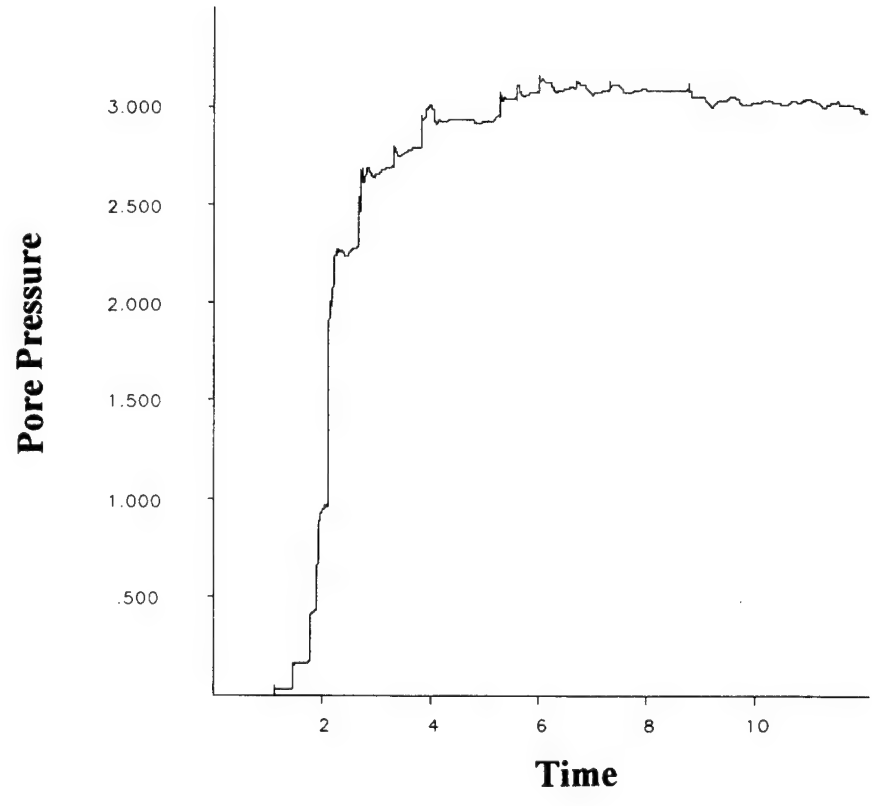

Figure 16. Confining stress and pore pressure layer 1.

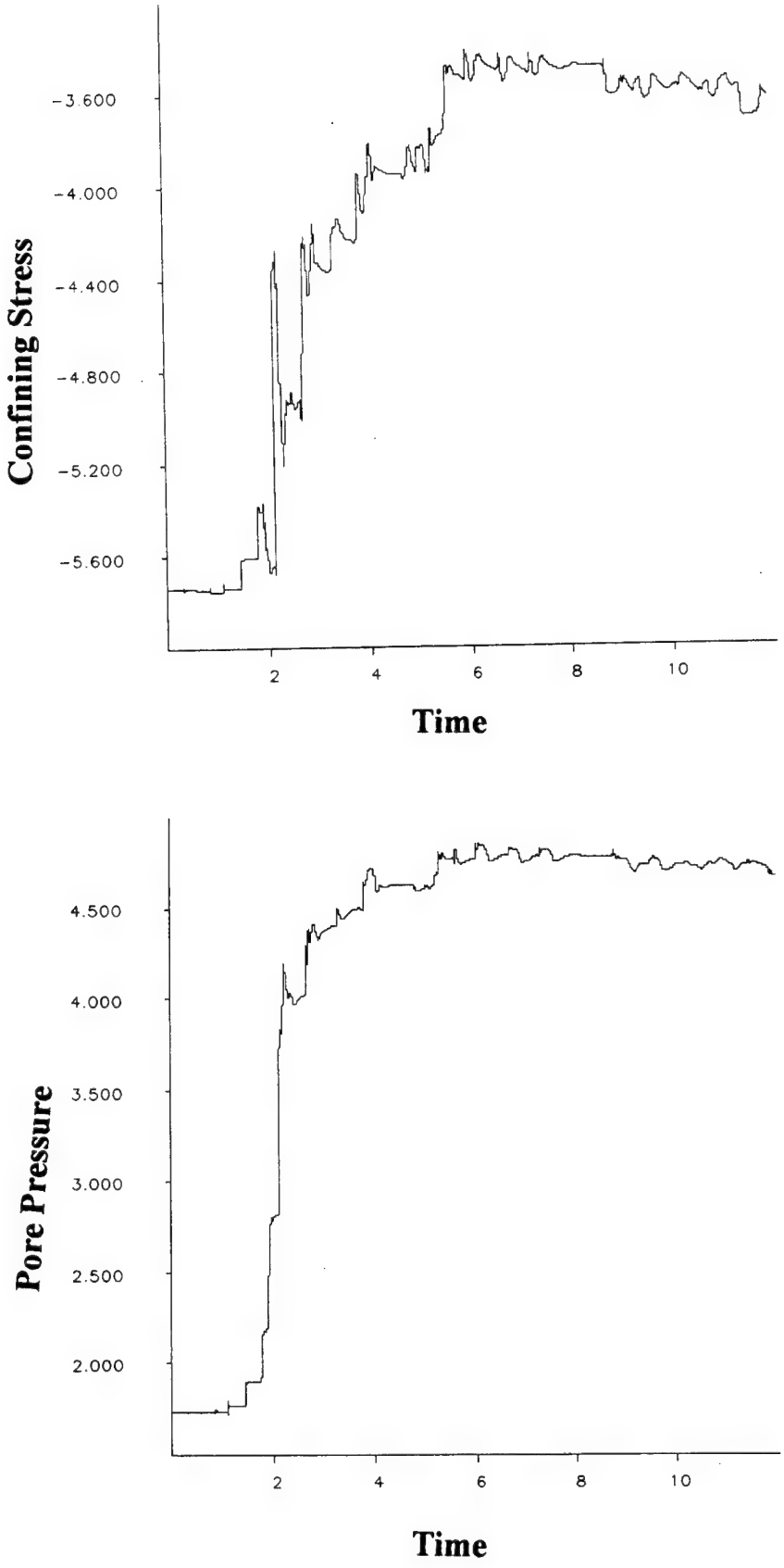

Figure 17. Confining stress and pore pressure layer 2.

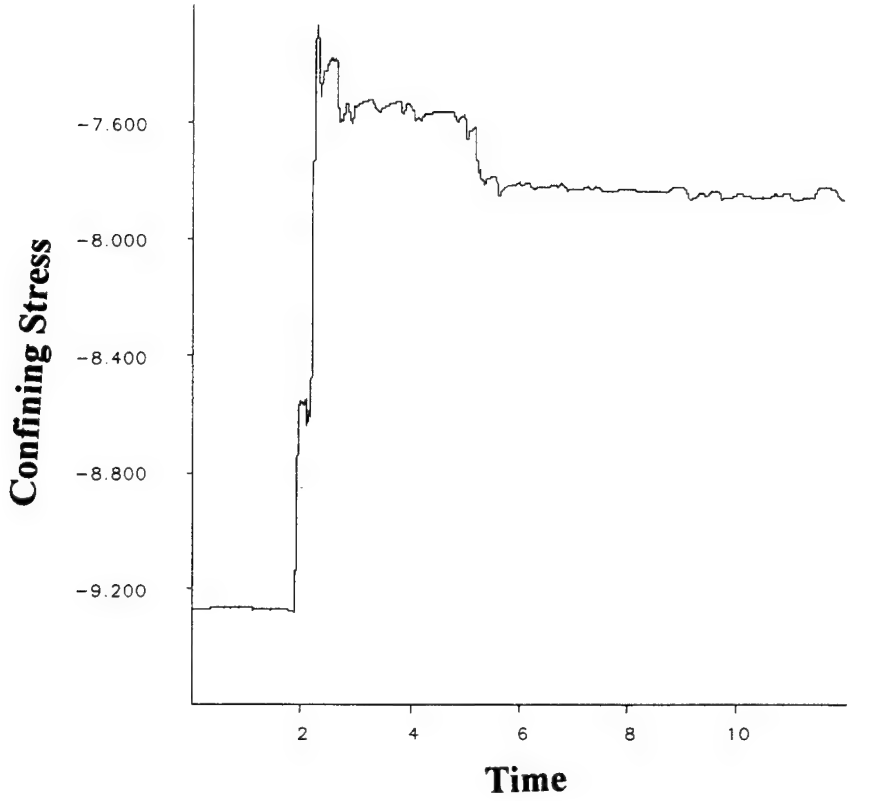

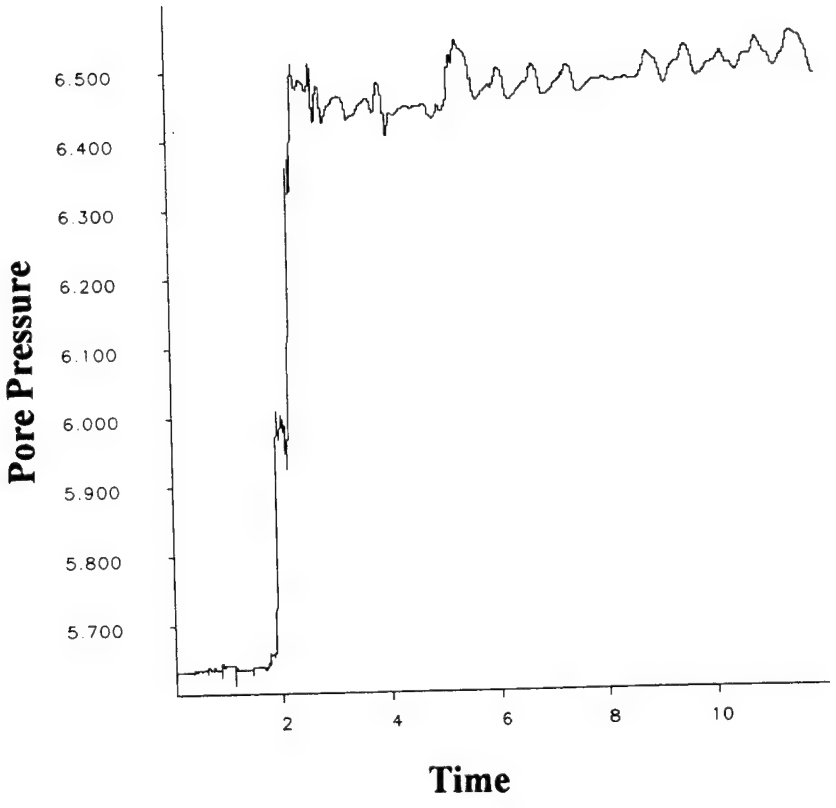

Figure 18. Confining stress and pore pressure layer 3.

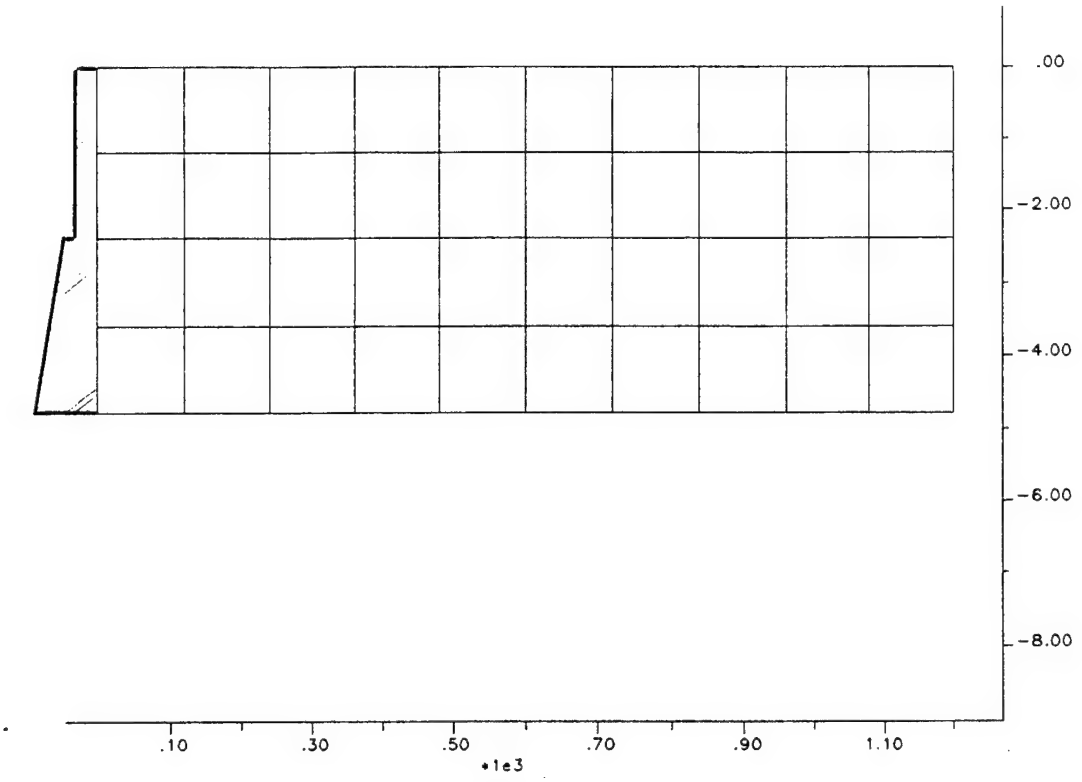

Figure 19a FLAC grid and drydock wall.

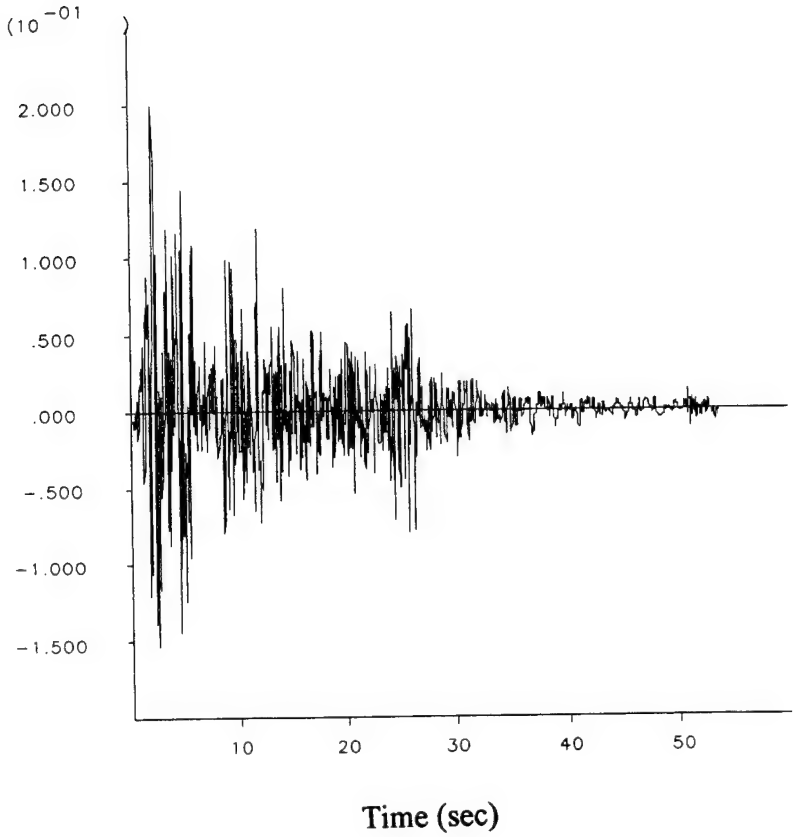

Figure19b El Centro earthquake.

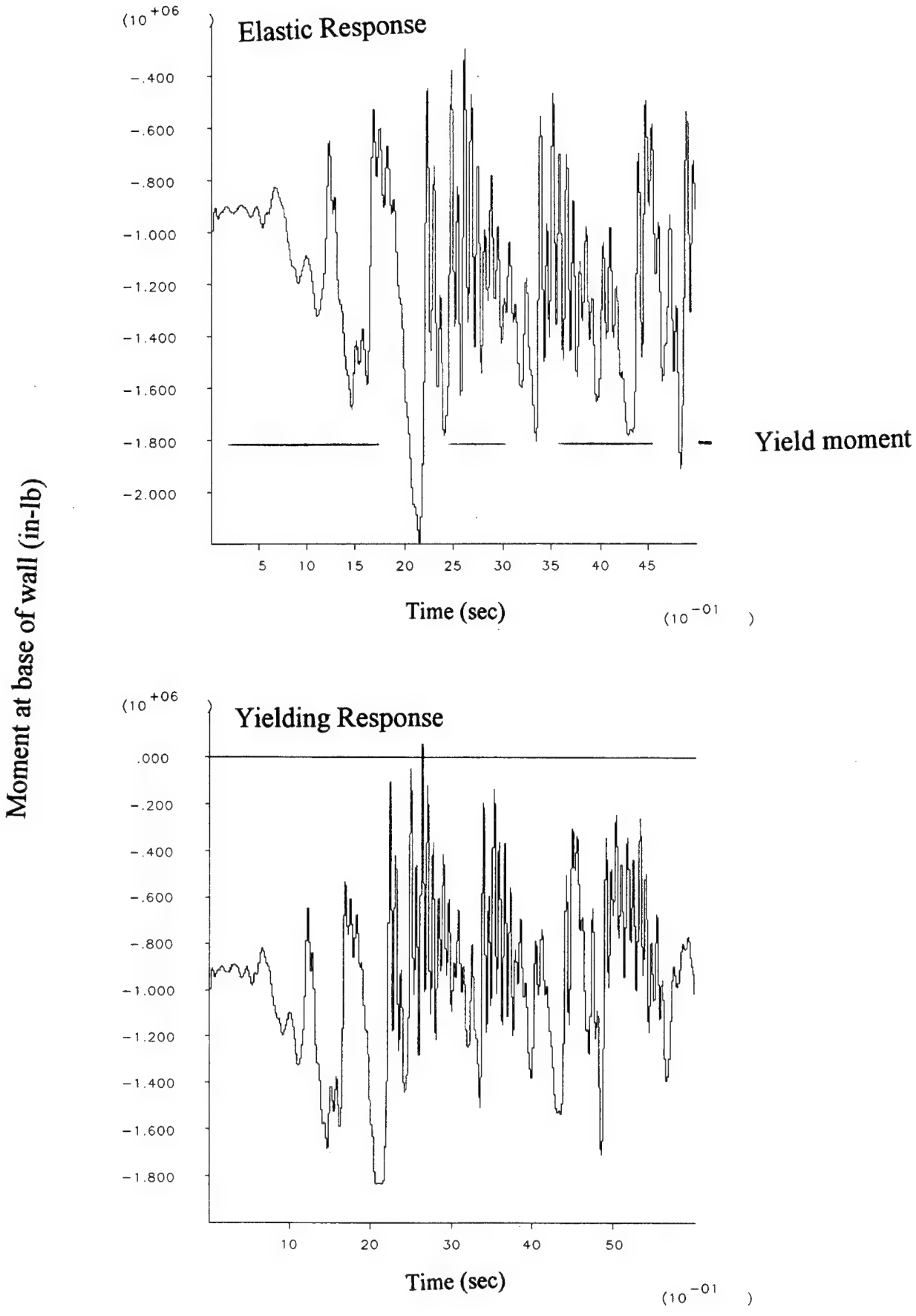

Figure 20. Moment in drydock wall.

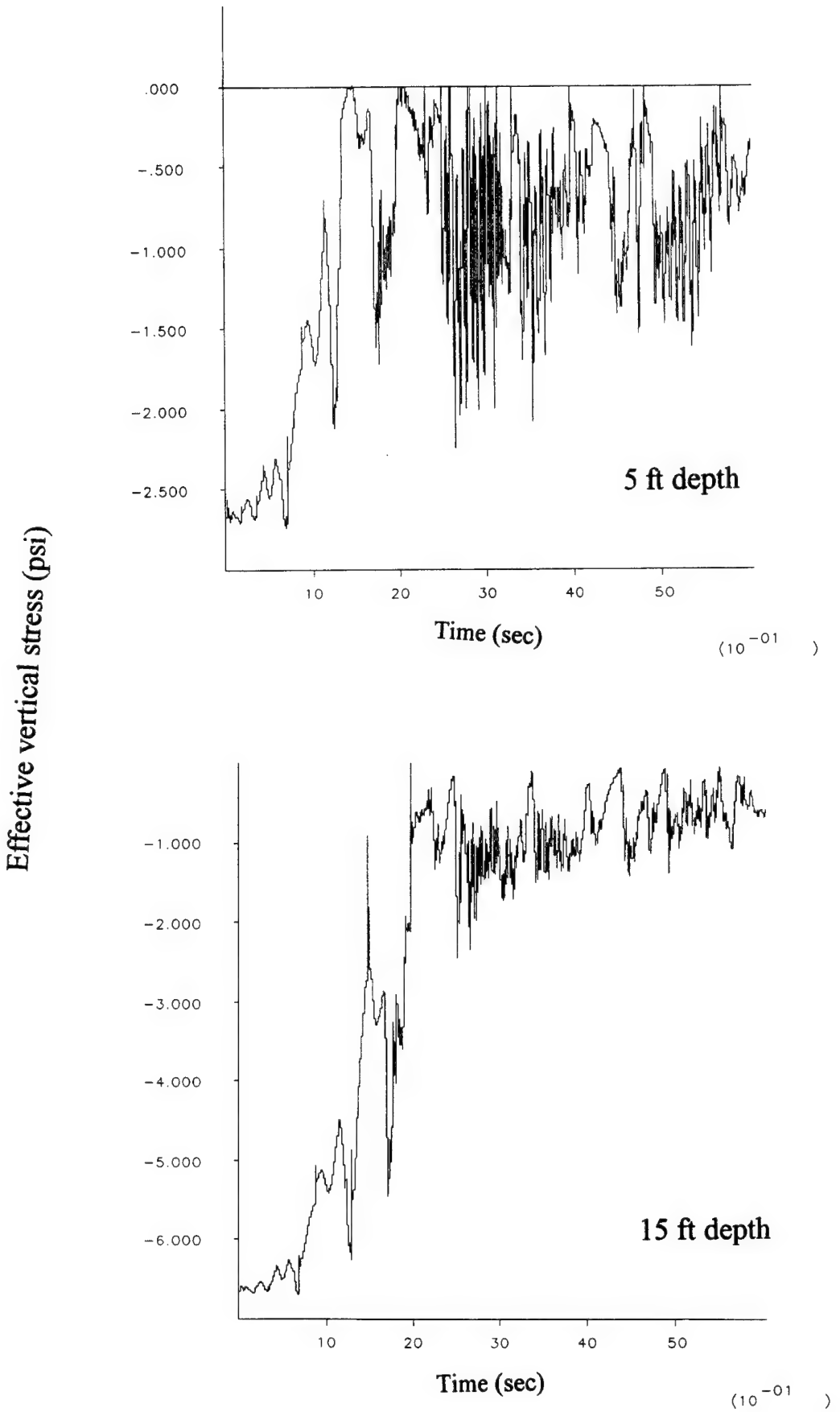

Figure 21a. Effective vertical stress.

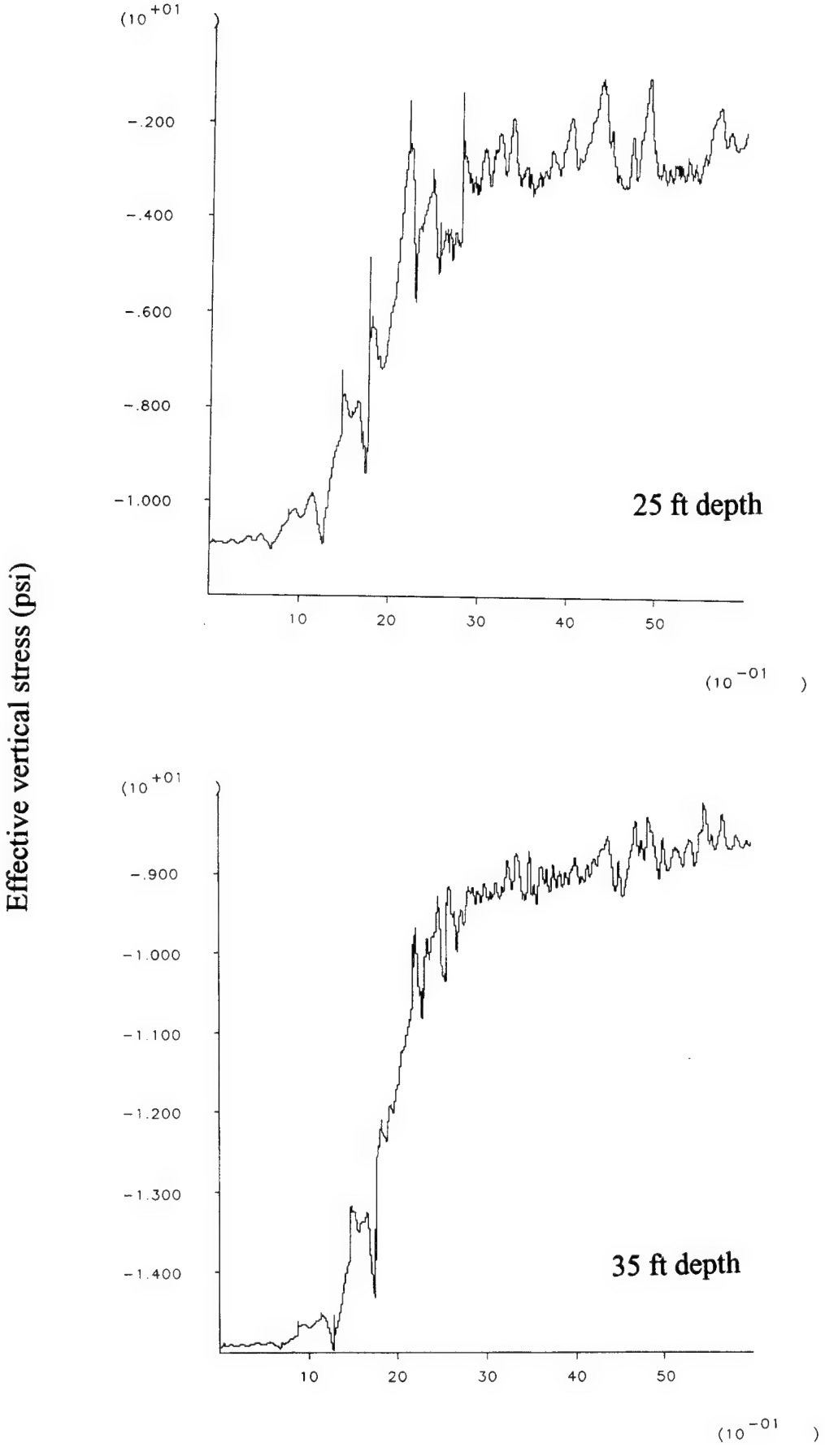

Figure 21b. Effective vertical stress.

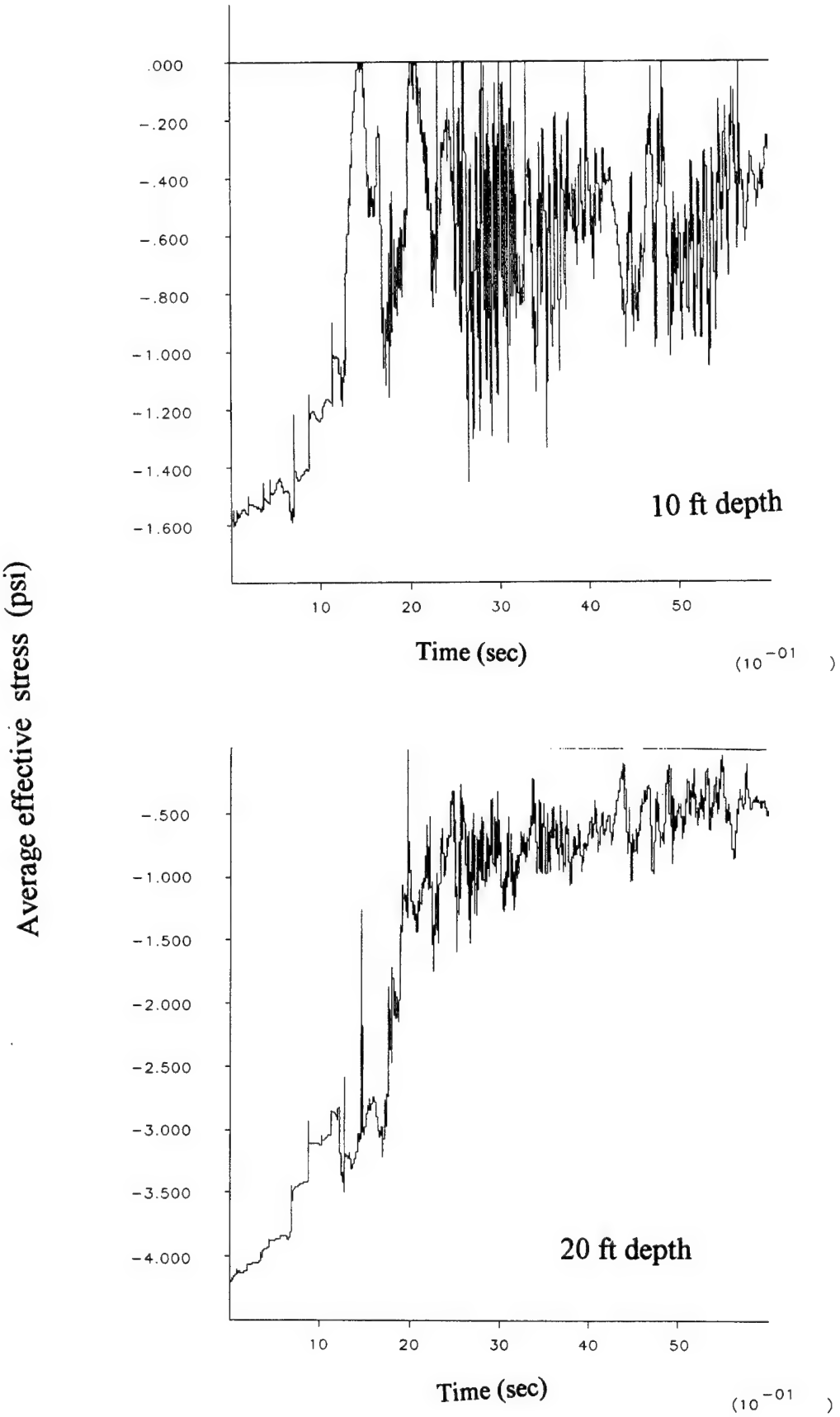

Figure 22a. Average effective stress.

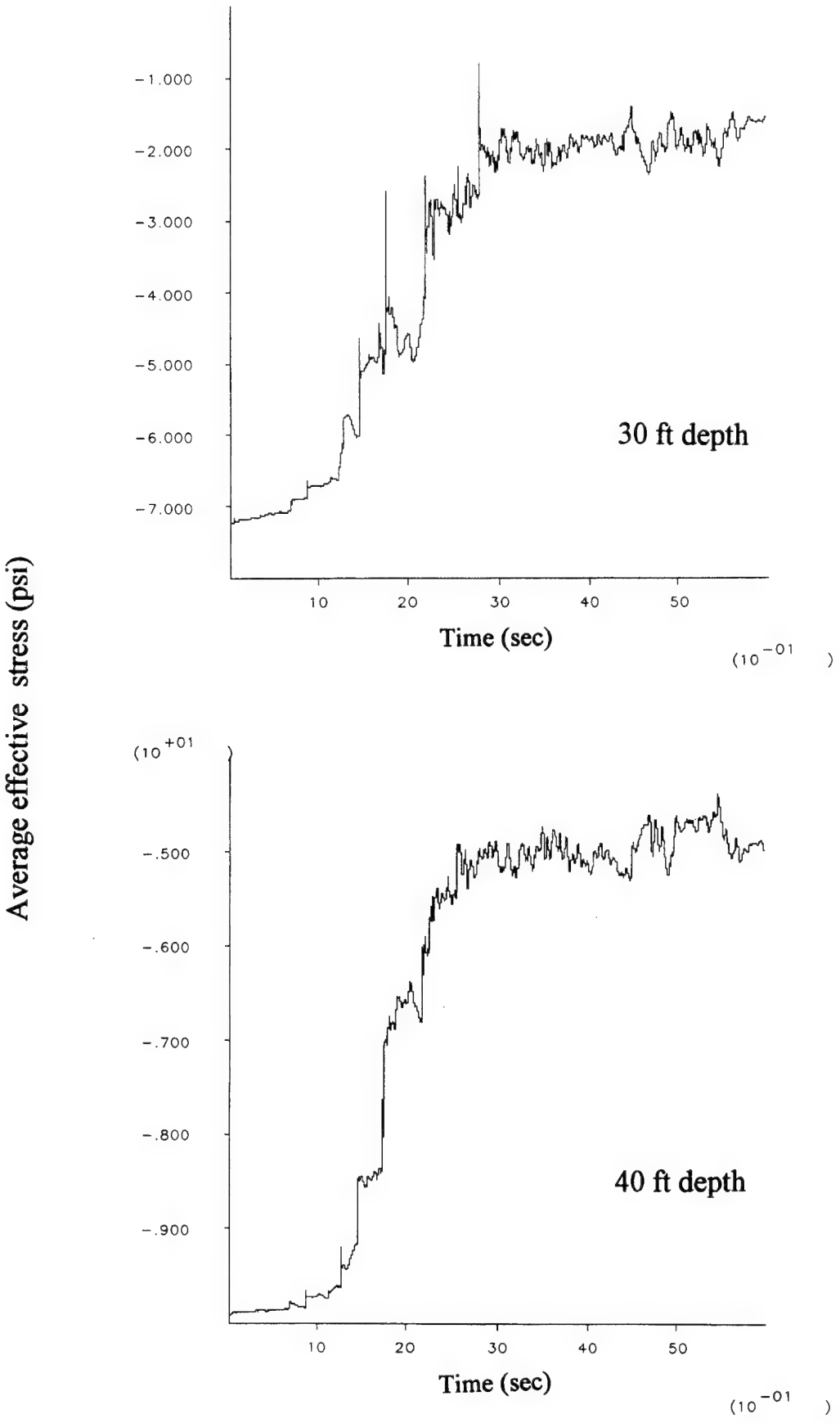

Figure 22b. Average effective stress.

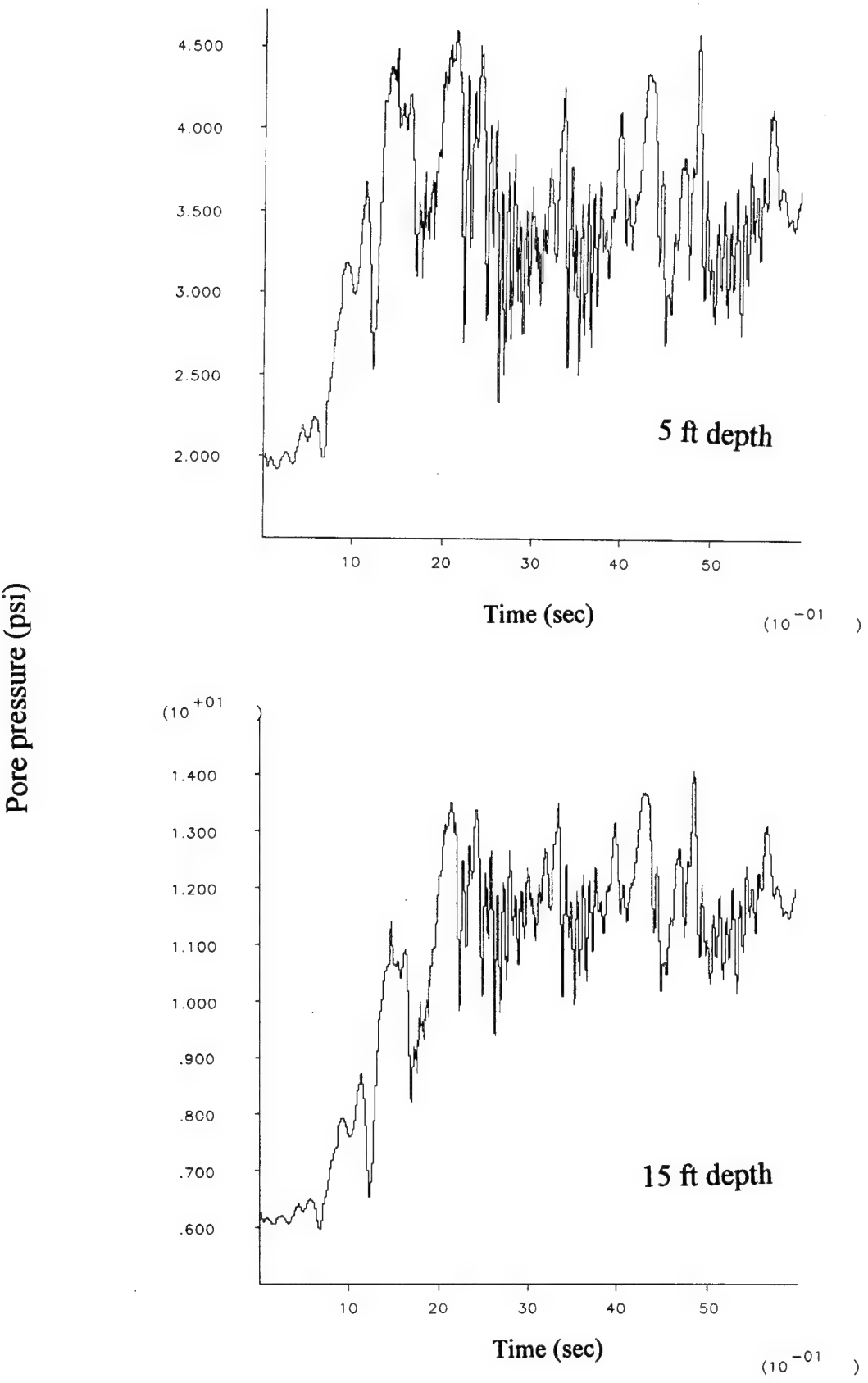

Figure 23a. Pore pressure.

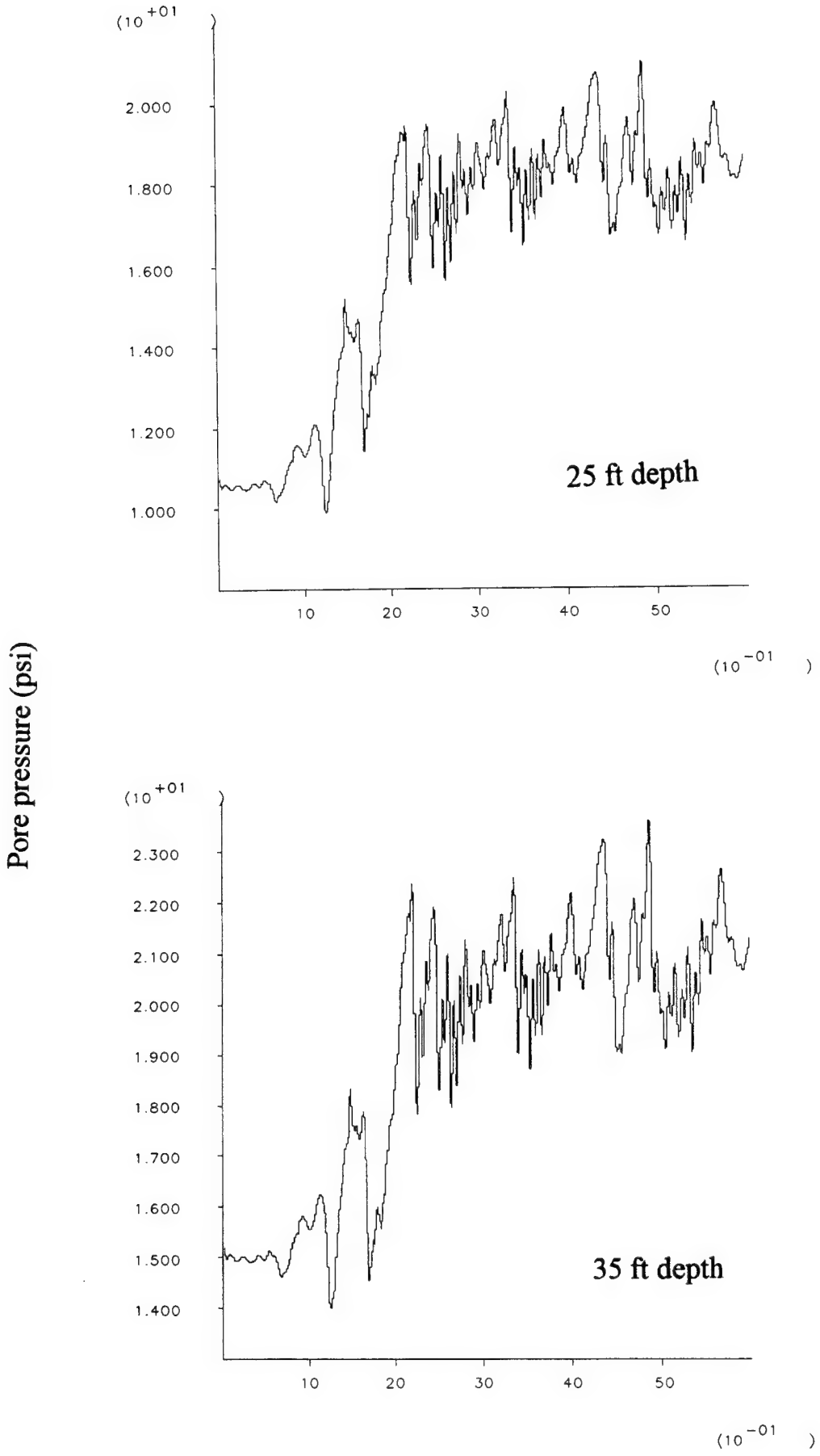

Figure 23b. Pore pressure.

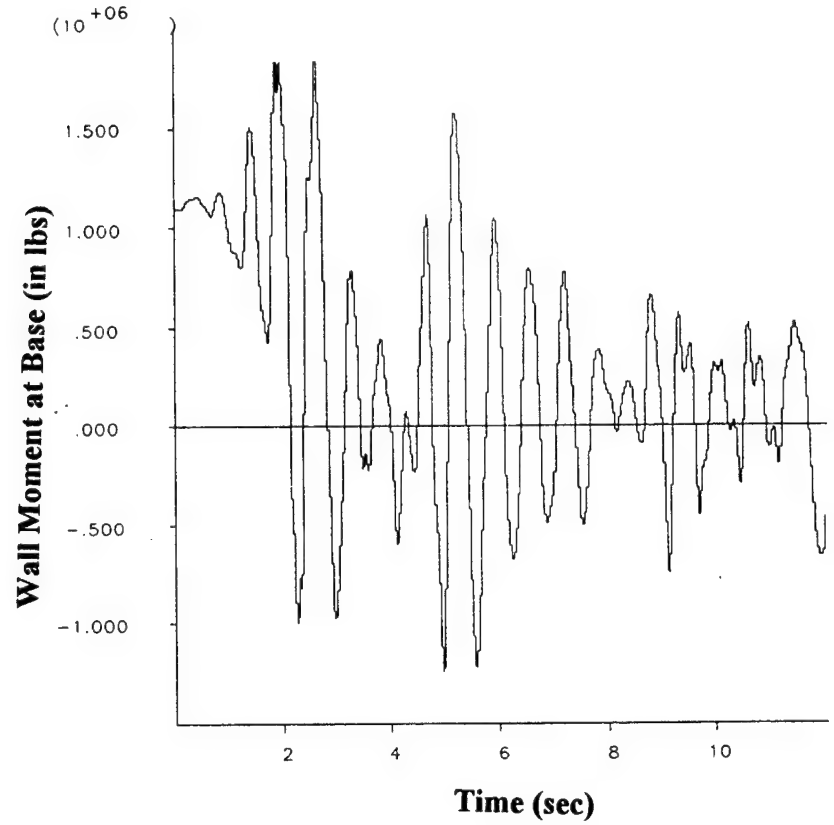

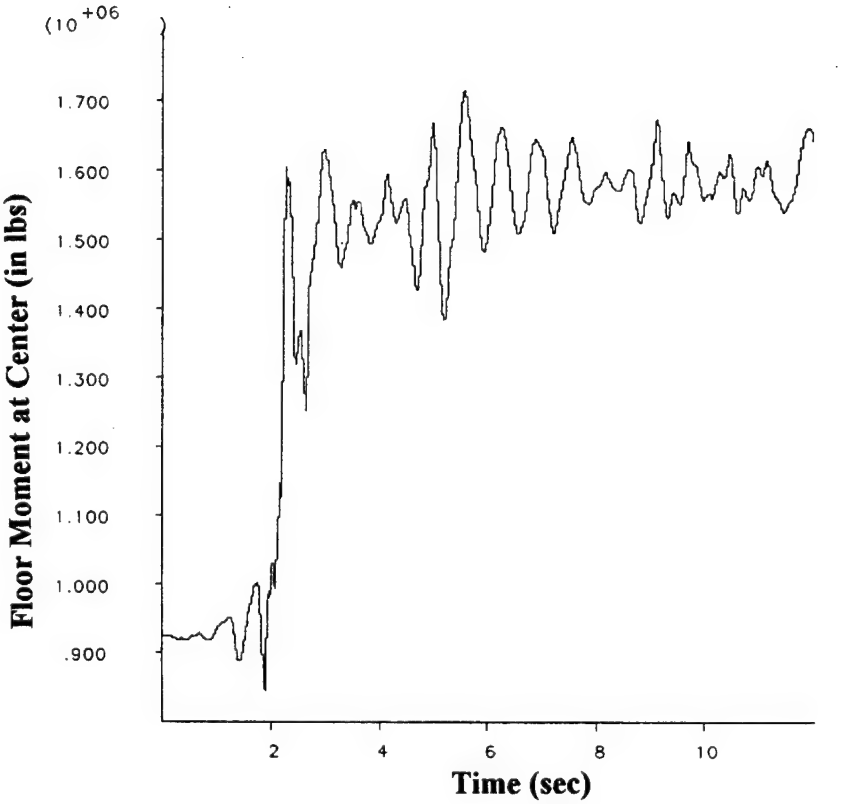

Figure 24. Moments in wall and floor, drydock empty.

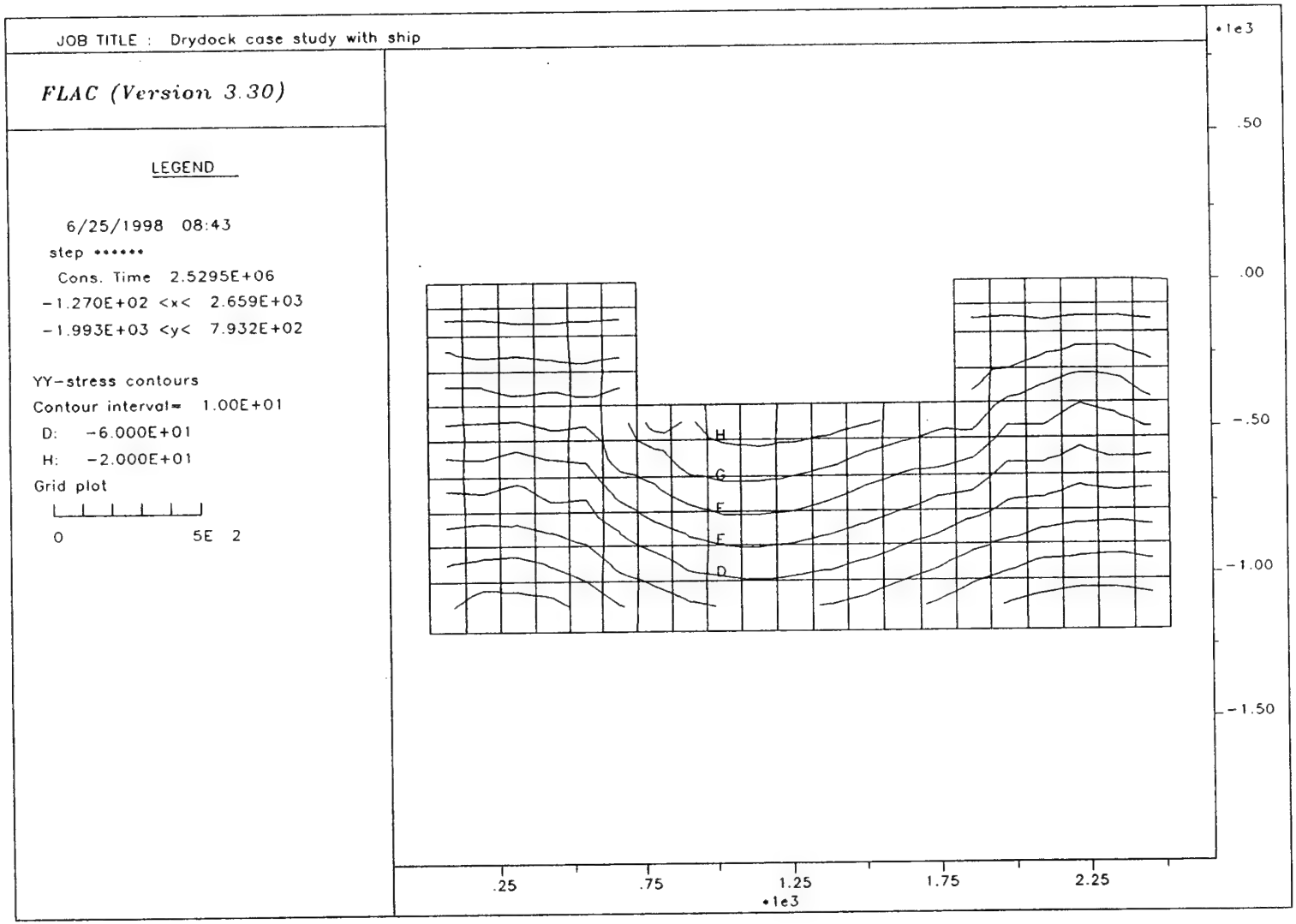

Figure 25. Vertical stress, dock empty.

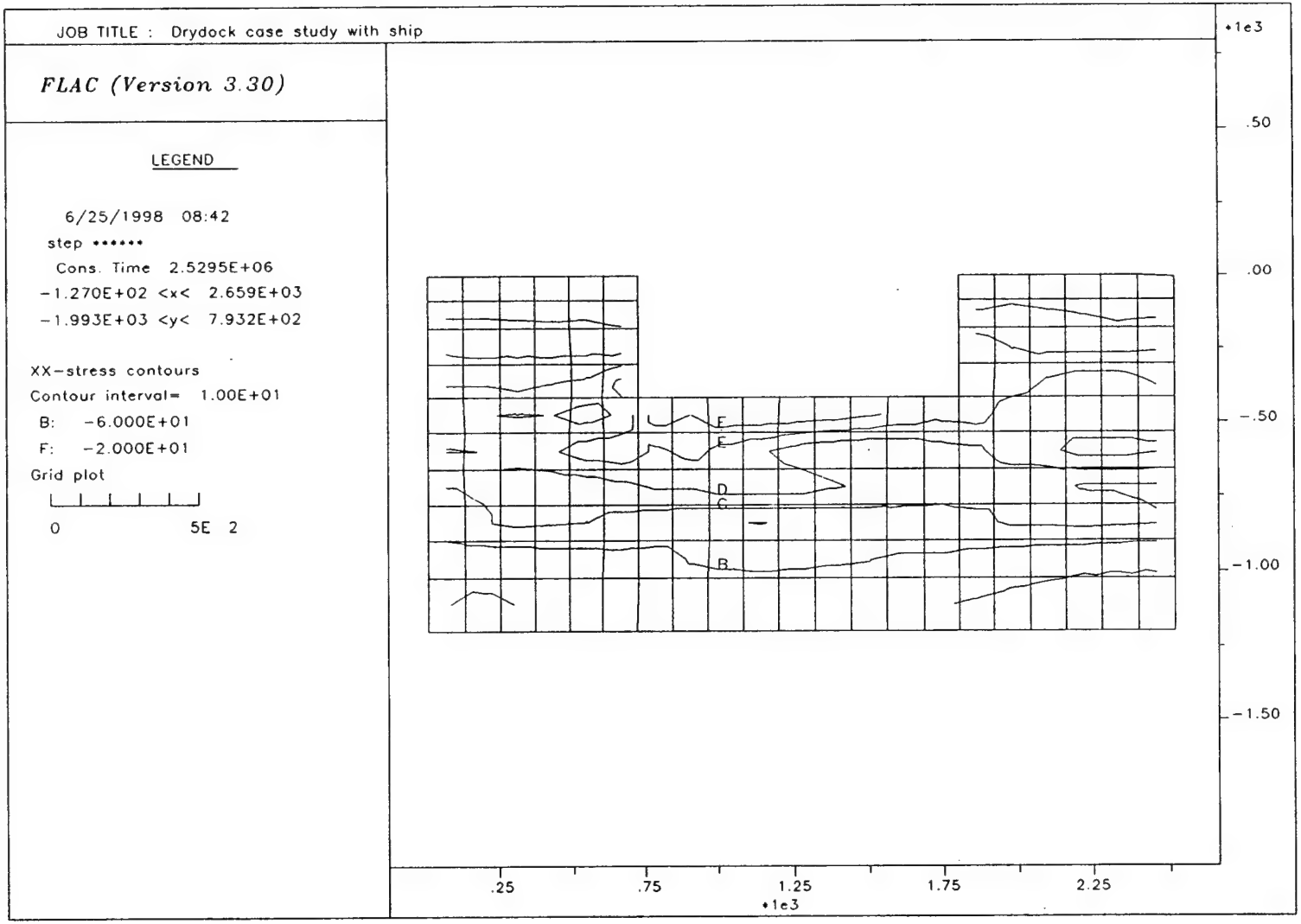

Figure 26. Horizontal stress, dock empty.

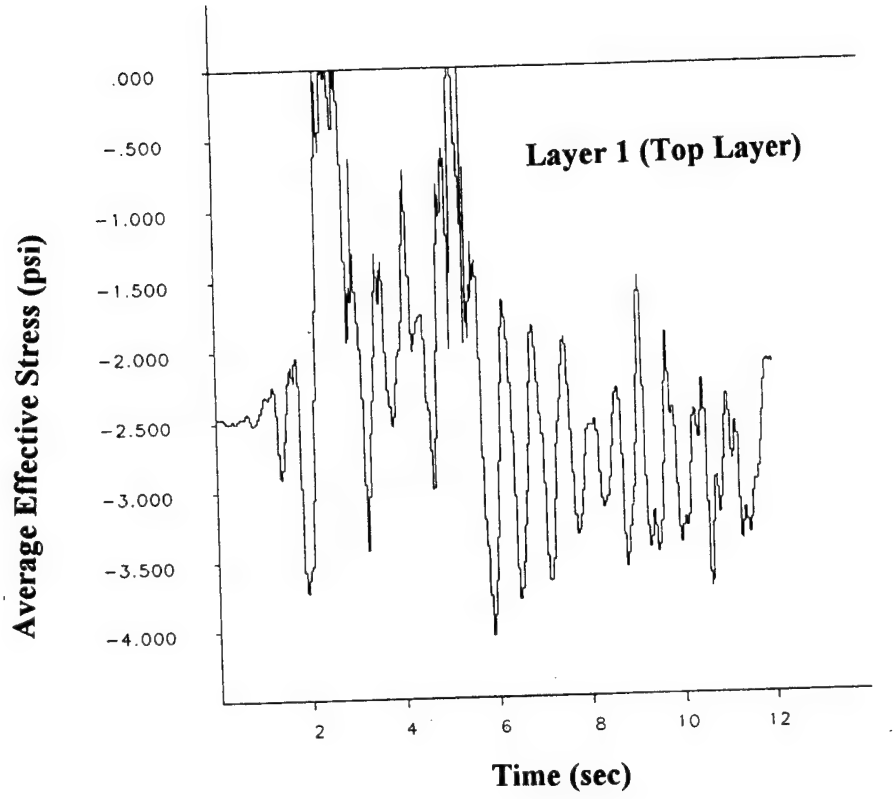

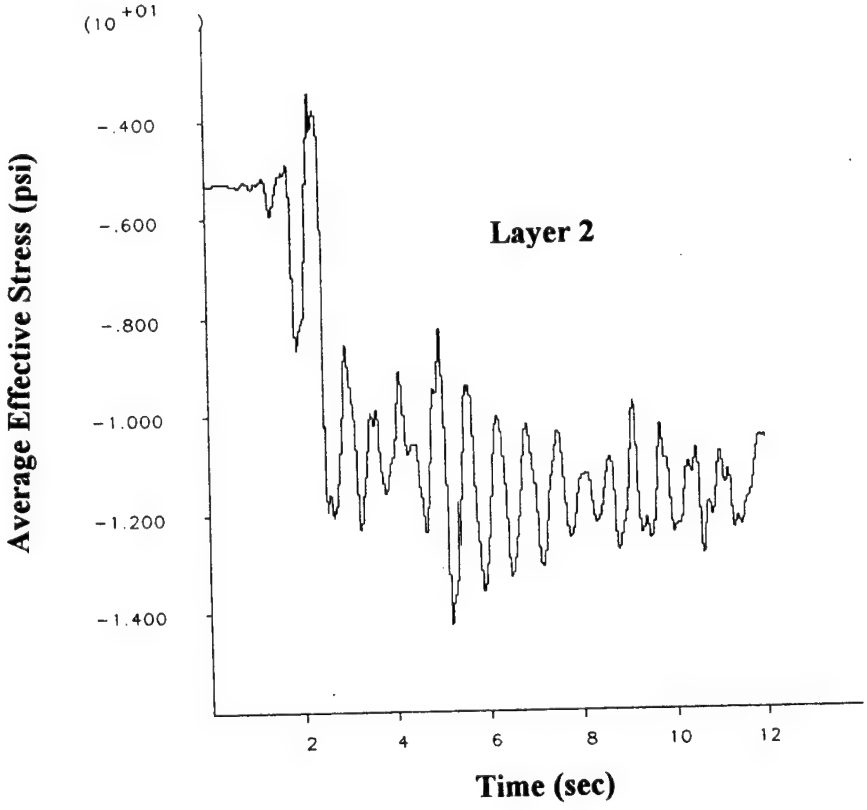

Figure 27a. Effective average confining stress, drydock empty.

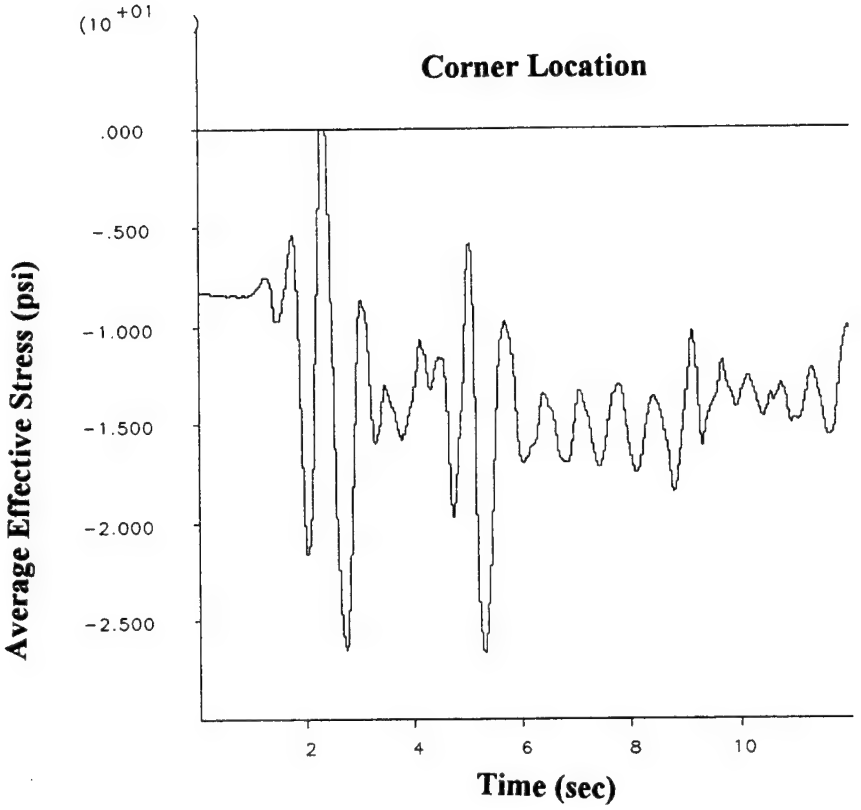

Figure 27b. Effective average confining stress, drydock empty.

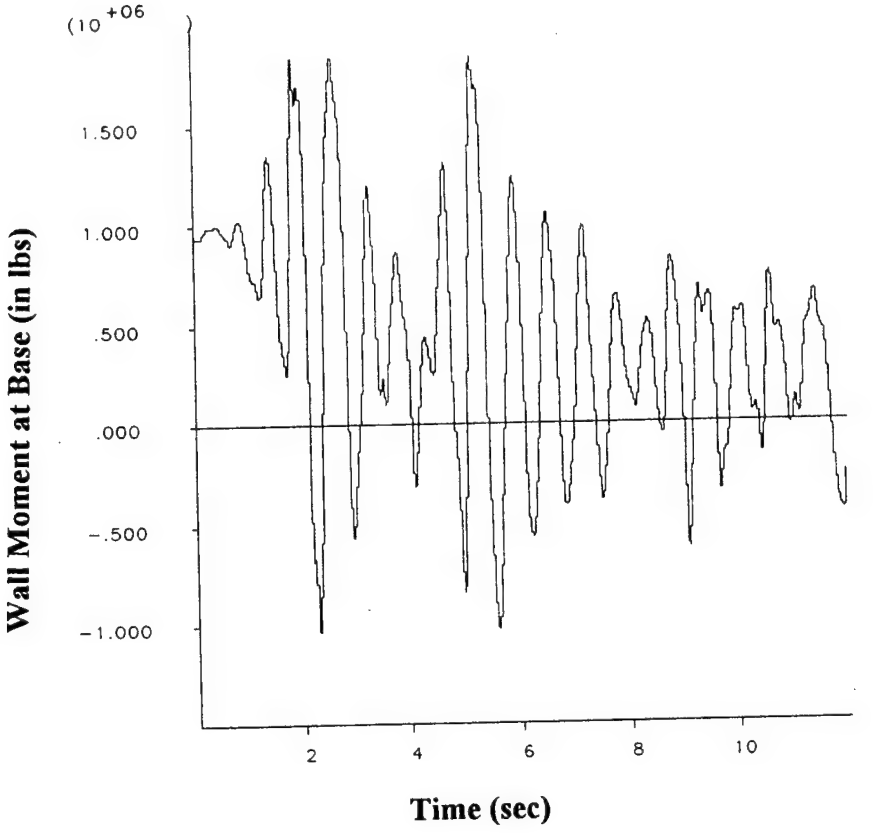

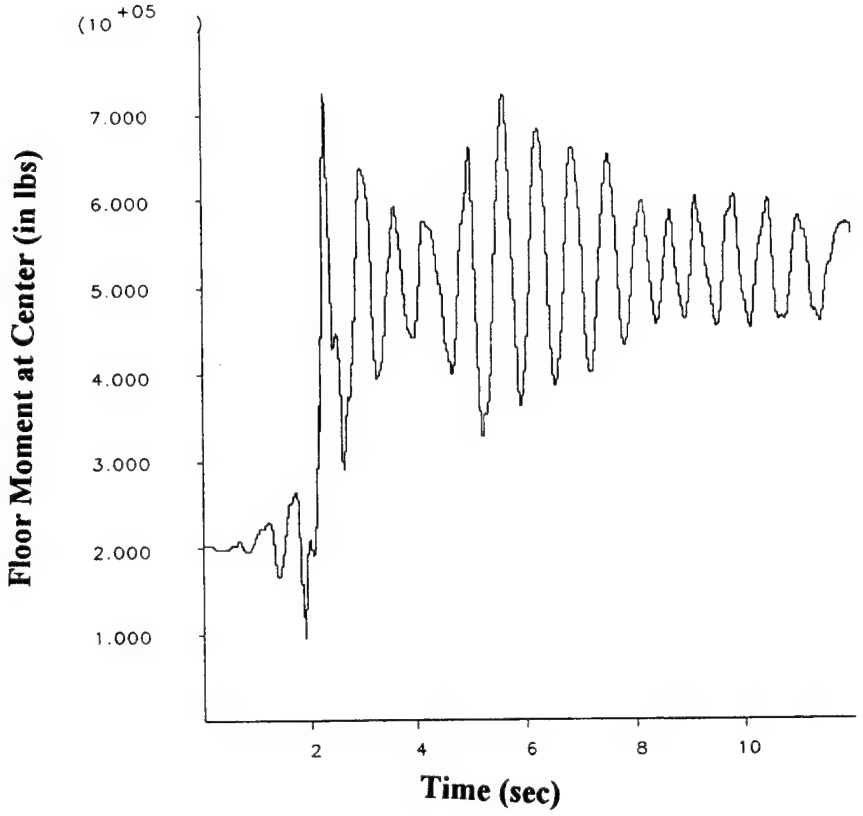

Figure 28. Moments in wall and floor, with ship.

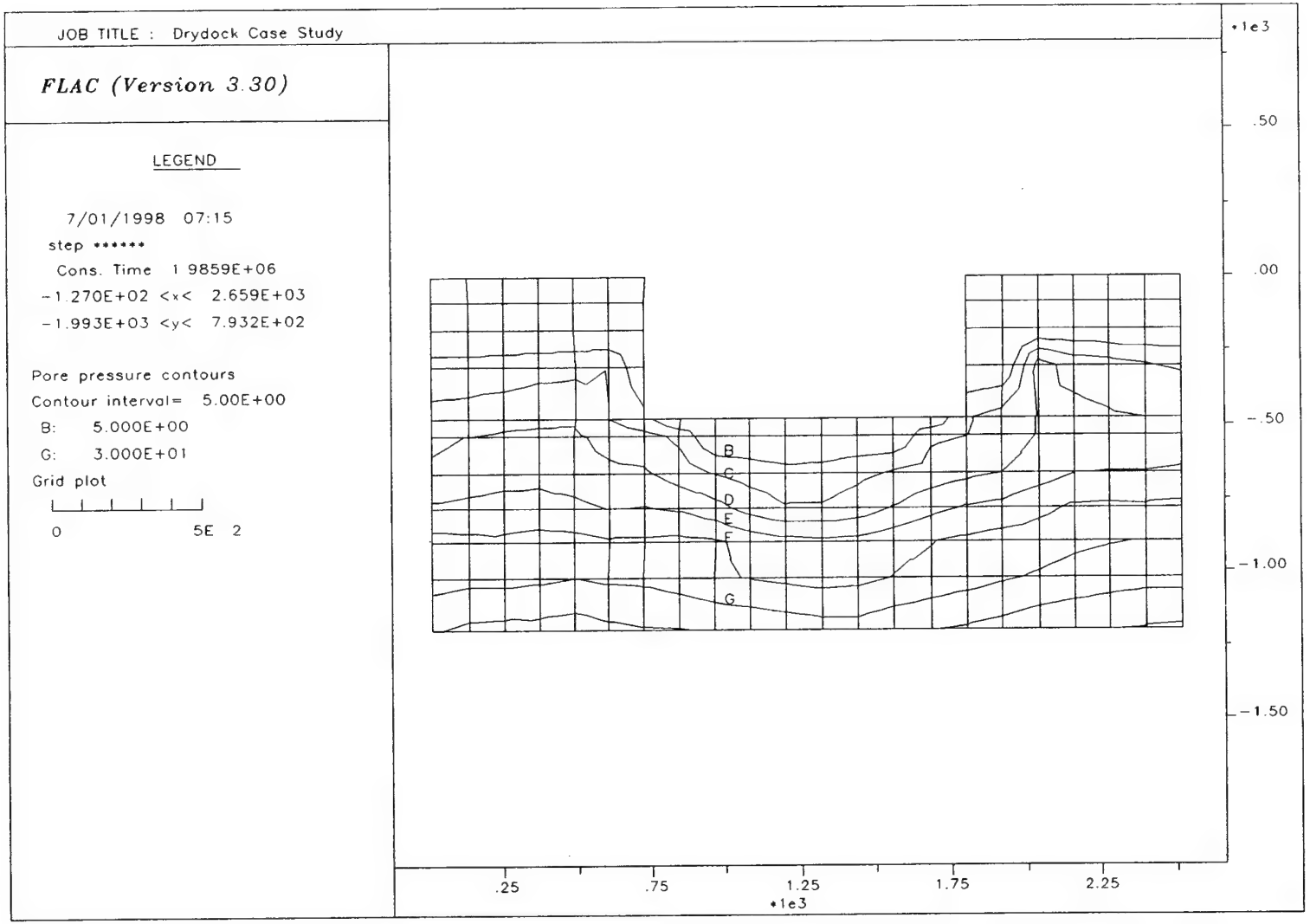

Figure 29. Pore pressure contours.

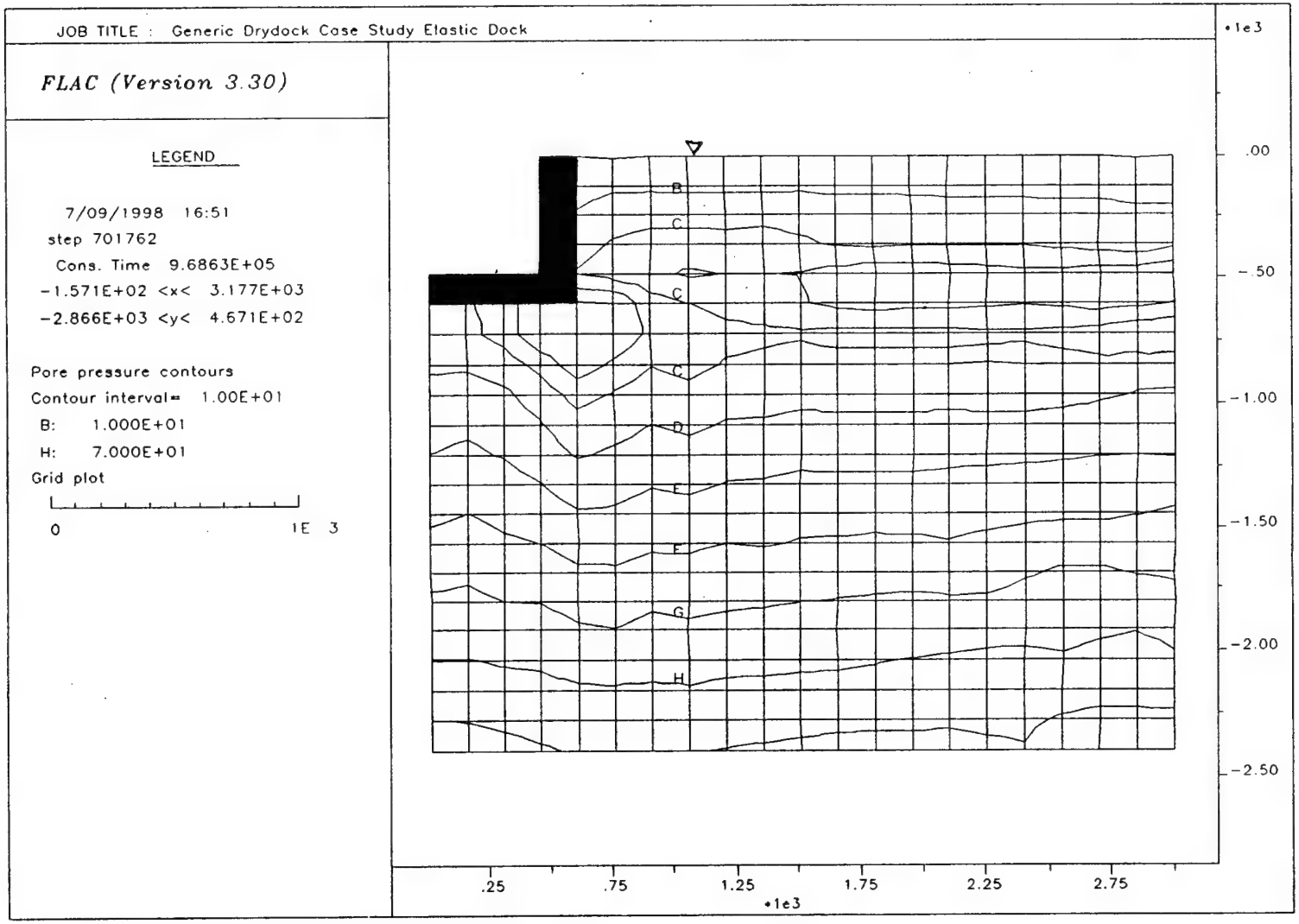

Figure 30. Pore pressure contours.

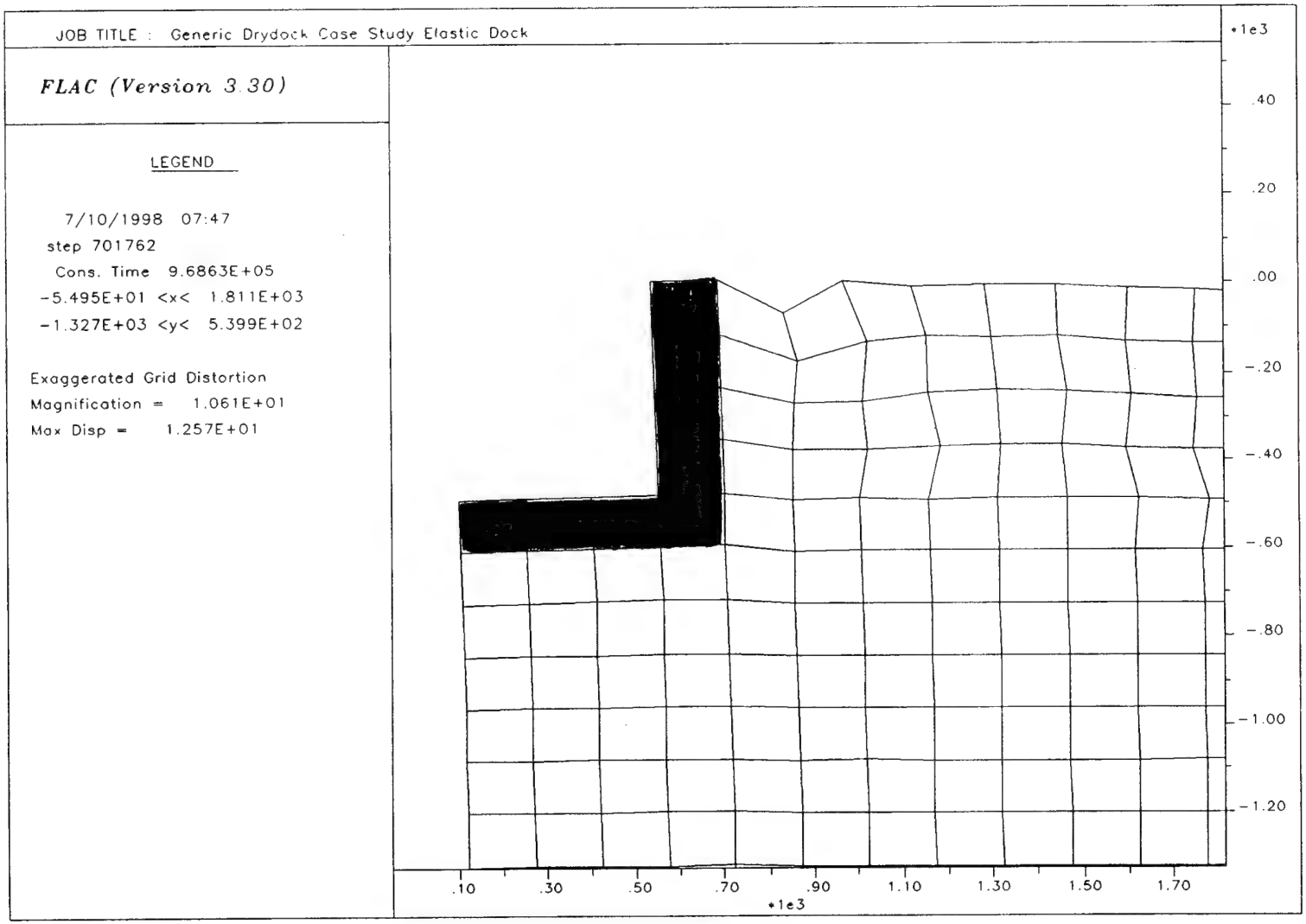

Figure 31. Magnified soil grid deformation.

Figure 32. Drydock wall static moment.

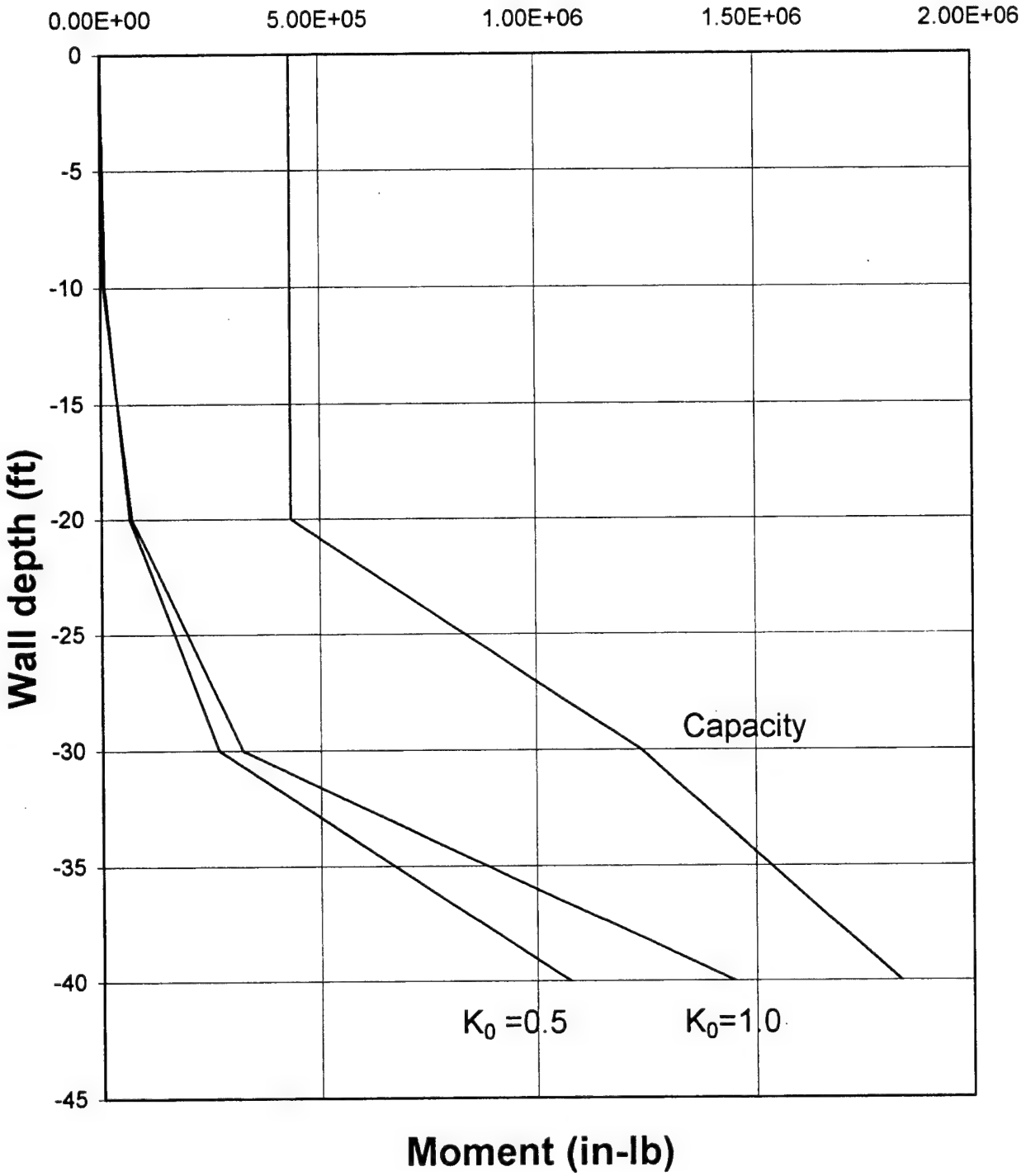

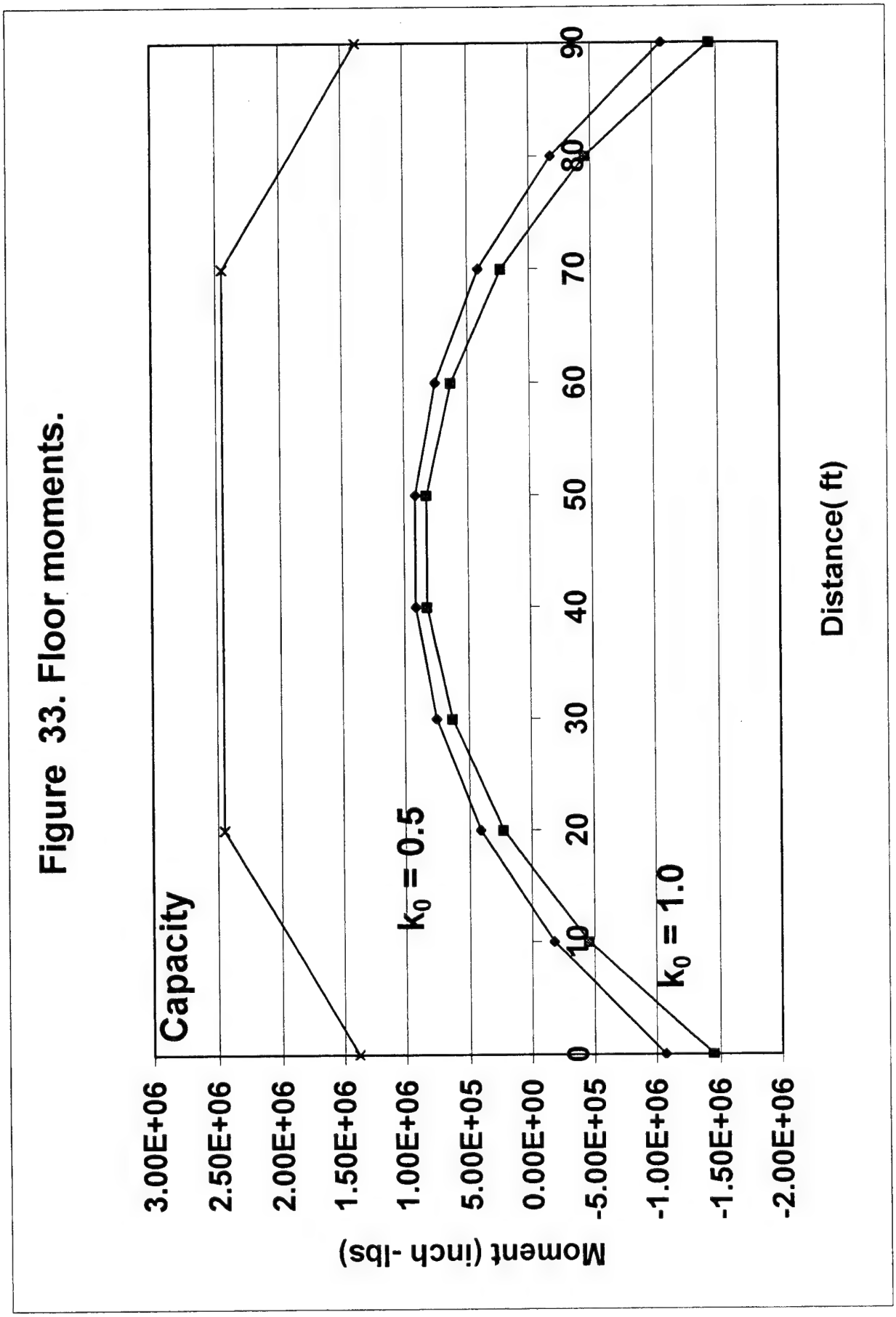

Figure 33. Floor moments.

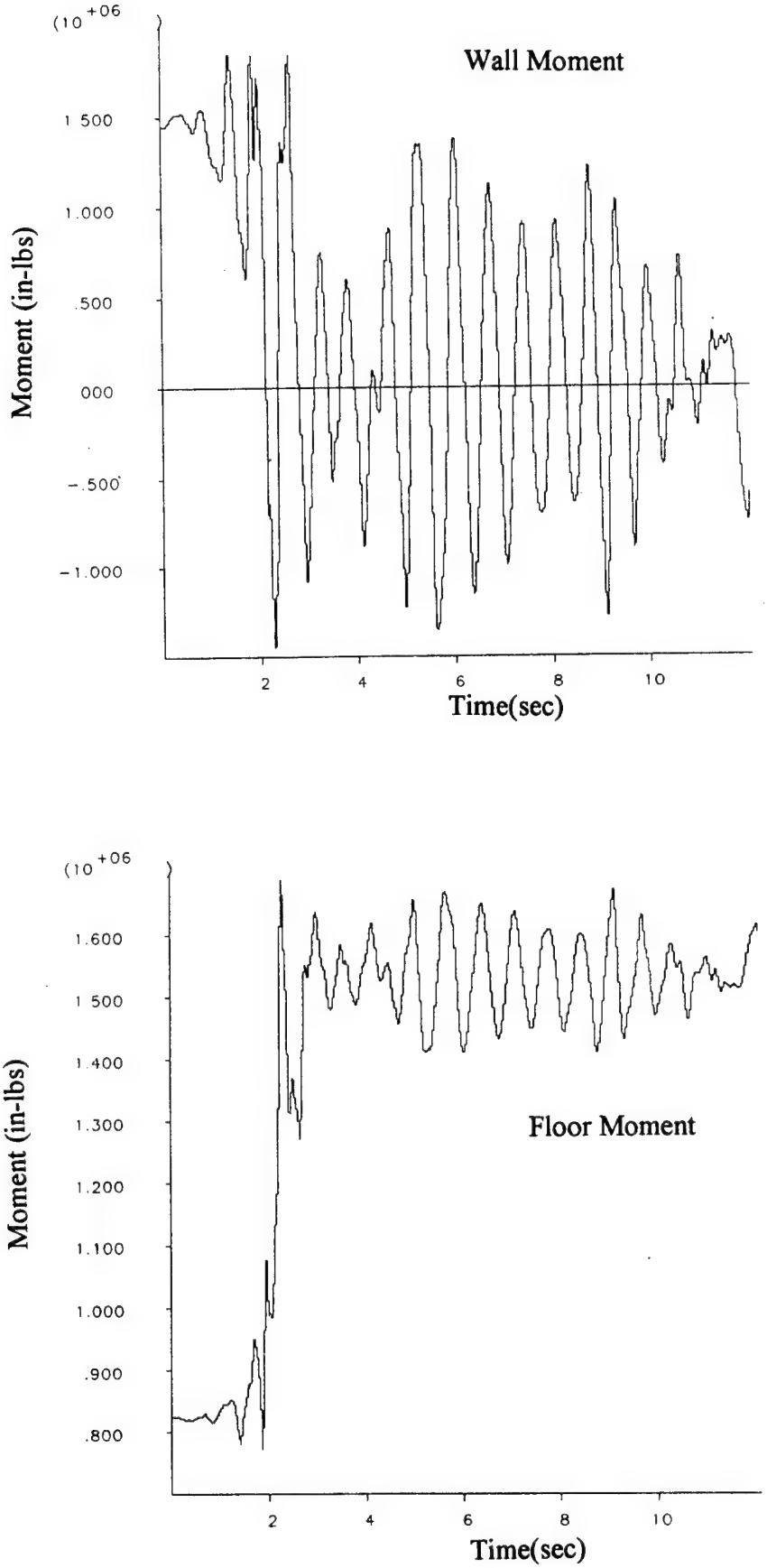

Figure 34. Drydock floor and wall dynamic moments.

Figure 35. Probability of not exceeding acceleration.

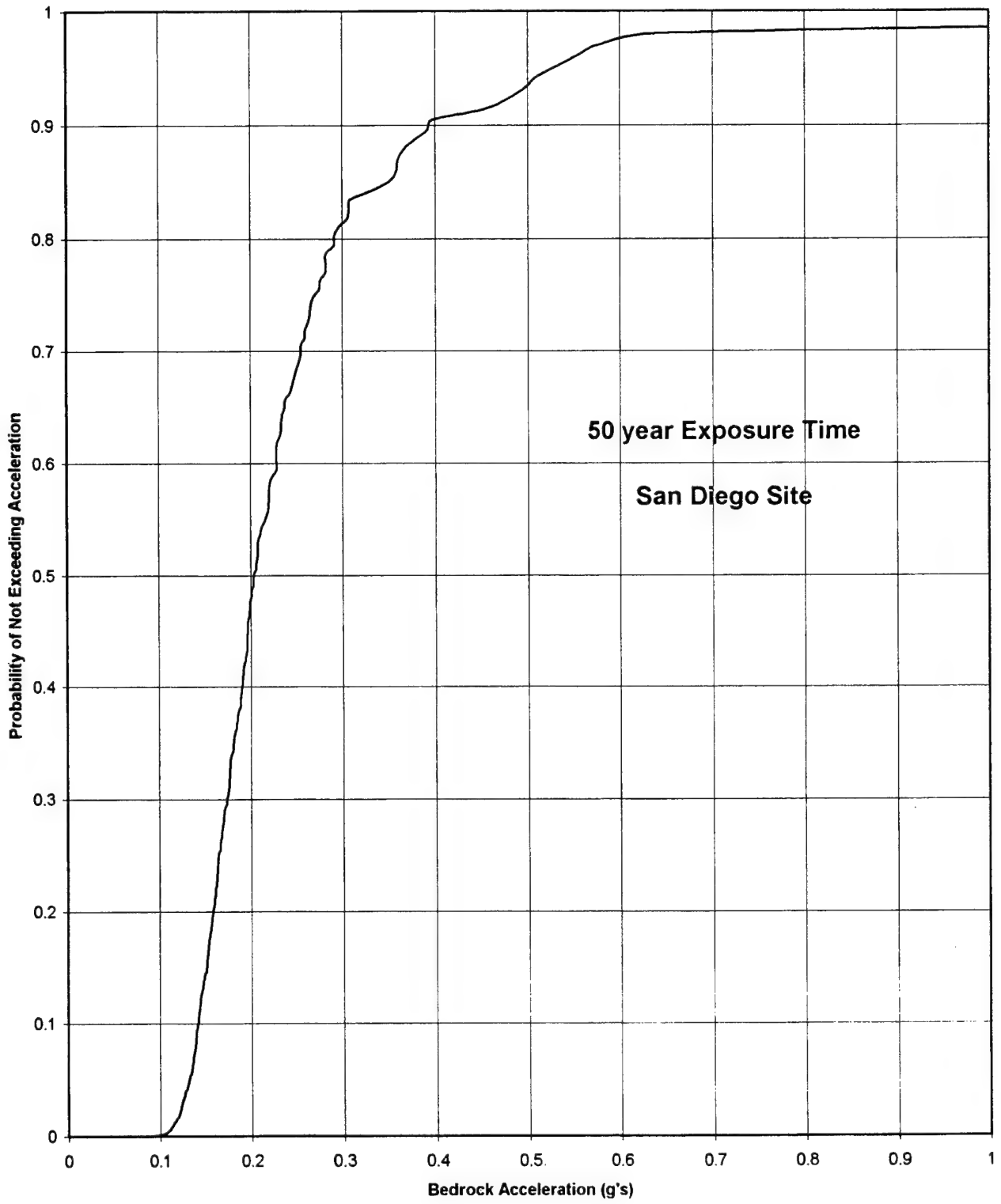

Figure 36 . Probability distribution

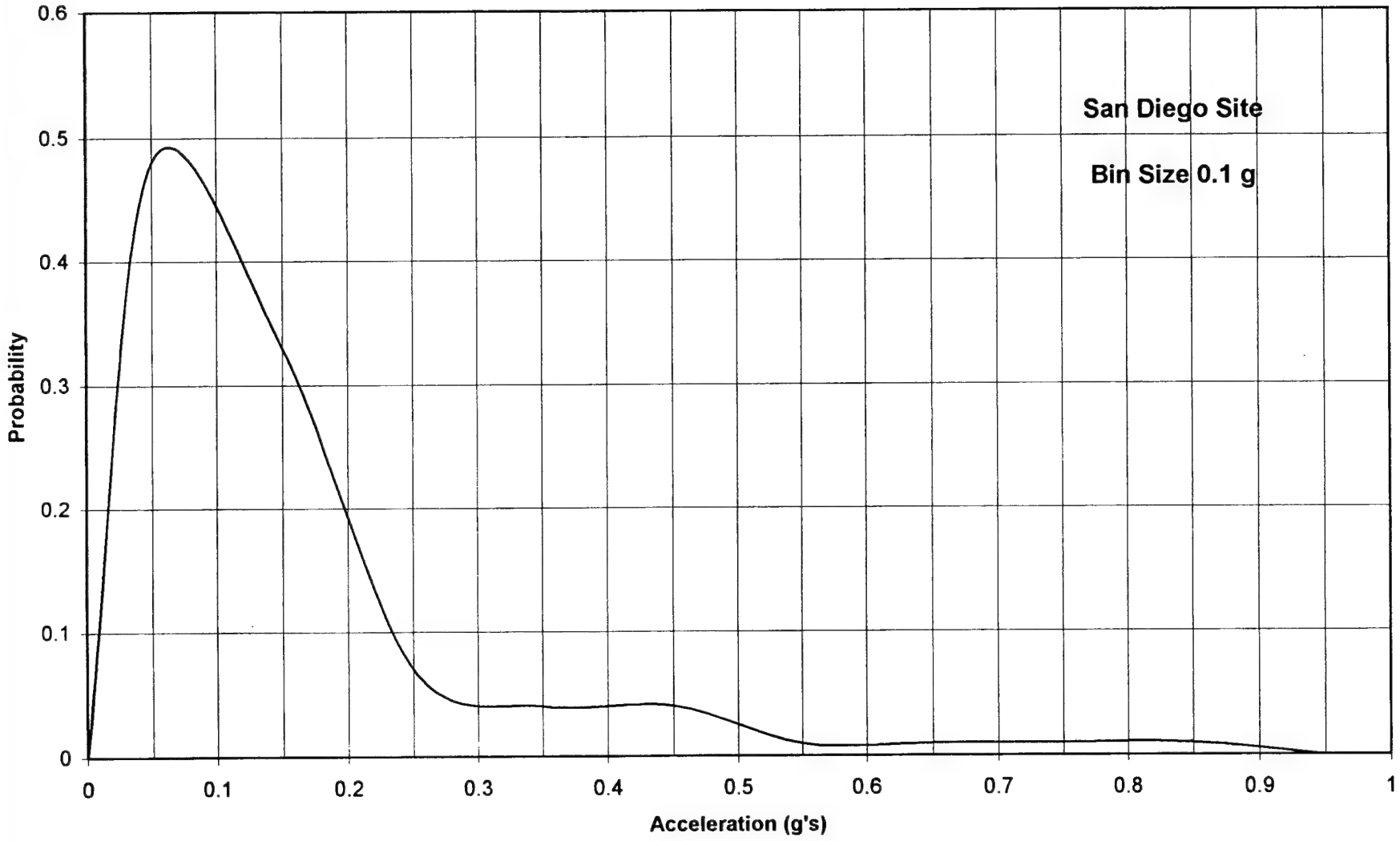

Figure 37. Damage and earthquake return time.

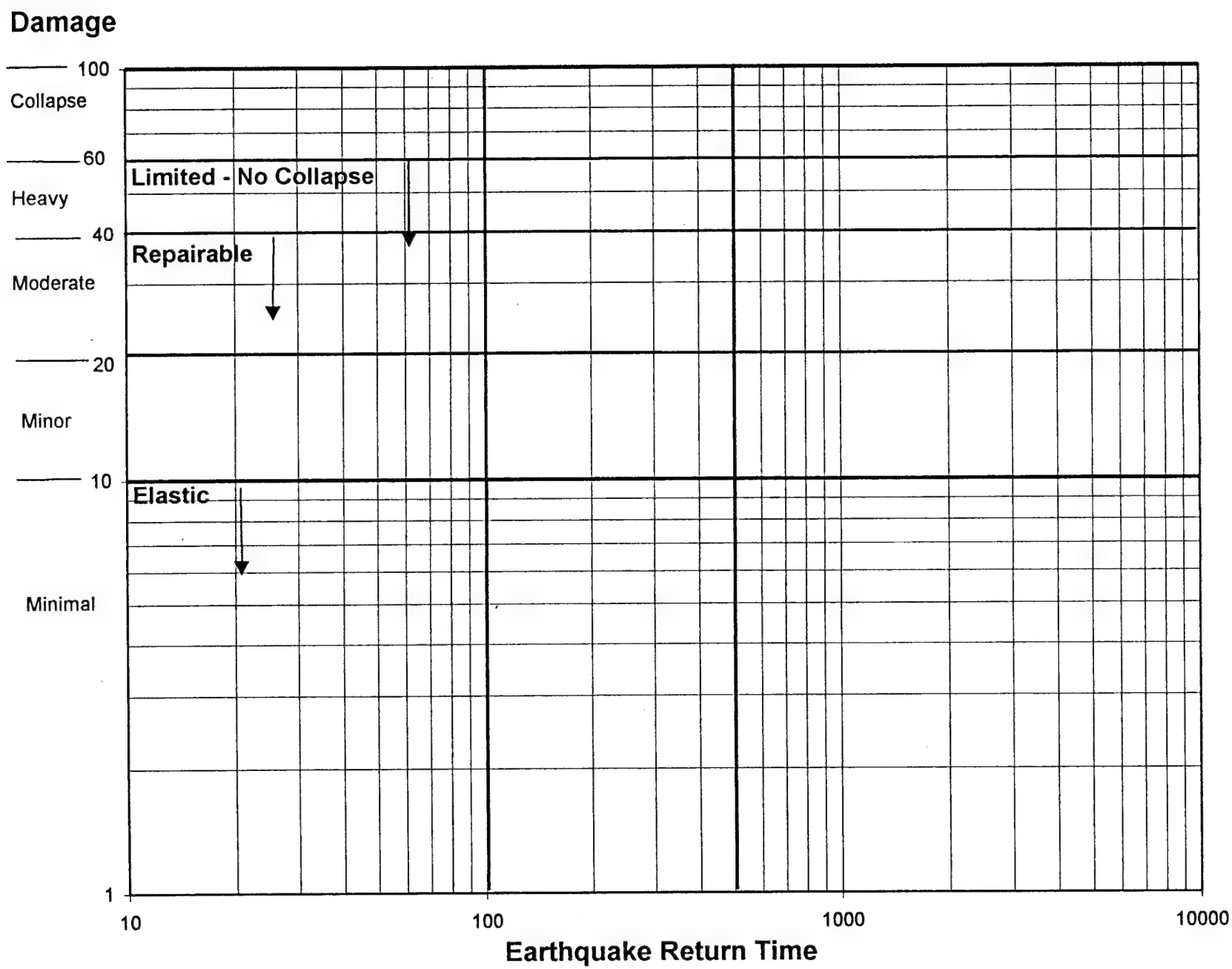

Figure 38. Drydock damage.

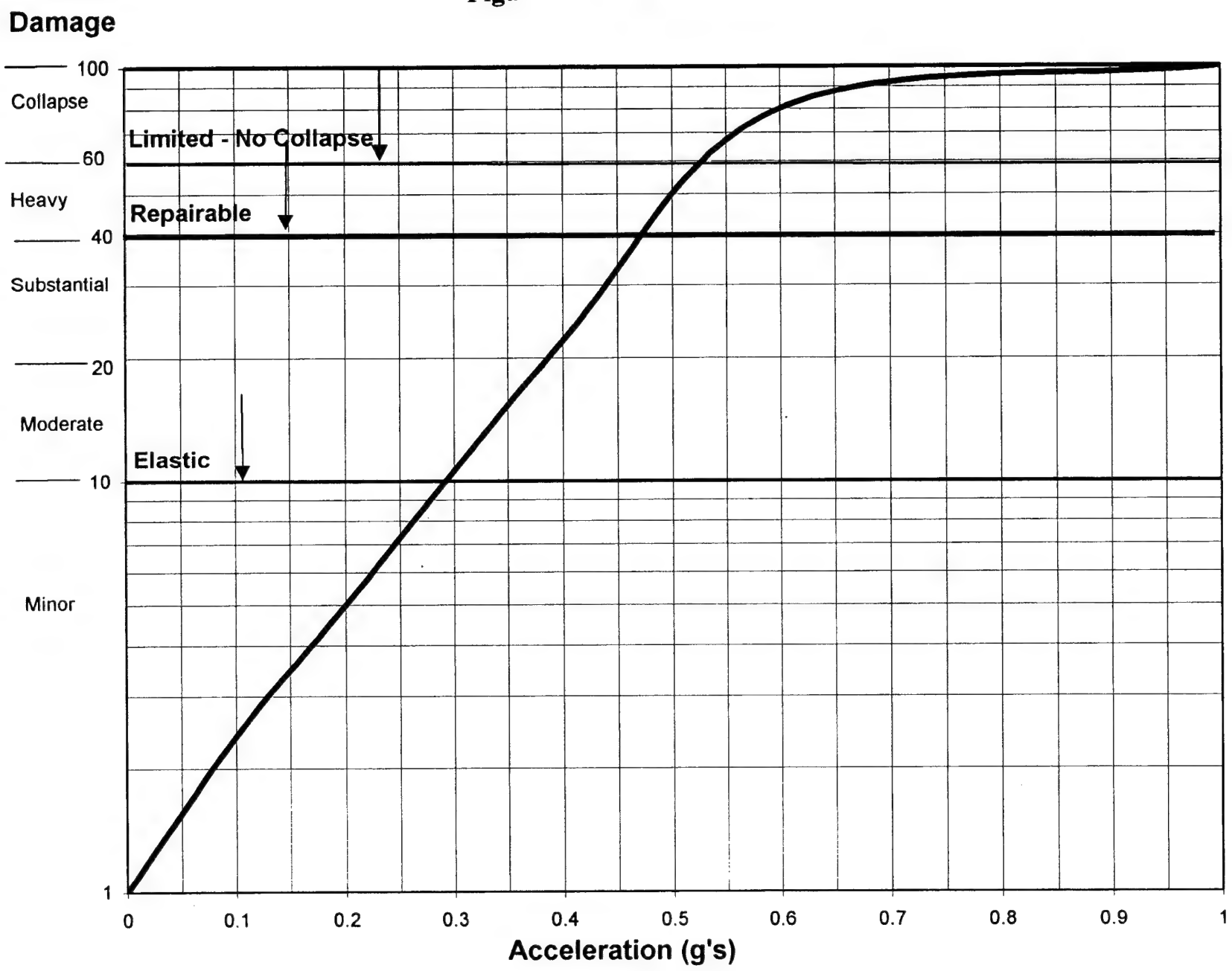

Figure 39. Drydock damage as a function of return time.

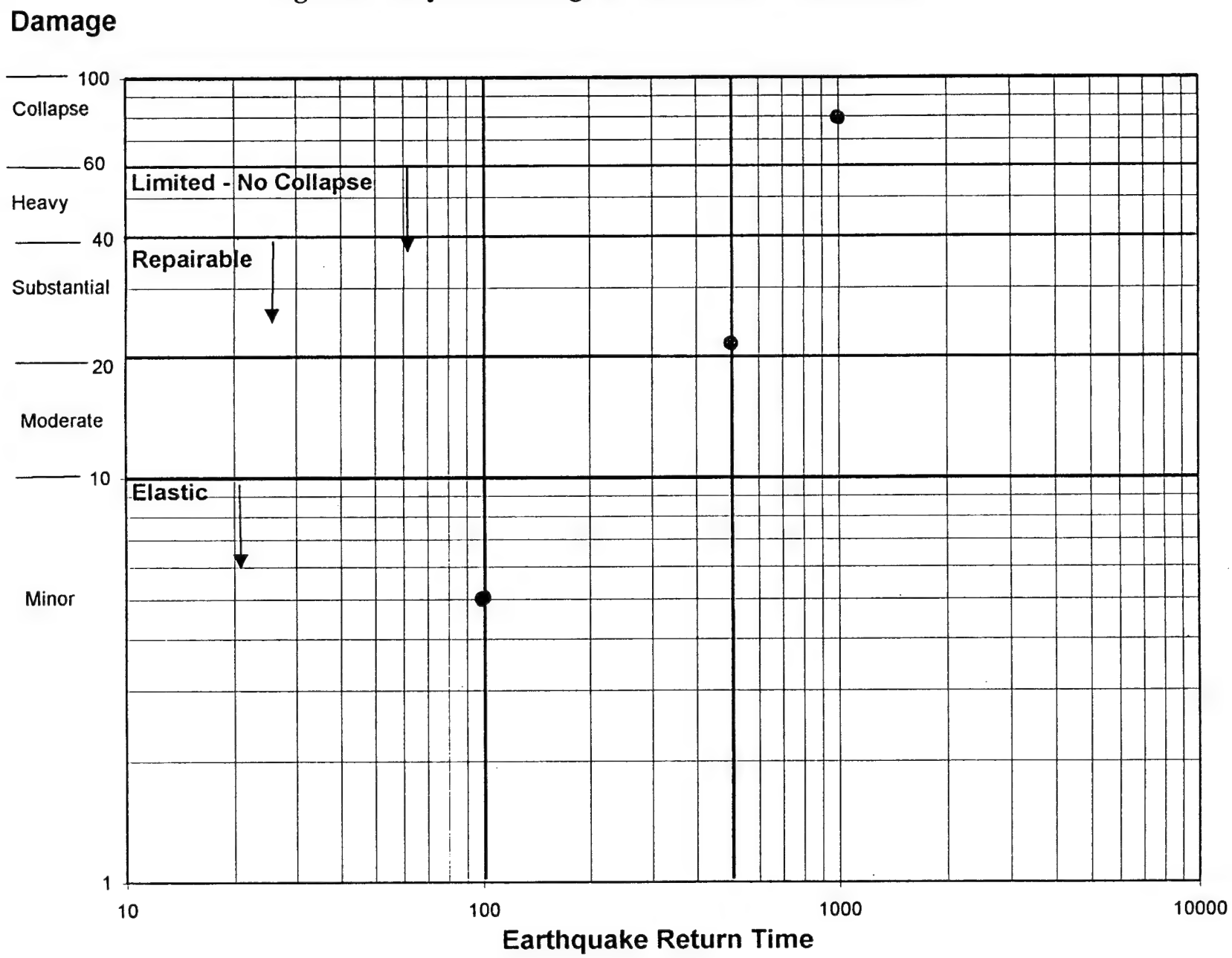

Figure 40. General damage criteria.

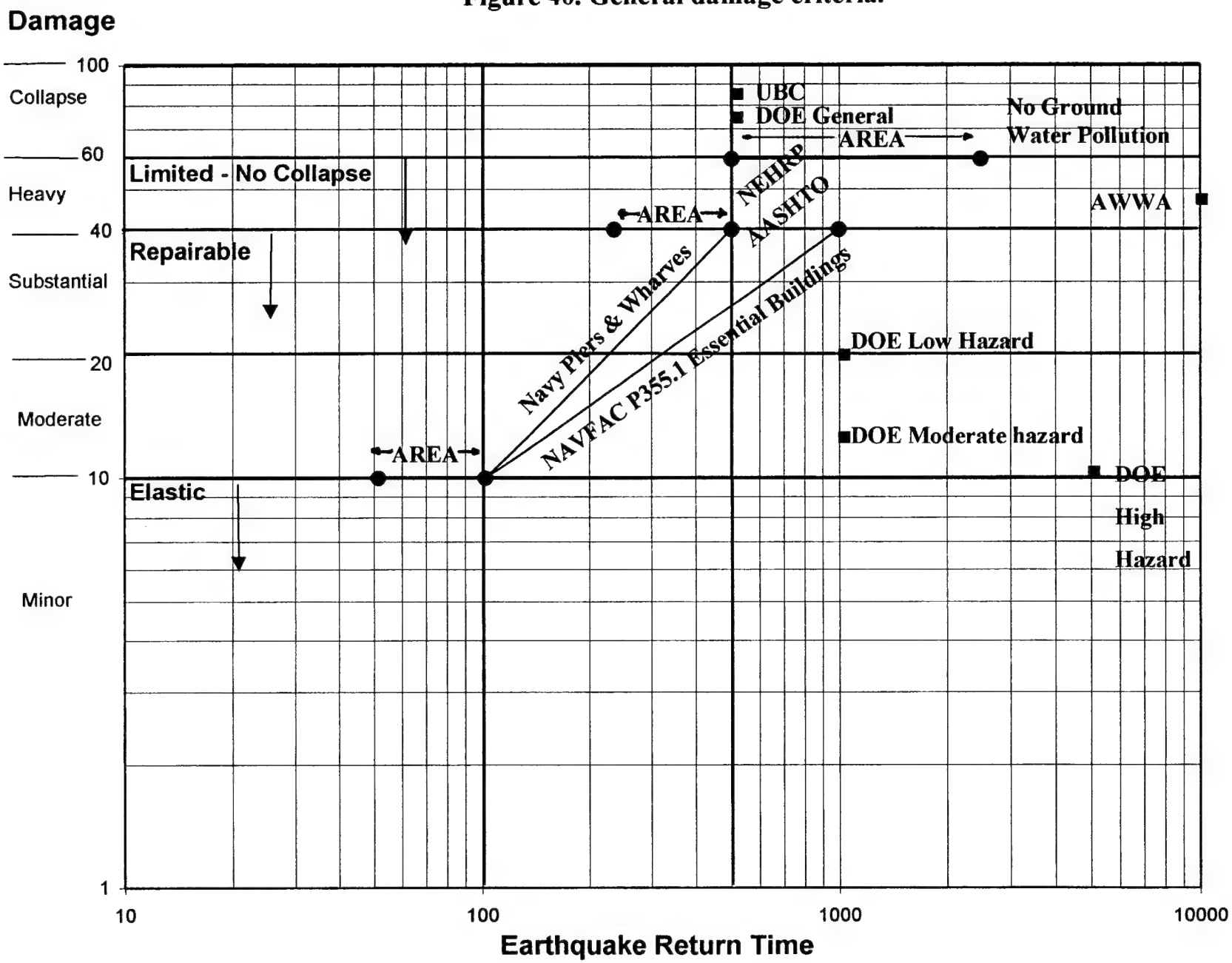

APPENDIX

Equivalent Properties Of

Reinforced Concrete Section

Yield-Stress Moment And Moment Of Inertia

The initial yield moment of a reinforced-concrete cross section may be defined as the moment required for the steel in tension or the concrete in compression to just reach its yield limit. The reinforcement provided in actual construction must be governed by the former case; therefore, only the derivation for the under-reinforcement case (steel-in-tension yield) is described below. For typical cross section of a reinforced-concrete, the strain diagram is assumed linear and A and A' are the areas of the steel reinforcement in tension and compression, respectively. The strain level in tension steel is ε_t, in concrete is ε_c, and in compression steel is ε'. The strains are related by the following equations:

$$\frac{\varepsilon_t}{\varepsilon_c} = \frac{d - Kd}{Kd} = \frac{-(1-K)}{K}$$

$$\frac{\varepsilon'}{\varepsilon_c} = \frac{d' - Kd}{Kd} = \frac{-((d'/d) - K)}{K}$$

(1)

The stresses in steel are as follows:

$\sigma_s = -n\,\sigma_c\,(1-K) / K$ stress in tension steel (2a)

$\sigma_s' = -n\,\sigma_c\,((d'/d)-K) / K$ stress in compression steel (2b)

where $n = E_S/E_c$, the ratio of modulus of elasticity of steel to concrete.

Denoting the area of steel as a fraction of the area of the concrete section, i.e.,

$$p = A_s /(b\,d)$$

$$p' = A_s' / (b\,d) \qquad (3)$$

The equation of equilibrium becomes

$$\sigma_s A_s + \sigma_s' A_s' + \tfrac{1}{2}\,\sigma_c\,K\,b\,d = 0$$

(4)

This can be rewritten after some arrangement into the form

$$K^2 + 2(np + np')\,K - (2np + 2np'\,d'/d) = 0$$

Therefore the solution of K becomes

$$K = [\,(2np + 2np'\,d'/d) + (np + np')^2]^{1/2} - (np + np') \qquad (5)$$

The yield moment for the under reinforcement case is

$$M = \sigma_s\,As\,(d - Kd/3) + \sigma_s'\,A_s'\,(d' - K\,d/3)$$

or (6)

$$M = A_s\,J\,d\,\sigma_s$$

where

$$J = 1 - K/3 + (p'/p)\,(d'/d - K)(d'/d - K/3)/\,(1-K) \qquad (7)$$

If the solution of Equation 5 is such that K > d'/d, then the stress in compression steel is

$$\sigma_s' = 2n\,\sigma_c\,(d'/d - K)\,/\,K = 2\,(d'/d - K)\,\sigma_s\,/\,(1 - K) \qquad (8)$$

The equation of equilibrium for this case becomes

$$\sigma_s\,A_s + 1/2\,\sigma_c\,K\,b\,d - E_c\,\varepsilon'\,A' = 0 \qquad (9)$$

After some rearrangement, and the use of Equation 3, K becomes

$$K = \{\,2[np + (2n - 1)p'\,d'/d\,] + [np + (2n \_\ 1)p']^2\,\}^{1/2} \qquad (10)$$

$$-[np + (2n - 1)p']$$

The form of Equation 6 remains the same except that for this case, j is defined as

$$j = 1 - K/3 - (\,(2n - 1)\,K - 2n\,d'/d)\,(p'/p)(d'/d - K/3)\,/\,(n(1-K)) \qquad (11)$$

The transformed section moment of inertia is given by

$$I_c = 1/3\,b\,K\,d^3 + n\,A_s\,(d - Kd)^2 + (n - 1)\,A_s'\,(Kd - d')^2 \qquad (12)$$

The value of I_c is the moment of inertia of the cracked concrete section of width b considering the compression concrete area and steel areas transformed into equivalent concrete areas and computed about the centroid of the transformed section. I_c may also be calculated from

$$I = F\, bd^3 \qquad (13)$$

The coefficient F varies as the modular ratio n and the amount of reinforcement used.

Ultimate Strength Moment Capacity

The ultimate unit resisting moment M_u of a rectangular section of width b with tension reinforcement only is given by

$$M_u = A_s f_y (d - a/2) \qquad (14)$$

where

A_s = area of tension reinforcement, sq in

a = static design yield stress for reinforcement, psi

f_y = distance from extreme compression fiber to centroid of tension reinforcement, in.

d = depth of equivalent rectangular stress block = $A_s f_y / 0.85\, b\, f_c'$, in.

b = width of compression face, in.

f_c' = static ultimate compressive strength of concrete, psi

The reinforcement ratio p is defined as

$$P = A_s / bd \qquad (15)$$

For a rectangular section of width b with compression reinforcement, the ultimate unit resisting moment is

$$M = (As - As') f_y (d - a/2) + A_s' f_y (d - d') \qquad (16)$$

where

A_s' = area of compression reinforcement, in.

d' = distance from extreme compression fiber centroid-of compression reinforcement, in.

a = depth of equivalent rectangular stress block

Equation 16 is valid only when the compression steel reaches the value f_y at ultimate strength, and this condition is satisfied when

$$p - p' > 0.85 K_1 [(f_c' d') / (f_y d)] [87,000/(87,000 - f_y)] \quad (18)$$

If p - p' is less than the value given by Equation 18 or when compression steel is neglected, the calculated ultimate unit resisting moment should not exceed that given by Equation 14. The quantity p - p' must not exceed 0.75 of the value of P_b.

Modulus Of Elasticity

The modulus of elasticity of concrete Ec may be computed by

$$E_c = w^{1.5} \quad 33 (fc')^{½} \quad psi \quad (19)$$

for values of w between 90 and 155 lb/ft^3, where w is the unit weight of concrete and normally equal to 145 lb/ft^3.

The modulus of elasticity of reinforcing steel E_s is

$$E = 29,000,000 \text{ psi} \quad (20)$$

The modular ratio n is

$$n = E_s / E_c \quad (21)$$

and may be taken as the nearest whole number.

ACI Code Approach For Computing Moment Of Inertia For Deflection

Since finite element analysis techniques require a characterization of the stiffness of the structural element, it is important to review several approaches for estimating moment of inertia.

The ACI code states that where deflections are to be computed, those which occur immediately on application of load shall be computed by the usual methods or formulas for elastic

deflections. Deflections shall be computed taking the modulus of elasticity for concrete as specified in Equation 19 and taking the effective moment of inertia as follows.

$$Ic = (M_{cr} / M_a)^3 I_g + [1 - (M_{cr} / M_a)^3] I_{cr} \leq Ig \qquad (22)$$

where

$$M_{cr} = f_r I_g / y_t \qquad (23)$$

and

$f_r = 7.5 (f_c')^{1/2}$

I_{cr} = moment of inertia of cracked section transformed to concrete

I_c = effective moment of inertia for computation of deflection

I_g = moment of inertia of gross concrete section about the centroidal axis, neglecting the reinforcement

M_a = maximum moment in member at stage for which deflection is a being computed

M_{cr} = cracking moment

y_t = distance from centroidal axis of gross section, neglecting the reinforcement, to extreme fiber in tension

Special provisions are included for lightweight aggregate.

Equivalent Modulus Approach For Computing Deflection

Another approach for stiffness evaluation is the equivalent modulus. Assume that the displacements in a reinforced concrete beam are in the following form:

$$u(x,y,z) = (\partial W(x)/ \partial x)\ z = - W'(x)z$$

$$v(x,y,z) = 0 \qquad (25)$$

$$w(x,y,z) = W(x)$$

and the strains

$$\varepsilon_{xx} = (\partial^2 W(x) / \partial x^2) z = - W'' (x)z$$

$$\varepsilon_{zz} = \varepsilon_{yy} = \varepsilon_{xz} = \varepsilon_{xy} = \varepsilon_{yz} = 0 \tag{26}$$

Assuming that the vertical stress $\sigma_{zz} = 0$

$$(\lambda + 2G)\,\varepsilon_{zz} + \lambda\,(\varepsilon_{xx} + \varepsilon_{yy}) = 0$$

$$\varepsilon_{zz} = -[\lambda / (\lambda + 2G)]\,(\varepsilon_{xx} + \varepsilon_{yy}) = -[\lambda / (\lambda + 2G)]\,W''(x)z \tag{27}$$

and

$$\sigma_{xx} = (\lambda + 2G)\,\varepsilon_{xx} + \lambda\,(\varepsilon_{zz}) = [(\lambda + 2G) - (\lambda^2 / (\lambda + 2G))]\,\varepsilon_{xx}$$

$$= [E / (1 - \nu^2)]\,\varepsilon_{xx} = (D/I)\,\varepsilon_{xx} = -(D/I)\,W''(x)z \tag{28}$$

where

$$D = EI / (1 - \nu^2)$$

Now the moment M_x is given by

$$M_x = -b \int_{-h/2}^{h/2} \sigma_{xx} z\,dz$$

$$M_x = DW''(x) \tag{29}$$

From the strain distribution

$$W''(x) = \varepsilon_t / [(1 - k)\,d] \tag{30}$$

$$\varepsilon_t = (1 - k)\,dW''(x)$$

Moment of the section is then given by

$$M = A_s\,jd\;\sigma_s = A_s\,jd\,E_s\,\varepsilon_t \tag{31}$$

$$M = A_s\,j\,E_s(1 - k)\,d^2\;W''(x) = DW''(x)$$

Also

$$D = A_s\,j\,E_s\,(1 - k)\,d^2 = EI / (1 - \nu^2)$$

Therefore the effective E for the concrete section is given by

$$E = A_s j E_s(1 - k) d^2 (1 - \nu^2) / I \qquad (32)$$

where I is I_g,

Average Moment of Inertia

An alternative approach used in blast resistant design uses the average moment of inertia of the cracked and gross moments of inertia.

Analysis By Equivalent Beam

A brief comparison study was conducted to evaluate the ability to duplicate the load-deflection history observed in test data and to duplicate failure modes and ultimate resistance. Beam elements were selected as the most direct technique to represent the test beams, using an elasto-plastic material model. The material model for elasto-plastic beams requires definition of a rectangular section, elastic modulus, Poisson's ratio, and yield stress. The decision was made to use the actual beam cross section dimension thus implicitly specifying a gross moment of inertia.

Tension Failure There were three choices for determination of stiffness namely:

(1) ACI approach using Equation 23, to determine effective I and concrete modulus

(2) Average approach using to determine average I_a and concrete modulus and

(3) Equation 32 to determine effective E and gross I.

The results of 1 and 3 were identical; however 2 gave a stiffness 1.28 times greater The conclusion in this case is that gross moment of inertia is effective only at very low loads (less than 10 percent of ultimate moment). The use of cracked moment of inertia is a better representation of behavior.

Compression Failure The cracked moment of inertia was used to estimate stiffness. The analysis is dependent upon the solution process. A finite element implicit analysis with equibrilibium checking terminated prematurely. The solution without equilibrium check terminated with a stiffness matrix not being positive-definite at the point when a full plastic moment developed at mid-span indicating a failure mechanism. It is important to note that the finite element representation does not give any indication of the type of failure or stress condition in the actual beam. Thus it is necessary to analyze the actual section to determine its failure mode. Initial observation would be misleading and indicates a tension failure having large yield capacity. The actual failure was a sudden brittle compression failure.

Shear Failure The cracked moment of inertia was used to estimate the stiffness. The stiffness in this analysis is greater than the actual. This is a limitation of an elasto-plastic model when the beam exhibits early nonlinearities. Although the initial stiffness is in agreement, the overall stiffness is about half that originally estimated based on a cracked section. This is attributed to the shear mode of failure. The results of the analysis show that the shear stress of the cross section would be exceeded. However, the user must adjust the results since no internal failure mechanism exists for shear. The exact occurrence of the point of shear failure is unknown since the beam computationally yields rapidly and the exact failure shear stress is not known. The burden is placed upon the user to note shear failures since the solution will proceed. This is a critical limitation in cases of multicomponent structures since the solution would not be valid past the point of shear failure.

Material Models for Concrete

Drucker-Prager Model it is convenient to derive relationships which are based upon terms that are independent of axis orientation. There are functions of the stress or strain tensors which have the same definition regardless of the coordinate system in which they are defined. They are called the stress or strain "invariants" J_1 and J_2, where J1 and J2 are defined as the first and second stress invariant respectively. The first invariant of the stress tensor J1 equals three times the average hydrostatic stress or pressure. The first invariant is generally used in constitutive relationships to introduce the influence of volumetric or hydrostatic effects. The shearing, or deviatoric portion of the stress or strain tensor is referred to as the deviatoric. The invariants of the deviatoric are distinguished by primes. The first invariant of the stress deviatoric, Ji = 0 indicating the absence of volumetric effects. The second invariant of the stress deviatoric, J2' is a function of the maximum shearing stresses. It is also related to the shear stress acting on the octahedral plane which is the plane perpendicular to a line equidistant from the 3 major axes in principle stress space. The normal and shear stresses acting on this plane are defined as:

$$\sigma_{oct} = 1/3 \ \sigma_{ii} = p$$

$$\tau_{oct} = 1/3 \ [(\sigma_{11} - \sigma_{22})^2 + (\sigma_{22} - \sigma_{33})^2 + (\sigma_{33} - \sigma_{11})^2]^{1/2}$$

The second invariant of the deviatoric is generally used to provide an axis-independent means of introducing the influence of shearing behavior. Once plastic deformation is initiated, the constitutive equations of elasticity are no longer valid. Because plastic strains depend upon the entire loading history of the material, plastic stress-strain relations very often are given in terms of strain increments - the so-called incremental theories. By neglecting the elastic portion and by assuming that the principal axes of strain increment coincide with the principal stress axes, the Levy-Mises equations relate the total strain increments to the deviatoric stress components through the equations

$$d\varepsilon_{ij} = s_{ij}\, d\,\lambda$$

Here the proportionality factor $d\lambda$ appears in differential form to emphasize that incremental strains are being related to finite stress components. The factor $d\lambda$ may change during loading and is therefore a scalar multiplier and not a fixed constant. The above represents the flow rule for a rigid-perfectly plastic material. If the strain increment is split into elastic and plastic portions according to

$$d\varepsilon_{ij} = d\varepsilon^{\,E} + d\varepsilon_{ij}^{\,P}$$

and the plastic strain increments related to the stress deviator components by

$$d\varepsilon_{ij}^{\,P} = s_{ij}\, d\,\lambda$$

the resulting equations are known as the Prandtl-Reuss equations. This represents the flow rule for an elastic-perfectly plastic material. They provide a relationship between the plastic strain increments and the current stress deviators but do not specify the strain increment magnitudes.

The theories of plasticity utilized are generally limited to isotropic incremental flow theories for isotropic time-independent materials subjected to small strains under isothermal conditions. Yielding is generally defined to occur at some experimentally observed stress state. For example, a van Mises yield condition limits the square root of the second invariant of the stress deviatoric to some constant value, A.

$$\sqrt{J'^2} = A$$

For the Drucker-Prager yield condition the maximum shear stress is related to some function of the volumetric stress, -

$$\sqrt{J'^2} = A + \alpha J_1$$

where A and *a* are constants and the square root of J_2 is generally used to maintain units of stress. For the uniaxial strain or the biaxial shear test,

$$\sqrt{J'^2} = (1/\sqrt{3})(\sigma_1 - \sigma_3)$$

$$J_1 = 3P = (\sigma_1 + 2\sigma_3)$$

The square root of the second invariant of the stress deviatoric, J2' may be plotted against P (equal to one-third the value of the first stress invariant, J1) in order to evaluate A and α.

A straight line approximation for A and α in terms of cohesion, c, and friction angle, ϕ, from a Mohr-Coulomb diagram, are:

$$A = 6c \cos\phi / [\sqrt{3} (3 - \sin \phi)]$$

$$\alpha = 2 \sin \phi / [\sqrt{3} (3 - \sin \phi)]$$

Murtha and Crawford demonstrate that A and α can be computed directly for concrete. This means all of the measured data is included in the calculation of A and α and that no dependence on parameters c and ϕ is necessary. This is accomplished by computing J_1 and J_2' at intervals of 0.2 along the σ_1/f_c' axis. Values of σ_1/f_c' (i = 1, 2, 3) were computed for various points on the curves and from these values J1 and J2 were computed. The results are shown in Figure 1 where A = 0.48 f_c' and α = 0.09. In effect, Figure 1 demonstrates that the Drucker-Prager Model matches the envelopes of concrete in the compression quadrant.

Using the above to derive an equivalent ϕ and c gives ϕ = 12.5° and c = 0 395 f_c

Mohr-Coulomb The generalized Mohr-Coulomb behavior may be used to produce the following failure law for compression-compression zone.

$$3J_2 + \sqrt{3}\, \beta\, \sigma\, J_1 + \alpha\, J_1^2 = \sigma^2$$

where β, σ and α are material constants. For biaxial stress Kupfer evaluated these constants as

$$\beta = \sqrt{3}$$

$$\alpha = 1/5$$

$$\sigma = f_c'/3$$

In the tension-compression zone and tension-tension zones, failure may be defined by a series of straight lines based on the tensile strength of concrete.

References

Mrutha R and J. Crawford, NCEL TM 51-78-6 "A Evaluation of Material Model Performance"

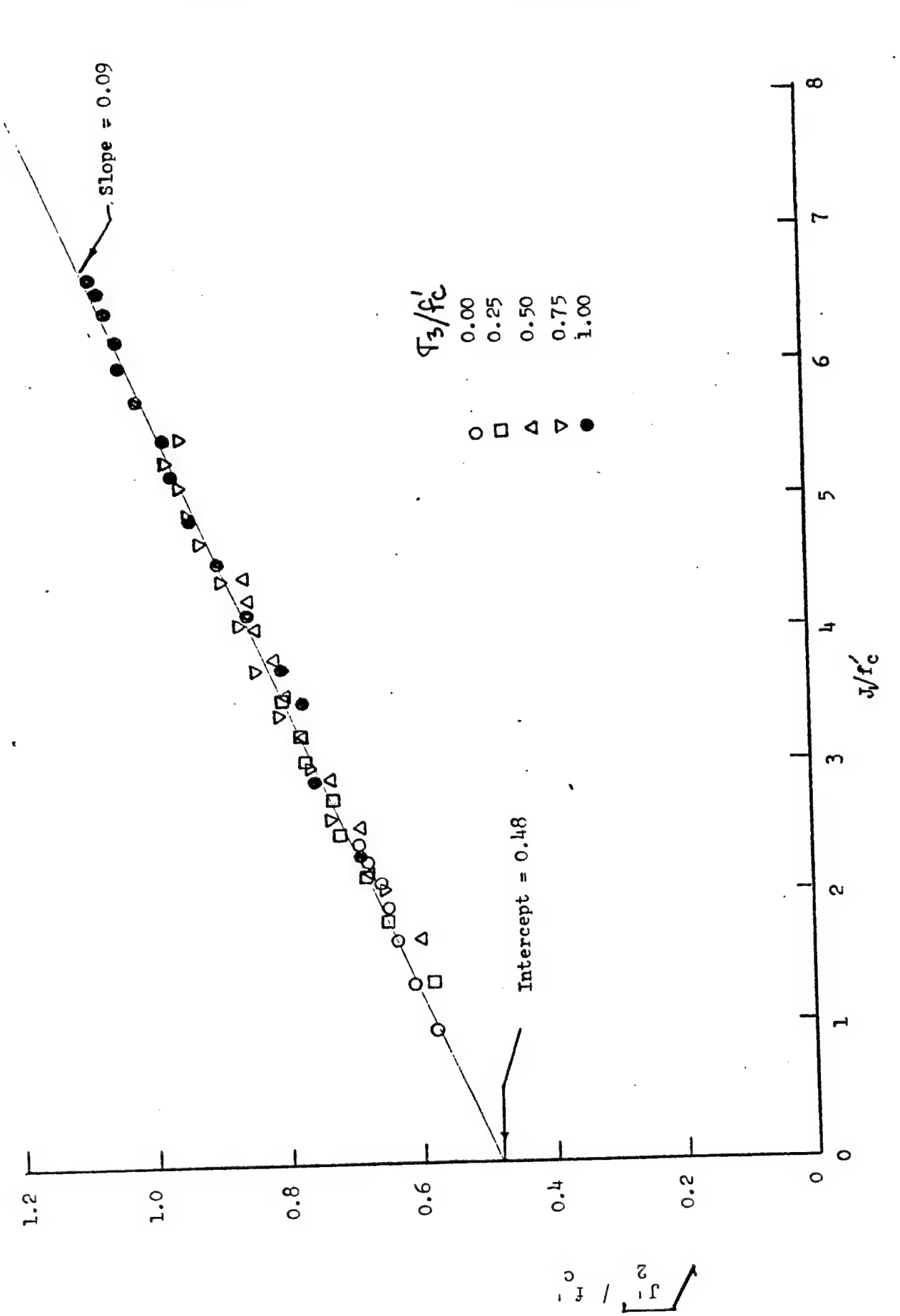

Figure A1. Drucker - Prager failure envelope.

APPENDIX

Soil Properties

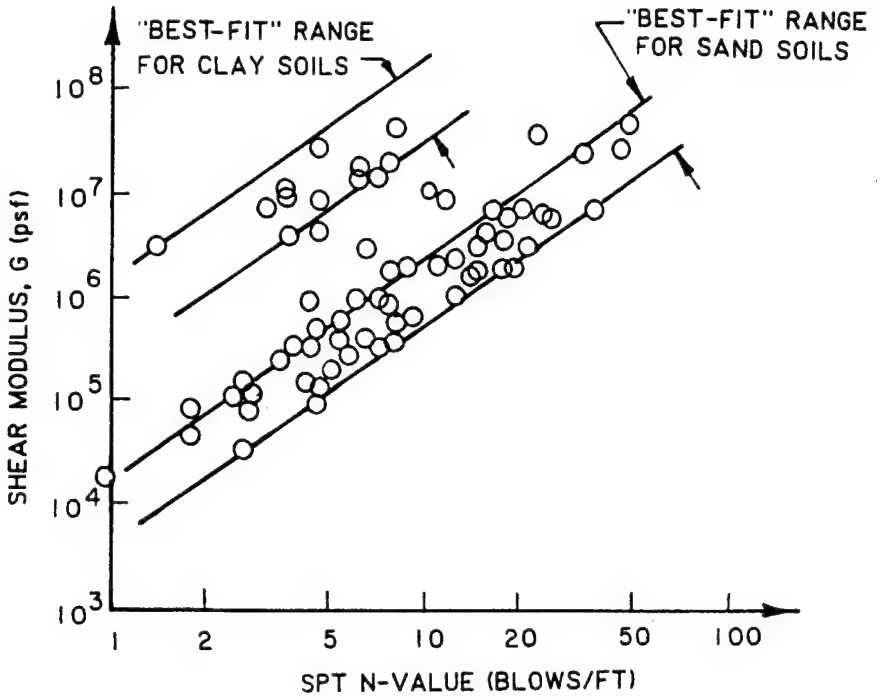

Figure 1. Variation in shear modulus of sands and clays with SPT N-value (Kanai 1966) (as presented in Ohsaki and Iwasaki 1973)

$$K = \frac{E}{3(1-2\nu)}$$

$$G = \frac{E}{2(1+\nu)}$$

Selected elastic constants (laboratory-scale) for rocks [adapted from Goodman, 1980]

	E (GPa)	ν	K (GPa)	G (GPa)
Berea sandstone	19.3	0.38	26.8	7.0
Hackensack siltstone	26.3	0.22	15.6	10.8
Bedford limestone	28.5	0.29	22.6	11.1
Micaceous shale	11.1	0.29	8.8	4.3
Cherokee marble	55.8	0.25	37.2	22.3
Nevada Test Site granite	73.8	0.22	43.9	30.2

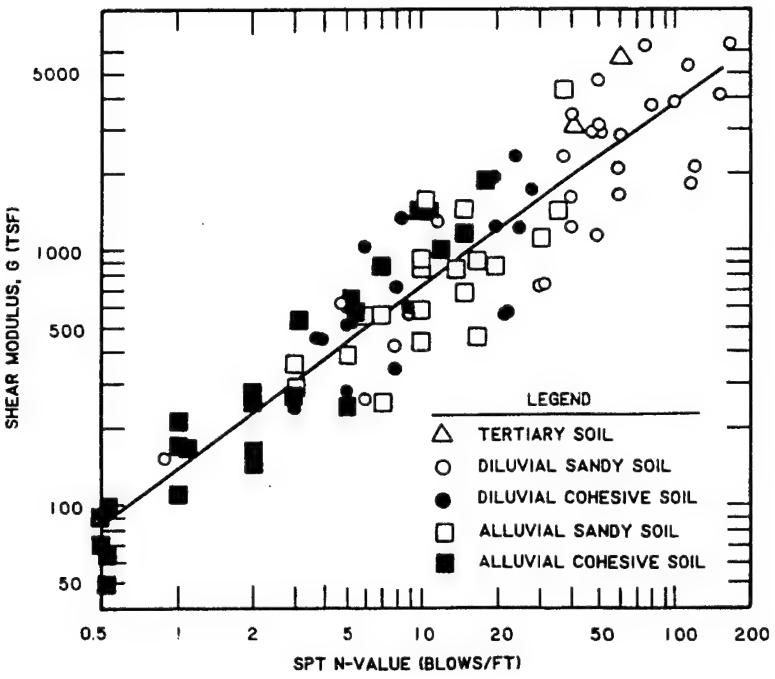

. Correlation between SPT N-value and G using data from Ohta et al. (1970) (as presented by Ohsaki and Iwasaki 1973)

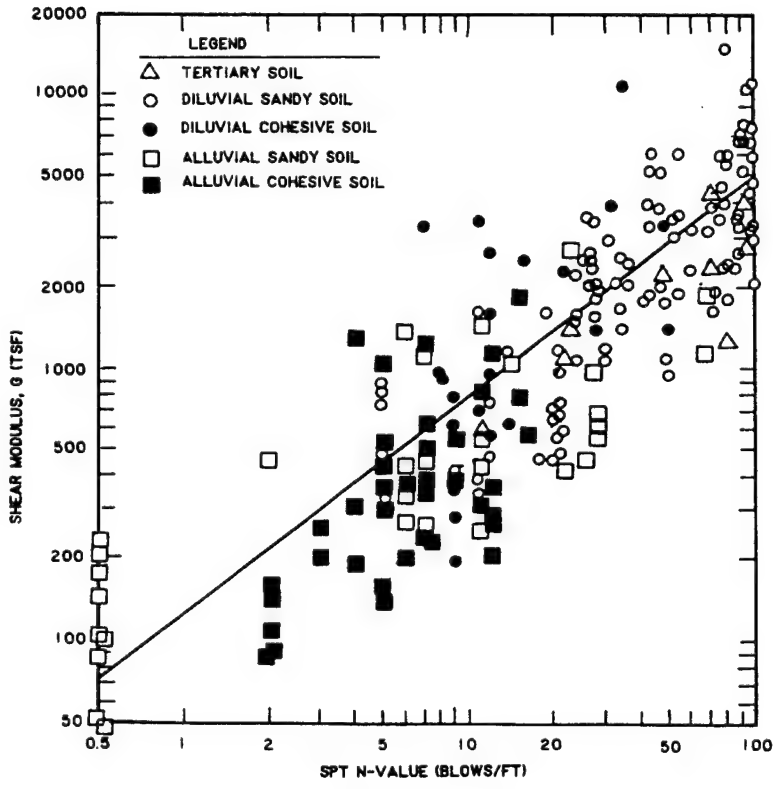

Correlation between SPT N-value and G (performed by Ohsaki and Iwasaki 1973)

	cohesion	friction angle	
		peak	residual
	(kPa)	(degrees)	(degrees)
gravel	—	34	32
sandy gravel with few fines	—	35	32
sandy gravel with silty or clayey fines	1.0	35	32
mixture of gravel and sand with fines	3.0	28	22
uniform sand — fine	—	32	30
uniform sand — coarse	—	34	30
well-graded sand	—	33	32
low plasticity silt	2.0	28	25
medium to high plasticity silt	3.0	25	22
low plasticity clay	6.0	24	20
medium plasticity clay	8.0	20	10
high plasticity clay	10.0	17	6
organic silt or clay	7.0	20	15

Typical values for dilation angle [Vermeer and de Borst (1984)]

dense sand	15°
loose sand	< 10°
normally consolidated clay	0°
granulated and intact marble	12° – 20°
concrete	12°

Soil Material	$\bar{\phi}_{tc}$ (degrees) Loose	Dense
Sand, round grains, uniform	27.5	34
Sand, angular grains, well-graded	33	45
Sandy gravels	35	50
Silty sand	27 to 33	30 to 34
Inorganic silt	27 to 30	30 to 35

Source: Terzaghi and Peck (4), p. 107.

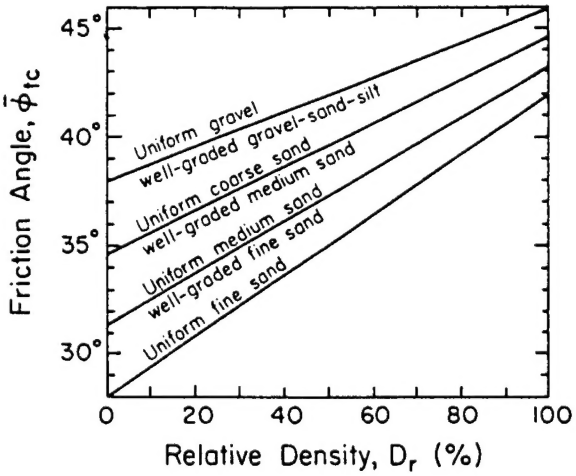

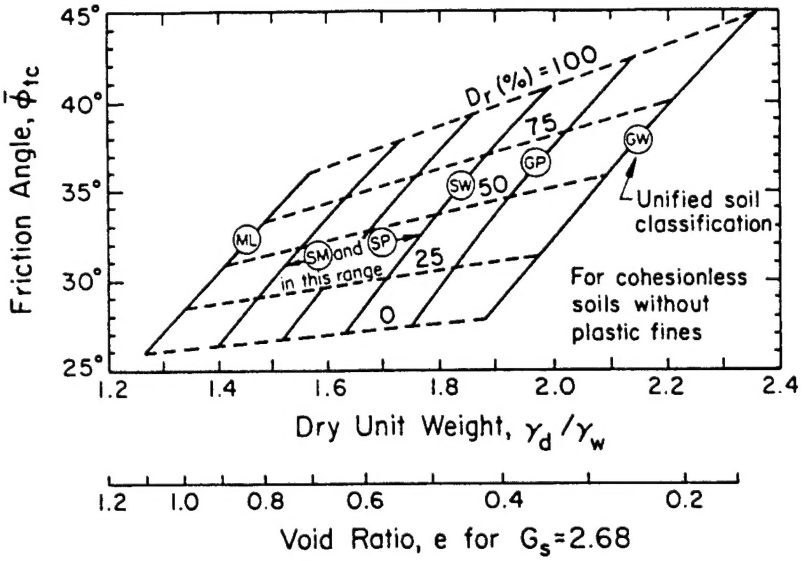

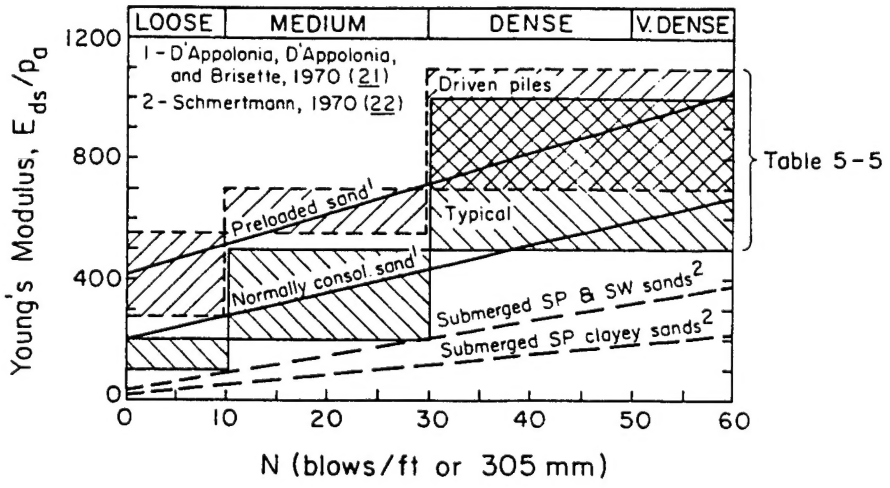

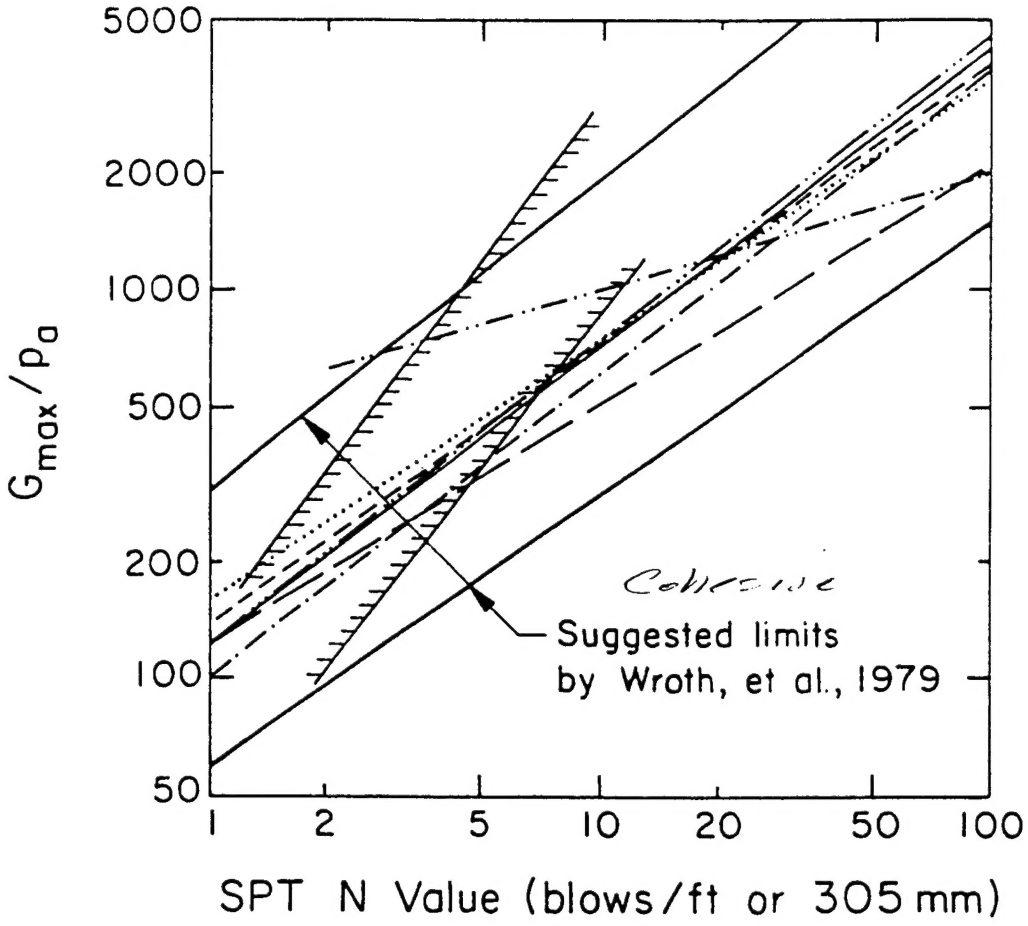
5000
2000
1000
500
200
100
50
G_{max}/p_a
Cohesive
Suggested limits
by Wroth, et al., 1979
1
2
5
10
20
50
100
SPT N Value (blows/ft or 305 mm)

TYPICAL RANGES OF DRAINED POISSON'S RATIO

Soil	Drained Poisson's Ratio, ν_d
Clay	0.2 to 0.4
Dense sand	0.3 to 0.4
Loose sand	0.1 to 0.3

Type	s_u (psi)	ε_{50} (%)	γ_b (pcf)
Underconsolidated clays	0.35-1.0	2	20-25
Normally consolidated soils at depth z, in.	1.0 + 0.0033z	2-1	25-50
Overconsolidated soils based on consistency:			
medium stiff	3.5-7.0	1.0	50-65
stiff	7.0-14	0.7	
very stiff	14-28	0.5	
hard	over 28	0.4	

Type	Standard Penetration Blow Count, N	ϕ (deg)	D_r (%)	γ_b (pcf)
Very loose to loose	<10	28-30	0-35	45-55
Medium dense	10-30	30-36	35-65	55-65
Dense	30-50	35-42	65-85	60-70
Very dense	50+	40-45	85-100	60-70